NAVAL POSTGRADUATE SCHOOL
Monterey, California

THESIS

VIBRATION MEASUREMENTS ON THE PHALANX ELECTRO-OPTICAL STABILIZATION SYSTEM

by

James E. Schmidt

September, 1996

Thesis Advisor: Steven R. Baker

Approved for public release; distribution is unlimited.

REPORT DOCUMENTATION PAGE

Form Approved OMB No. 0704-0188

1. AGENCY USE ONLY *(Leave blank)*	2. REPORT DATE	3. REPORT TYPE AND DATES COVERED
	September 1996	Master's Thesis

4. TITLE AND SUBTITLE VIBRATION MEASUREMENTS ON THE PHALANX ELECTRO-OPTICAL STABILIZATION SYSTEM

5. FUNDING NUMBERS

6. AUTHOR(S) James E. Schmidt, LCDR USN

7. PERFORMING ORGANIZATION NAME(S) AND ADDRESS(ES)
Naval Postgraduate School
MONTEREY CA 93943-5000

8. PERFORMING ORGANIZATION REPORT NUMBER

9. SPONSORING/MONITORING AGENCY NAME(S) AND ADDRESS(ES)
Naval Surface Warfare Center, Dahlgren, Virginia

10. SPONSORING/MONITORING AGENCY REPORT NUMBER

11. SUPPLEMENTARY NOTES The views expressed in this thesis are those of the author and do not reflect the official policy or position of the Department of Defense or the U.S. Government.

12a. DISTRIBUTION/AVAILABILITY STATEMENT
Approved for public release; distribution is unlimited.

12b. DISTRIBUTION CODE

13. ABSTRACT *(maximum 200 words)*

The installation of the new PHALANX Surface Mode (PSUM) upgrade will enable the PHALANX to handle a wider range of threats, such as a small boat approaching the ship. The objective of the research described in this thesis was to measure the vibration of a prototype forward looking infrared (FLIR) camera stabilizer system during live-fire tests to evaluate its performance. Uniaxial, triaxial, and angular accelerometers were mounted at 19 different locations on the stabilizer and on the camera. Acceleration data were collected during eight live fire tests conducted at a Navy range, and the results analyzed. The power spectral densities (PSD) of the input linear accelerations at the stabilizer mounting points and the resulting linear accelerations at key locations on the stabilizer were calculated. The azimuth and elevation angular displacements of the FLIR camera mount were also calculated. The azimuth and elevation angular displacement of the plane of the stabilizer pedestal mounting points were also calculated.

Recommendations are made for follow-on studies.

14. SUBJECT TERMS PHALANX, M61A1, Gatling Gun, PHALANX Surface Mode Upgrade			15. NUMBER OF PAGES 155
			16. PRICE CODE
17. SECURITY CLASSIFICATION OF REPORT Unclassified	18. SECURITY CLASSIFICATION OF THIS PAGE Unclassified	19. SECURITY CLASSIFICATION OF ABSTRACT Unclassified	20. LIMITATION OF ABSTRACT UL

NSN 7540-01-280-5500

Standard Form 298 (Rev. 2-89)
Prescribed by ANSI Std. 239-18 298-102

Approved for public release; distribution is unlimited.

VIBRATION MEASUREMENTS ON THE PHALANX ELECTRO-OPTICAL STABILIZATION SYSTEM

James E. Schmidt
Lieutenant Commander, United States Navy
B.A., John Carroll University, 1985

Submitted in partial fulfillment
of the requirements for the degree of

MASTER OF SCIENCE IN ENGINEERING ACOUSTICS

from the

NAVAL POSTGRADUATE SCHOOL
September 1996

ABSTRACT

The installation of the new PHALANX Surface Mode (PSUM) upgrade will enable the PHALANX to handle a wider range of threats, such as a small boat approaching the ship. The objective of the research described in this thesis was to measure the vibration of a prototype forward looking infrared (FLIR) camera stabilizer system during live-fire tests to evaluate its performance. Uniaxial, triaxial, and angular accelerometers were mounted at 19 different locations on the stabilizer and on the camera. Acceleration data were collected during eight live fire tests conducted at a Navy range, and the results analyzed. The power spectral densities (PSD) of the input linear accelerations at the stabilizer mounting points and the resulting linear accelerations at key locations on the stabilizer were calculated. The azimuth and elevation angular displacements of the FLIR camera mount were also calculated. The azimuth and elevation angular displacement of the plane of the stabilizer pedestal mounting points were also calculated.

Recommendations are made for follow-on studies.

TABLE OF CONTENTS

I. INTRODUCTION

The PHALANX Close-In Weapons System (CIWS) is a six-barrel gatling gun that fires 20mm tungsten bullets at 4,500 rounds a minute. Its is the last defense against incoming high speed airborne targets at short range and is installed on almost every ship in the U.S. Navy. However, the PHALANX CIWS is unable to be employed against the less sophisticated weapons and tactics that a terrorist or third world nation might employ against a U.S. Navy ship. For example, the current PHALANX system is incapable of engaging an adversary using a small boat to approach the ship. The installation of the new PHALANX Surface Mode (PSUM) upgrade with a infrared imaging/tracking system will enable the PHALANX to counter these types of threats.

The PHALANX system currently employs a single operating mode in which it operates totally automatically against high speed airborne targets. Using its own radar, the PHALANX searches for incoming contacts. Then, after the radar acquires a contact that meets preselected criteria, the contact is designated a hostile target and the gun is automatically aimed and fired at the target. All of these actions must, and do, occur automatically within seconds to destroy an incoming high speed target before it hits the ship.

For numerous reasons, the Naval Surface Warfare Center (NSWC), at Dahlgren, Virginia, desired to modify the PHALANX system to operate in a non-automatic mode against possible surface targets. Against this type of target, NSWC envisioned the PHALANX engaging a target without using the radar to aim the gun. The gun would be manually aimed and fired by an operator in a totally new, manual mode of operation.

This new mode of operation and modification program is named the PHALANX Surface Mode (PSUM) upgrade. Hughes Missile Systems Company (HMSC) developed and built a prototype with a forward looking infrared (FLIR) camera. The new PSUM system consists of the FLIR camera and a stabilizer. (Hughes Missile Systems Company, 1996, p. 4). The FLIR camera is mounted on the stabilizer and the stabilizer is mounted on the side of the PHALANX's radome cover, aligned with the boresight of the gun. Figure 1.1 shows a line drawing of the prototype stabilizer mount and FLIR camera. Figure 1.2 shows a line drawing of the prototype mounted on the side of the PHALANX CIWS radome.

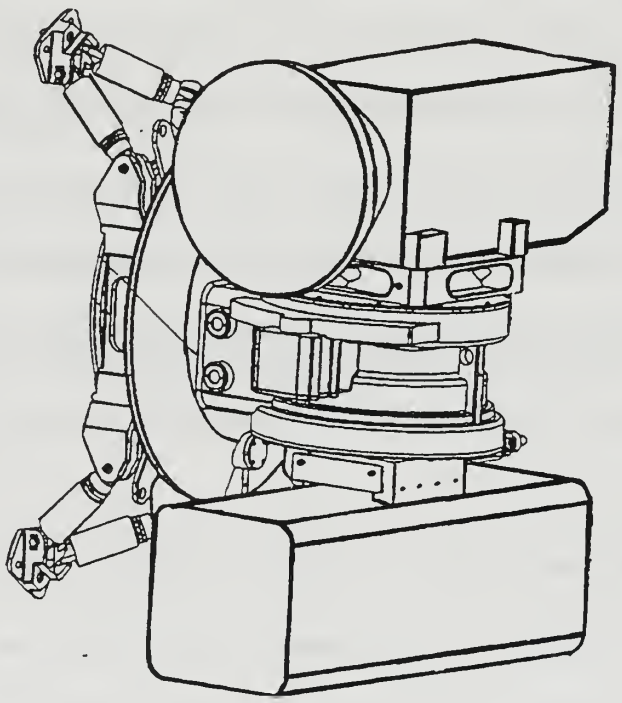

Figure 1.1. Prototype stabilizer and FLIR camera mount.

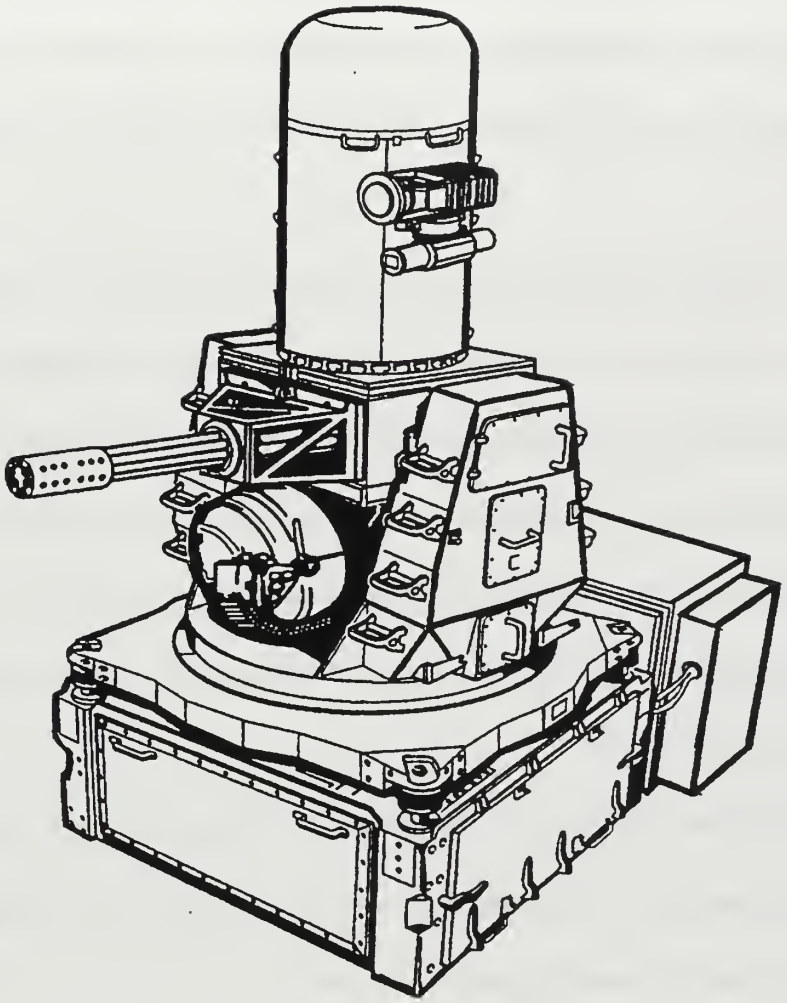

Figure 1.2. Mounting of the prototype stabilizer and FLIR camera on the side of a PHALANX CIWS radome.

It was determined by HMSC that, to properly aim the gun, the image from the FLIR camera must have less then 100 micro radians rms of angular jitter (displacement) across the gun's boresight when the gun is fired. The stabilizer subsystem was designed to reduce the input accelerations from the radome at the three pedestal mounts to less than 100 micro radians rms of angular jitter at the FLIR camera mount. The stabilizer

consists of a three-footed pedestal with passive isolation, elevation and azimuth servo-controlled rotators, and a mounting pad for the FLIR camera. Provision for mounting a television (TV) camera beneath the FLIR camera is provided for but is not included in this upgrade.

Live-fire testing of the prototype FLIR camera and its stabilizer was conducted at NSWC, Dahlgren, Virginia. NPS was tasked to measure the input accelerations to the stabilizer at the pedestal feet and the angular displacements at the FLIR camera mount. Hughes made simultaneous optical measurements of angular jitter using a point target. The NSWC approved test plan to accomplish this is enclosed as Appendix A.

This thesis is organized as follows. Chapter II discusses the equipment used for the test and calibrations.

Chapter III discusses the locations and mounting of the accelerometers and a description each of the eight live fire-tests, as outlined in the test plan. This chapter includes the post-test and data analysis goals of the tests.

Chapter IV discusses the results of the calibrations conducted prior to and after the live-fire tests. This chapter includes the results of the signal analyzer input channel calibrations, the accelerometer calibrations, and the comparison of angular acceleration measurements made with linear accelerometers to those made with angular accelerometers.

Chapter V discusses the results of the live-fire tests: the power spectral densities (PSDs) of the input accelerations at the pedestal mounts, the angular accelerations and displacements at the FLIR camera mount , and the azimuthal and elevation motion of the

plane of the pedestal mounts.

Chapter VI includes conclusions and recommendations for further analysis.

II. TEST AND CALIBRATION EQUIPMENT

A brief description of the test equipment employed during the live-fire tests and the calibrations conducted in the lab at NPS is described below. A detailed description of the calibrations performed is provided in Chapter IV.

A. TEST EQUIPMENT

The major equipment used during the live-fire tests consisted of the following: one Scientific Atlanta Model SD390 8-channel signal analyzer, three PCB model J353B04 uniaxial linear accelerometers, three PCB model 354B33 triaxial linear accelerometers, four Kistler model 8832 Translational Angular PiezoBEAM (TAP) accelerometers and their associated electronic units. For each item, a brief description, the calibrations conducted, and its configuration during the live-fire test are described below.

1. The Scientific Atlanta SD390

The Scientific Atlanta Model SD390 is an 8-channel dynamic signal analyzer (Scientific Atlanta, 1996, p 1-1). It is basically a DOS/Windows computer with custom hardware and software. Each channel has an independent 16-bit A/D converter, with a maximum sampling rate exceeding 100 kHz with only two channels operating. When all eight channels are active, the maximum sampling rate is 40 kHz. The SD390 was used for recording accelerometer data. A calibration of each SD390 channel was conducted, and is described in Chapter IV. A listing of some of the SD390's specifications is included as Appendix B.

For the live-fire tests, the SD390 was manually triggered, then began sampling all eight channels at 25.6 kHz for 7.2 seconds. For most of the live-fire tests, the firing event

lasted approximately 5 seconds and the sampling began approximately 1.5 seconds before the gun began to fire. The time record covered the ramp-up, steady state, and ramp-down vibrations of the stabilizer. The 25.6 kHz sampling rate exceeds the maximum bullet firing rate of 80 Hz by more than a factor of 250, allowing data processing for frequencies well in excess of 2 kHz. A total of 184,320 samples per channel were recorded; the data for all eight channels for one firing requires 2.7 MB of memory. After a test firing the data were given a cursory review and stored on the internal hard disk. The data were later analyzed using MATLAB (Math Works, 1992, p.1). The conversion of the stored data files from the analyzer's format into a MATLAB-readable file and the subsequent data analysis are described in Chapter V.

2. Uniaxial Linear Accelerometers

Three uniaxial linear accelerometers were used to collect data during the live-fire tests. One was used as a reference, to relate the acceleration measured at one set of locations for one test firing to those at another set for another firing. The uniaxial linear accelerometers were PCB Model J353B04 piezoelectric accelerometers (PCB Vibration & Shock catalog, 1993, p. 5). The accelerometers are small (½-in hex, 0.8-in H), lightweight (10 g), electrically-isolated, employ a quartz sensing element, and have a built-in charge amplifier. The frequency response of the accelerometers (± 5 %) are 1 Hz to 7 kHz. They have a 10-32 tapped hole for mounting onto a mounting base. They require an external 4 mA constant-current source, which was provided by the SD390 analyzer. A complete listing of the accelerometer's specifications and the manufacturer's calibration is included as Appendix C.

For the live-fire tests, the reference uniaxial accelerometer was screw-mounted to an adhesive mounting base bonded with epoxy to one of the pedestal feet. At the mounting location, the surface of the stabilizer was slightly roughened with fine sand paper and wiped clean. Then a small amount of epoxy was used to adhesively bond the mounting base to the stabilizer foot. The epoxy was allowed to cure overnight before the test firings. The exact location of the reference and all other accelerometers by location number is provided in Chapter III.

3. Triaxial Linear Accelerometers

The triaxial linear accelerometers used for the tests were three PCB Model 354B33 piezoelectric accelerometers (PCB Vibration & Shock catalog, 1993, p. 65). These are also small (0.8-in hex, 0.4-in H), lightweight (15.5 g), electrically-isolated units which employ quartz sensing elements and have a built-in charge amplifier. The accelerometers have a hole in their center for a 10-32 through-bolt to be inserted for mounting. This allows the accelerometers to be rotated for easy axis alignment. The frequency response of the accelerometers (± 5 %) is 1 Hz to 2 kHz. They also require an external 4 mA constant current source, which was provided by the SD390 analyzer. A complete listing of the triaxial accelerometer's specifications and the manufacturer's calibrations is included as Appendix D.

For the live-fire tests, triaxial accelerometers were mounted to the stabilizer with the through-bolt in four different ways. The most common method employed was to bolt the accelerometer to an adhesive mounting base bonded to the structure with epoxy. The method used on the pedestal feet was to bolt the accelerometer to a tapped hole in a bolt

manufactured at the Naval Postgraduate School (NPS) that replaced one bolt securing each of the pedestal feet. The third method was to screw the through-bolt directly in a taped hole on the structure. The fourth method was to bolt the accelerometer to an adhesively-bonded mounting base manufactured at NPS to fit the curvature of the infrared camera's curved lens housing. The exact method of mounting for each accelerometer by location is described in Chapter III.

4. Translational-Angular PiezoBEAM "TAP" Accelerometers

The angular accelerometers used for the tests were four Kistler Model 8832 Translational-Angular PiezoBEAM "TAP" accelerometer Systems (Kistler, 1995, p. 50). The TAP system is composed of a Kistler Model 8696 accelerometer and a Kistler Model 5130 signal coupler (includes a power supply). The accelerometers are small (5/8-in square, ½-in H), lightweight (10 g), units which employ two piezoelectric ceramic bimorph sensing elements and have built-in charge amplifiers. They are not electrically isolated. By summing and differencing the individual sensor outputs in the signal coupler, the TAP System provides one output signal proportional to the linear acceleration normal to the accelerometer base and another output proportional to the angular acceleration about an axis parallel to the accelerometer cable connector. The frequency response of the system (± 5 %) is 0.5 Hz to 2 kHz. The range for linear operations is ± 10 g, and ± 18,000 rad/s^2 for angular operations. These ranges are for pure linear or pure angular accelerations. They are derated when both linear and angular vibration are present. A complete listing of the accelerometer's specifications and the manufacturer's calibrations is included as Appendix E.

Because the TAP accelerometers have no provision for stud or screw mounting, all four were adhesively bonded to the structure with a cyanoacrylate ester "super glue" gelatin supplied by Kistler. The owner's manual recommends petro wax to affix the accelerometer, and each unit is supplied with petro wax for use at nominally 70° F. We were concerned that the ambient temperature at the test site may exceed this temperature. Therefore, we consulted with an application engineer at the manufacturer for the best solution. He advised us that it is acceptable to adhesively bond the outer edges of the bottom of the accelerometer, outside the cover plate, to the structure with super glue.

B. CALIBRATION EQUIPMENT

Additional significant equipment used for calibrations in the lab at NPS consisted of the following items: one Bruel & Kjaer model 8305S reference accelerometer, one Bruel & Kjaer model 4810 mini-shaker, one Hewlett-Packard HP3325B Synthesizer/Function generator, one Stanford Research Systems SR530 Lock-in Amplifier, and a Hewlett-Packard HP4192 LF Impedance Analyzer. A detailed description of the calibrations conducted is provided in Chapter IV.

1. Calibration Reference Accelerometer

One calibration-quality reference accelerometer was purchased for calibrating the accelerometers used for the measurements, described previously. The reference accelerometer was a Bruel & Kjaer NIST-traceable reference accelerometer type 8305S SN 1864983 calibrated in February 1996 by laser interferometer (Bruel & Kjaer, 1996, p.1). The reference accelerometer frequency response is within 0.5% from DC to 2 kHz, depending on the supporting mass. A Kistler 5010B Dual Mode Charge Amplifier

(Kistler, 1995, p.61) was used to convert the B&K 8305 output signal from pC into Volts. Additional information on the Bruel & Kjaer reference accelerometer and the manufacturer's calibration is listed in the specification sheet located in Appendix F. Additional information and manufacturer's calibration of the Kistler 5010B is located in Appendix G.

2. Bruel & Kjaer Mini-Shaker

A Bruel & Kjaer type 4810 mini-shaker was used for accelerometer calibrations (Bruel & Kjaer, 1987, p.1). The Bruel & Kjaer type 4810 mini-shaker is specifically designed for dynamic testing and calibration of accelerometers at frequencies from DC to 18 kHz. The maximum allowed current is 1.8 Amps rms; the maximum displacement is 6 mm. The result of these limitations on calibrations was to limit the acceleration of the shaker to a maximum of about 1.2 g.

3. HP3325B Synthesizer/Function Generator

The HP3325B Synthesizer/Function Generator was used as an accurate voltage source during the calibration of each channel of the SD390 (Hewlett & Packard, 1985, p.1). The error of its output voltage is specified as less than 0.2 percent, after a 20 minuet warmup.

4. Stanford Research Systems SR530 Lock-in Amplifier

The Stanford Research Systems SR530 Lock-in Amplifier (Stanford Research Systems, 1985, p.1) was used to measure accelerometer voltage magnitude and phase during accelerometer calibrations. The specified maximum measurement errors for voltage magnitude and phase at 100 Hz are 1% and 1 degree respectively.

5. Hewlett-Packard 4192 LF Impedance Analyzer

The Hewlett-Packard 4192 LF Impedance Analyzer (Hewlett-Packard, 19) was used to measure test accelerometer voltage gain magnitude and phase relative to the calibrations reference accelerometer. The specified maximum measurement errors for voltage gain and magnitude and phase at 100 Hz are 0.01% and 0.2% , respectively.

III. THE TEST PLAN

The test plan to measure the input accelerations to the stabilizer at the pedestal feet and the resulting angular accelerations at the FLIR camera mount was originally submitted on April 5, 1996. This plan was revised and the final version was submitted on June 10, and is included as Appendix A. The test plan was divided into nine different sections. The sections of the test plan are 1) Data collection, 2) Accelerometers, 3) Sensor Calibration, 4) Mounting of Accelerometers, 5) Accelerometer Mounting Locations, 6) Reference Accelerometers, 7) Description of Each Firing, 8) Post Test, and 9) Data Analysis. This chapter will explain more on sections 5) Accelerometer mounting locations and 7) Description of each firing.

A. ACCELEROMETER MOUNTING LOCATIONS

The accelerometer locations were divided into primary and secondary locations in the test plan. They were further sub-divided into linear and angular accelerometer locations on major components of the stabilizer. The primary accelerometer locations supported data collection for the "primary" firings. The primary firings are those which are essential to complete the requirements of the study, that is to measure the input accelerations at the pedestal feet and the rotational accelerations at the FLIR camera mount. The "secondary" accelerometer locations supported data collection in the secondary firings. The secondary firings were not essential to complete the study, but added to the quality of the study and could prove essential for any follow-on work, if required. The reasons for choosing the specific primary and secondary locations are discussed below.

1. Primary Locations

Thirteen primary accelerometer locations supported the primary firings in determining the input vibration at the pedestal feet and the angular jitter (displacement) at the FLIR camera mount. Figure 3.1 shows their locations. Locations 10 through 13 are included to honor a request by Pilkington Company (the camera manufacturer) to provide acceleration data on the FLIR camera case and lens housing.

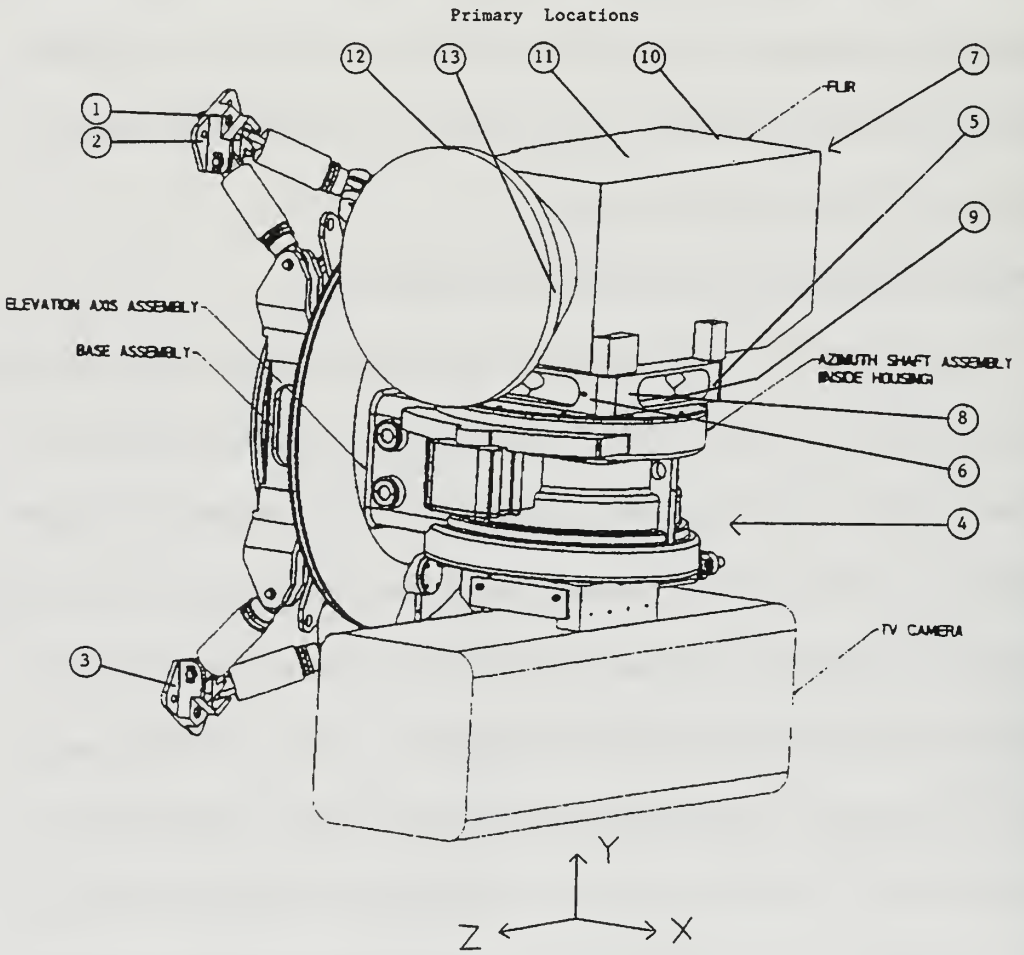

Figure 3.1. The thirteen primary accelerometer locations supported the primary firings.

One uniaxial accelerometer was designated as a reference. This accelerometer was mounted in the same location (1) and axis direction, and data were collected using this accelerometer for almost all of the eight live-fire tests. With the reference uniaxial accelerometer, data from one test firing can to be related to that of another. Below is a more detailed description of the primary types and locations.

a. Linear Accelerometer Locations on Pedestal Mounts

Location number one was directly over the top front pedestal mount alignment pin. The reference uniaxial accelerometer was stud-mounted at this location to a base which was bonded with epoxy to the pedestal foot directly over the alignment pin.

Locations numbers two through four were on bolt heads at each of the pedestal feet. The production bolts at these locations were replaced with bolts modified at NPS with a tapped hole in the bolt head. Triaxial accelerometers were screw-mounted on these bolt heads. A ½ -inch bushing was installed to space the accelerometers far enough away from the bolt head to ensure that the pedestal foot flange would not interfere with the accelerometer. Figure 3.2 shows a cut-away drawing of a replacement bolt and bushing. With a triaxial accelerometer mounted in this fashion at each pedestal foot, the acceleration of the pedestal feet can be determined in all axes.

b. Linear Accelerometer Locations on FLIR Mount ("rocky")

Location number five is on the left surface of the FLIR mount (when facing front) on an adhesive-bonded base as shown in Figure 3.5. This location was to be used for a second reference accelerometer, but was not used during the testing.

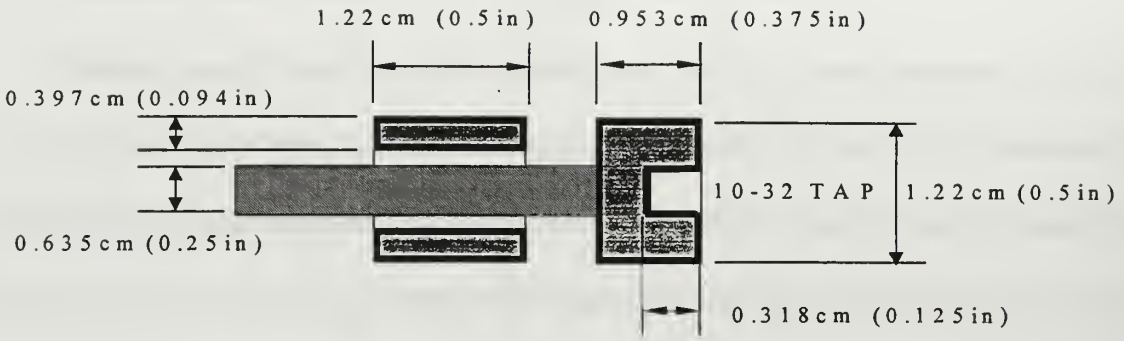

Figure 3.2. Cut away diagram of a replacement bolt and bushing.

Location number six is a screw hole on the front surface of the FLIR mount (when facing front), in the +Z-(gunbarrel) direction. The distances from this hole to the edges of the FLIR mount are shown in Figure 3.3. This location was used to mount a triaxial accelerometer. The data from this location, together with data from location number seven, can be used to determine the angular acceleration of the FLIR camera mount.

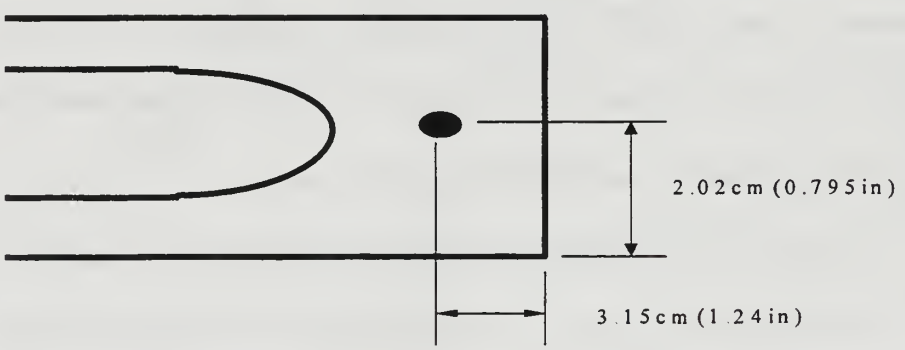

Figure 3.3. Accelerometer mounting location number six at a screw hole at the front surface of FLIR mount (when facing front).

Location number seven is at the rear surface of the FLIR mount, diagonally opposite of location six. The distance from this location to the edges of the FLIR mount are shown in Figure 3.4. This location was used to stud mount a triaxial accelerometer on a base bonded to the stabilizer with epoxy.

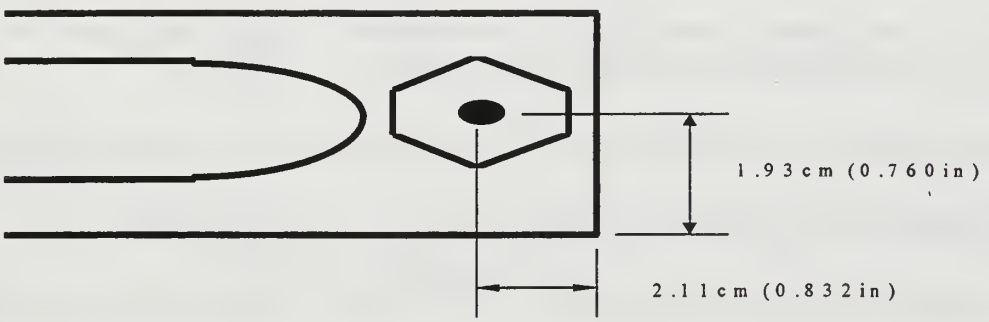

Figure 3.4. Accelerometer mounting location number seven is at the rear surface of FLIR mount, diagonally opposite of location six.

c. Angular Accelerometer Locations on FLIR Mount

Location number eight is on the left surface of the FLIR mount (when facing front) as shown in Figure 3.5. At this location a TAP accelerometer with the cable exiting up (+Y-direction) was bonded with super glue. The accelerometer provided angular acceleration of the FLIR mount about the Y-axis (azimuth) and linear acceleration in the +X-direction.

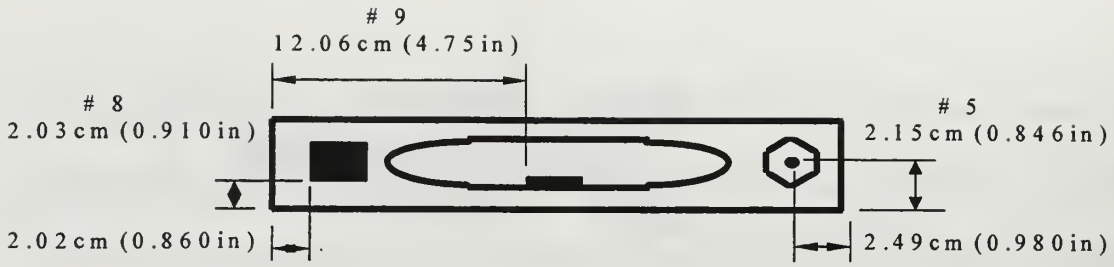

Figure 3.5. Accelerometer mounting location numbers five, eight, and nine on left surface of FLIR camera mount (when facing forward).

Location number nine is on top of the lower surface of the cutout on the left side of the FLIR mount (when facing front) as shown in Figure 3.5. At this location a TAP accelerometer was bonded with super glue with the cable exiting away from the stabilizer (+X) , the accelerometer can provide angular acceleration of the FLIR mount about the X-axis (elevation) and linear acceleration in the +Y-direction.

d. Linear Accelerometer Locations on FLIR Camera

Location number ten is on the top rear surface of the FLIR camera case seam (Pilkington location 10), as shown in Figure 3.6. This location was used to stud-mount a triaxial accelerometer to a base bonded with epoxy to the case. Data from this location, together with data from location number eleven can be used to determine the angular acceleration of the FLIR camera.

Location number eleven is on the top center surface of FLIR camera case seam (Pilkington location 4), as shown in Figure 3.6. This location was used to stud mount a

triaxial accelerometer to a base bonded with epoxy to the case.

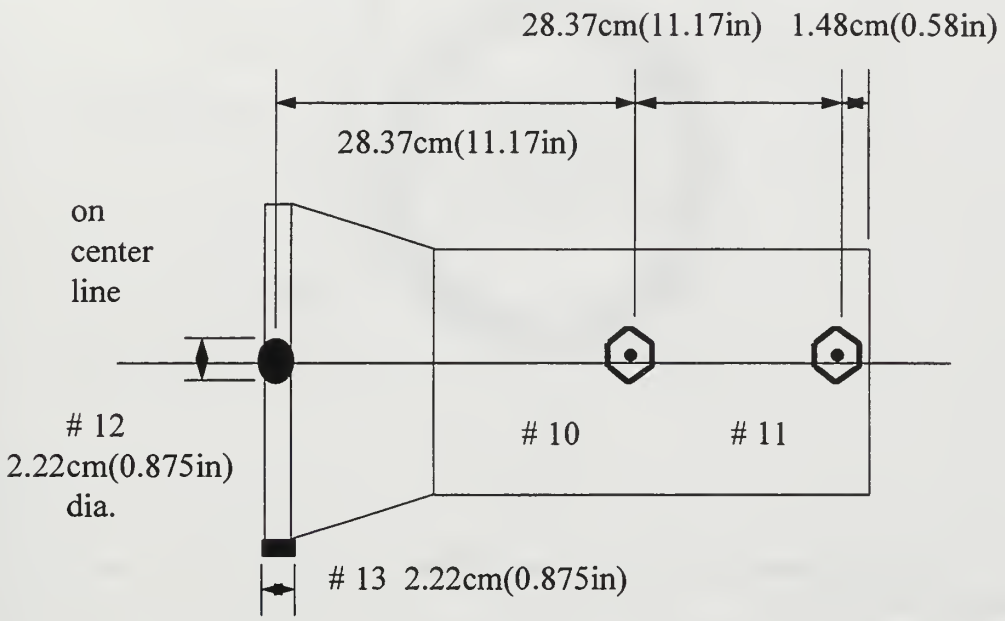

Figure 3.6. Accelerometer mounting locations number ten and eleven are on the FLIR camera case seams; twelve and thirteen are on the camera lens housing.

Locations twelve and thirteen are on the FLIR camera lens housing. Custom made stud-mount aluminum bases were machined at NPS to match the curvature of the outside of the FLIR camera lens housing. These were bonded to the lens housing with epoxy as shown in Figures 3.6 and 3.7. A triaxial accelerometer was stud-mounted on each base. Location number twelve is at the top of the housing; number thirteen is at the left side of the housing (when facing front).

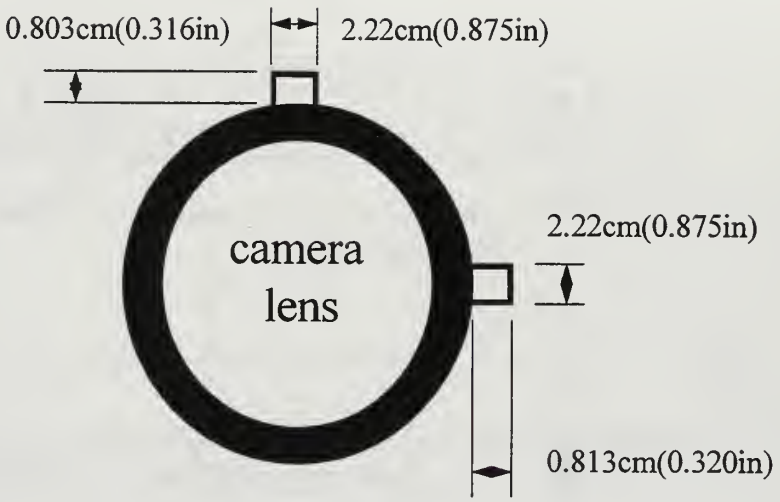

Figure 3.7. Accelerometer mounting locations number twelve and thirteen on the of FLIR camera lens housing.

2. Secondary Locations

Six secondary accelerometer locations supported the secondary firings. Figure 3.8 shows their locations, numbered 14 through 19. The secondary firings were not essential to complete the study, but added to the quality of this study and could prove essential for any follow- on work if required. The secondary accelerometer locations were sub-divided into linear and angular accelerometers.

a. Linear Accelerometer Locations on the Base Assembly

Locations number fourteen through sixteen are on the base assembly, as close as possible to each pedestal mount. Figure 3.9 gives the precise locations. These locations were used to stud- mount a triaxial accelerometer using an epoxy-bonded base.

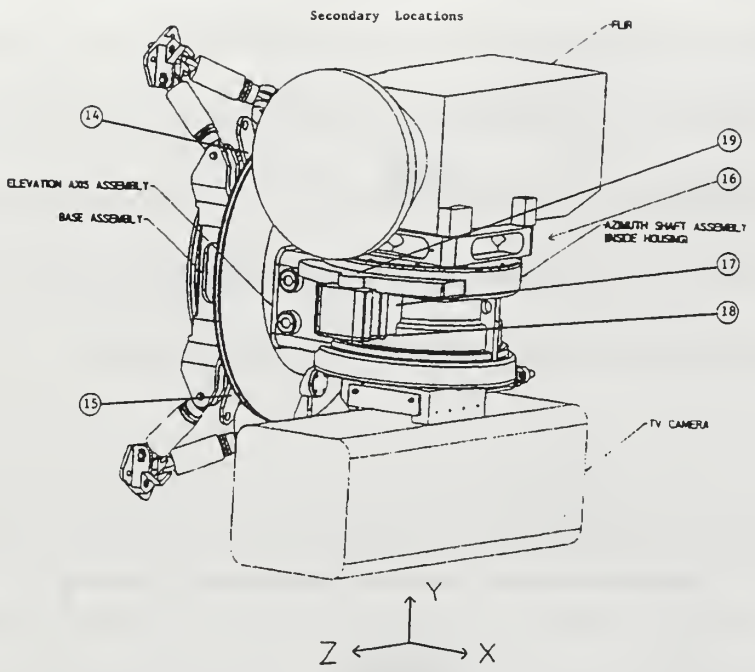

Figure 3.8. The six secondary accelerometer locations supported the secondary firings.

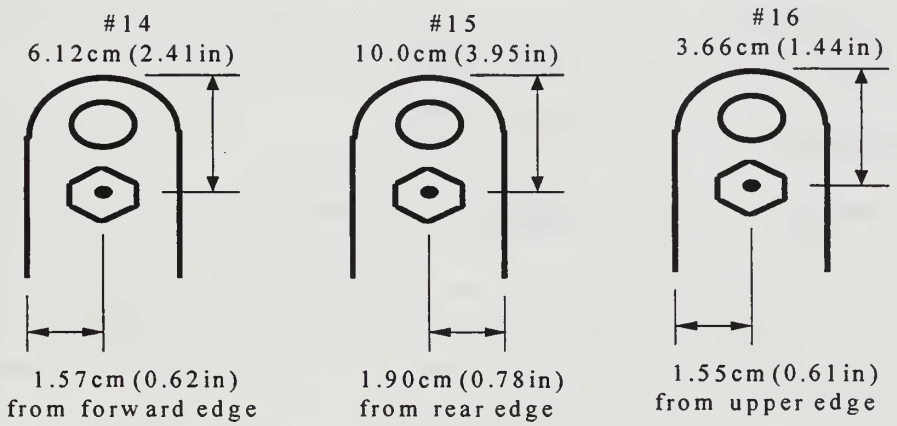

Figure 3.9. Accelerometer mounting locations number fourteen through sixteen are on the metal tabs protruding from the base assembly.

b. Angular Accelerometer Locations on Elevation Assembly

Location number seventeen is on the left surface of the flat box on the front of the azimuth shaft assembly (when facing front). At this location, a TAP accelerometer was bonded with super glue with the cable exiting up (+Y). The precise location is indicated in Figure 3.10. This accelerometer can provide angular acceleration of the FLIR mount about the Y-axis (azimuth) and linear acceleration in the +X-direction.

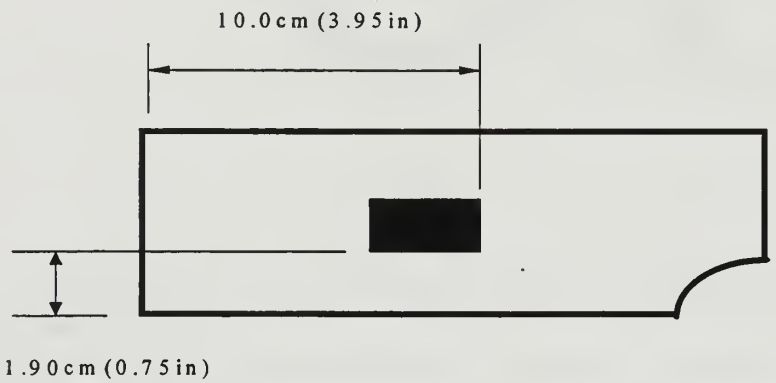

Figure 3.10. Accelerometer mounting location number seventeen on the left surface of the flat box on the front of the azimuth shaft assembly (when facing front).

Location number eighteen is on the bottom surface of the flat box on the front of the azimuth shaft assembly (when facing front). At this location, a TAP accelerometer was bonded with super glue with the cable exiting away from the stabilizer (+X). The precise location is indicated if Figure 3.11. The accelerometer can provide angular acceleration of the FLIR mount about the X-axis (elevation) and linear acceleration in the +Y-direction

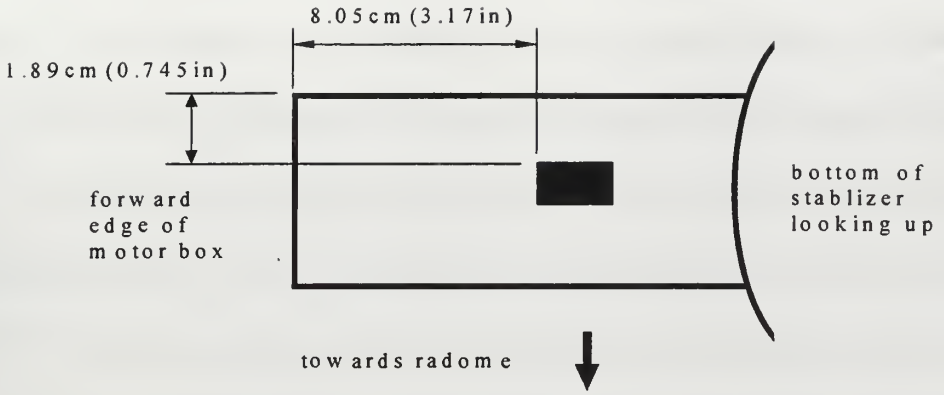

Figure 3.11. Accelerometer mounting location number eighteen on the bottom surface of the flat (motor) box on the front of the azimuth shaft assembly (when facing front).

Location number nineteen is on the front surface of the flat box on the front of the azimuth shaft assembly (when facing front). This location was used to stud mount a triaxial accelerometer to a base bonded with epoxy to the stabilizer. Figure 3.12 gives the precise location.

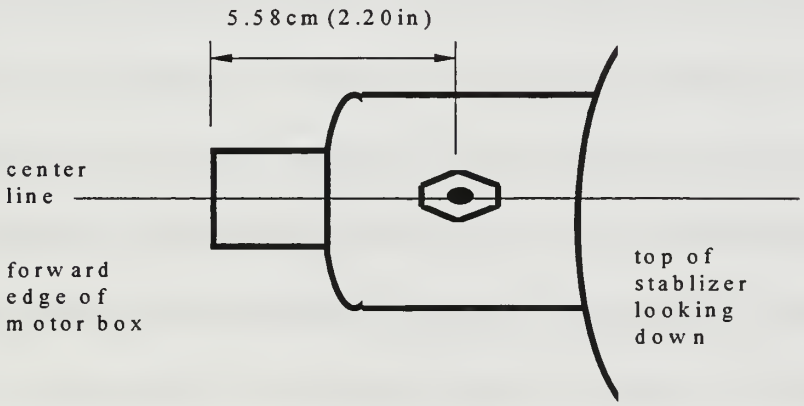

Figure 3.12. Accelerometer mounting location number nineteen on the front surface of the flat box on the front of the azimuth shaft assembly (when facing front).

B. DESCRIPTION OF EACH FIRING

Eight separate live-firings were designed, each with a different configuration of eight measurement accelerations, one for each SD390 channel. The primary test firings were designed to provide data on the input vibration at the pedestal feet and at the FLIR camera mount. These were the minimal firings required for this study. The secondary firings were designed to provide additional data to analyze the performance of the individual components of the stabilizer, if required. The objectives for each firing are discussed below.

1. Primary Firings

a. Firing One

The purpose of the first firing was to obtain the Z- and X-components of the input linear accelerations at the pedestal feet and the resulting azimuth and elevation angular accelerations of the FLIR camera mount. One single-axis (X) linear accelerometer was mounted at location one (top front foot). This accelerometer was employed for almost all firings as a reference. Triaxial accelerometers at the three pedestal feet measured the remaining Z- and X-components of input linear acceleration. Two angular accelerometers were mounted at locations eight and nine, on the FLIR camera mount ("rocky"), and measured its elevation and azimuth angular acceleration. The SD390 channel assignment, type of accelerometer, location number, and axis direction for acceleration data collected during the first firing are provided in Table 3.1.

b. Firing Two

The purpose of the second firing was to obtain the Y- and X-components of the input linear accelerations at the pedestal feet and the resulting azimuth and elevation angular accelerations of the FLIR camera mount. One single-axis (X) linear accelerometer (the reference) was mounted at location 1 (top front foot). Triaxial accelerometers at the three pedestal feet measured the remaining Y- and X-components of input linear acceleration. Two angular accelerometers, mounted at locations eight and nine on the FLIR camera mount ("rocky"), measured its elevation and azimuth angular acceleration. The SD390 channel assignment, type of accelerometer, location number, and axis direction for acceleration data collected during the second firing are provided in Table 3.1.

c. Firing Three

The purpose of the third firing was to accommodate Pilkington's request for vibration data on the FLIR camera housing. The reference accelerometer was employed on the top front pedestal foot (1X). Two triaxial accelerometers measured the X- and Y- components of linear acceleration at the rear and center of the top of the camera. From these measurements, elevation and azimuthal angular acceleration can be computed. The Z- component of linear acceleration was also measured at the center of the top of the camera, and the azimuthal and elevation angular acceleration of the FLIR camera mount were measured using angular accelerometers. The SD390 channel assignment, type of accelerometer, location number, and axis direction for acceleration data collected during the second firing are provided in Table 3.1.

d. Firing Four

The purpose of the fourth firing was to measure the vibration of the FLIR camera lens housing. The reference accelerometer was not employed during this test firing. Two triaxial accelerometers were mounted at locations twelve and thirteen on the lens housing outer rim and collected data in the X, Y, and Z axes. The SD390 channel assignment, type of accelerometer, location number, and axis direction for acceleration data collected during the fourth firing are provided in Table 3.1.

e. Firing Five

The purpose of the fifth firing was to measure the linear and angular acceleration of the elevation axis assembly. The reference accelerometer was employed on the top front pedestal foot (1X). Two angular accelerometers measured the elevation and azimuthal angular acceleration of the elevation axis assembly at positions 17 and 18. Angular accelerometers at positions eight and nine simultaneously measured azimuth and elevation angular acceleration of the FLIR camera mount. The triaxial accelerometer at location 19 simultaneously measured the linear component for all axes. The SD390 channel assignment, type of accelerometer, location number, and axis direction for acceleration data collected during the fifth firing are provided in Table 3.1.

	SD390 Channel assignment							
Firing	Accel type / location and axis direction							
	1	2	3	4	5	6	7	8
1	Uni / 1 X	Tri / 2 Z	Tri / 3 X	Tri / 3 Z	Tri / 4 X	Tri / 4 Z	TAP / 8 AZ	TAP / 9 EL
2	Uni / 1 X	Tri / 2 Y	Tri / 3 X	Tri / 3 Y	Tri / 4 X	Tri / 4 Y	TAP / 8 AZ	TAP / 9 EL
3	Uni / 1 X	Tri / 10 X	Tri / 10 Y	Tri / 11 X	Tri / 11 Y	Tri / 11 Z	TAP / 8 AZ	TAP / 9 EL
4	Tri / 12 X	Tri / 12 Y	Tri / 12 Z	Tri / 13 X	Tri / 13 Y	Tri / 13 Z	TAP / 8 AZ	TAP / 9 EL
5	Uni/ 1 X	Tri / 17 AZ	Tri / 18 EL	Tri / 19 X	Tri / 19 Y	Tri / 19 Z	TAP / 8 AZ	TAP / 9 EL

Table 3.1. The SD390 channel assignments, type of accelerometer, and location number including the axis direction for the primary firings.

2. Secondary Firings

a. Firing Six

The purpose of the sixth firing was to obtain the linear X- and Z-components of the input accelerations at the pedestal feet and the base assembly. The reference accelerometer was employed on the top front pedestal foot (1X). Triaxial accelerometers on the base assembly (locations 14, 15, 16) measured the X- and Z-components of linear acceleration of the base assembly. The SD390 channel assignment, type of accelerometer, location number, and axis direction for acceleration data collected during the sixth firing are provided in Table 3.2.

b. Firing Seven

The purpose of the seventh firing was to obtain the linear X- and Y-components of the input accelerations at two pedestal and base assembly locations. The reference accelerometer was employed on the top front pedestal foot (1X). Triaxial accelerometers on the base assembly (locations 14 and 15) measured the Y- and Z-components of linear acceleration of the base assembly .The SD390 channel assignment, type of accelerometer, location number, and axis direction for acceleration data collected during the seventh firing are provided in Table 3.2.

c. Firing Eight

The purpose of the eighth firing was to compare elevation and azimuthal angular acceleration measurements made with linear and angular accelerometers. Triaxial accelerometers were mounted at locations six and seven and collected linear acceleration data in the X-, Y-, and Z-directions. Angular accelerometers at positions eight and nine simultaneously measured azimuth and elevation angular acceleration. The SD390 channel assignment, type of accelerometer, location number, and axis direction for acceleration data collected during the eighth firing are provided in Table 3.2.

	SD390 Channel assignment							
Firing	Accel type / location and axis direction							
	1	2	3	4	5	6	7	8
6	Uni / 1 X	Uni/ 14 X	Uni/ 3 X	Tri / 15 X	Tri / 4 X	Tri / 16 X	TAP / 4 Z	TAP / 16 Z
7	Uni / 1 X	Uni/ 2 Y	Tri / 3 X	Tri / 3 Y	Tri / 14 X	Tri / 14 Y	TAP / 15 X	TAP / 15 Y
8	Uni / 6 X	Tri / 6 Y	Tri / 6 Z	Tri / 7 X	Tri / 7 Y	Tri / 7 Z	TAP / 8 AZ	TAP / 9 EL

Table 3.2. The SD390 channel assignments, type of accelerometer, and location number including the axis direction for the secondary firings.

IV. CALIBRATIONS

Several calibrations were conducted prior to the live test firings in the lab at NPS. The first was a calibration of the voltage gain magnitude for each channel of the SD390. The second was of the voltage gain magnitude and phase between channel one and the other channels of the SD390. The third was a system calibration of each accelerometer and its assigned SD390 channel as specified in the test plan. The fourth and fifth were comparisons of the angular acceleration calculated from the difference in the linear acceleration measured using two triaxial accelerometers and that measured using an angular accelerometer.

Two more calibrations were conducted after the live test firings. The first was to calibrate the triaxial accelerometers sensitivity magnitude and phase, and the second was a calibration of the reference uniaxial accelerometer. The equipment, procedures, and results of all the calibrations are described below.

A. ABSOLUTE CHANNEL AMPLITUDE CALIBRATION OF SCIENTIFIC ATLANTA SD390

1. Equipment

The SD390 channel voltage gains were calibrated using the voltage from a precise external signal generator, the HP3325B.

The HP3325B was set to output a 100 Hz sine wave at the same amplitude as the full scale setting of the SD390, namely 1, 5, or 10 Vp. The HP3325B is specified to produce a sine wave of frequency from 1 MHz to 100 kHz with an amplitude accuracy of ± 0.2 dB (2%), for output voltages up to 3 Vp-p and ±0.1 dB (1%) for output voltages

greater than 3 Vp-p.

A Kikusui DSS5020 Oscilloscope was used to verify the frequency and amplitude of the sine wave generated by the HP3325B. The DSS5020 has a sensitivity accuracy of ± 3% or better at 1 kHz at four to five divisions. The DSS5020 was used for a rough order of magnitude agreement of the HP3325B output.

2. Procedures

The calibrations were made using three different full scale voltage settings and two different sampling frequencies. The voltages were 1, 5, and 10 Vp and the sampling frequencies were 512 Hz and 25.6 kHz. The HP3325B function generator was allowed 30 minutes to warm up and then configured to produce a 100 Hz sine wave at the same voltage as the SD390 full scale setting. The DSS5020 was connected to the HP3325B. The sine wave's magnitude and frequency was confirmed with the DSS5020. Then the HP3325B was connected one at a time to each of the SD390's eight channels and the voltage reading of the channel recorded.

3. Results

The results of the HP3325B source referenced calibrations of each channel and voltage is listed in Tables 4-1. These results were used to correct the channel voltage of the SD390.

Channel number	1 Vp 512 Hz Fs	5 Vp 512 Hz Fs	10 Vp 512 Hz Fs	1 Vp 25.6 kHz Fs	5 Vp 25.6 kHz Fs	10 Vp 25.6 kHz Fs
1	0.9753	4.972	9.875	0.9431	4.753	9.449
2	0.9763	4.974	9.876	0.9409	4.747	9.430
3	0.9921	5.072	10.07	0.9550	4.789	9.509
4	0.9940	5.076	10.08	0.9579	4.807	9.553
5	0.9976	4.980	9.886	0.9482	4.776	9.486
6	0.9787	4.992	9.911	0.9498	4.811	9.560
7	0.9772	4.971	9.872	0.9414	4.786	9.512
8	0.9785	4.982	9.894	0.9555	4.758	9.456

Table 4.1 The SD390 channel voltage reading when each channel is set to 1, 5, or 10 Vp full scale voltage and a sampling frequency of 512 Hz or 25.6 kHz for a 100 Hz input signal with the same amplitude as the full scale setting.

B. RELATIVE CHANNEL AMPLITUDE AND PHASE BETWEEN CHANNELS OF SCIENTIFIC ATLANTA SD390

1. Equipment

The relative channel amplitude and phase between channel one and the other seven channels of SD390 was measured using the SD390 Signal Source Generator (SSG) as the source signal.

A Kikusui DSS5020 Oscilloscope was used to verify the frequency and amplitude of the sine wave generated by the SSG.

2. Procedures

The SD390 SSG was set to deliver a 100 Hz, 300 mVp, 1Vp, or 5 Vp sine wave. This was connected to channels one to eight. The transfer function magnitude and phase was recorded relative to channel one. The sampling frequency was 512 Hz.

3. Results

The results of the observed magnitude and phase relative to channel one for each channel and sine wave voltage are listed in Table 4-2.

	300 mVp		1 Vp		5 Vp	
Channel number	magnitude (V)	phase (deg)	magnitude (V)	phase (deg)	magnitude (V)	phase (deg)
1	Ref	Ref	Ref	Ref	Ref	Ref
2	1.003	360	1.006	360	1.001	360
3	1.023	360	1.002	360	1.021	360
4	1.020	360	1.023	360	1.020	360
5	1.008	360	1.009	360	1.005	360
6	1.006	360	1.008	360	1.005	.052
7	1.004	360	1.007	360	1.001	360
8	1.007	0.011	1.009	0.56	1.004	360

Table 4.2 The transfer function magnitude and phase between channel one and each SD390 channels with a 300 mVp, 1 and 5 Vp sine waves and full scale settings and a sampling frequency of 512 Hz.

C. LINEAR ACCELEROMETER CALIBRATION

1. Equipment

The acceleration source was a Bruel & Kjaer type 4810 mini-shaker, which is designed for dynamic testing of small objects and calibration of accelerometers at frequencies from DC to 18 kHz. During the calibration of the accelerometers, the shaker was limited by current and weight of the accelerometer to a maximum acceleration of about 1.2 g's.

The mini-shaker was driven by a Hewlett-Packard Model 467A Power Supply/Amplifier set up as a X1 amplifier. The HP467A is rated to provide up to 10 V and 1 Amp peak from D.C. to 1 MHz.

The calibration reference accelerometer was a Bruel and Kjaer NIST-traceable reference accelerometer type 8305S, SN 1864983, which had been factory calibrated in February 1996 by laser interferometer. The calibration reference accelerometer frequency response is within 0.5% from DC to 2 kHz , depending on the supporting mass. The charge sensitivity of this accelerometer is 0.1261 pC/g or 0.1286 pC/ m/s^2.

A Kistler 5010B Dual Mode Charge Amplifier was used to convert the B&K 8305S output from pC into Volts. The 5010B was set for 0.126 pC/MU (measurement unit) and 10 V/MU. The maximum output voltage magnitude of the 5010B is 10 V.

After processing by the Kistler 5010B, the voltage of the calibration reference accelerometer was measured and displayed by a Stanford Research Systems SR530 lock-in amplifier. The lock-in amplifier's reference voltage input was connected to the SD390 signal generator output and the SR530's channel A input to the Kistler 5010B output. The maximum input voltage of the SR530 is 500 mVrms. Therefore, the maximum g's available for calibrations was about 0.6 to 1.2 g's (depending on current and weight).

The triaxial linear accelerometers calibrated were three PCB Model 354B33. These were stud-mounted to the top of the reference accelerometer for measurements in the (accelerometers) Z axis direction and were mounted to a right-angle fixture as shown in Figure 4-1 for X- and Y- axis measurements. The frequency response of the accelerometers (± 5 %) is 1 Hz to 2 kHz. The actual accelerometers used were model

354B33 SN 453, 454 and 455. The required external 4 mA constant current source was provided by the SD390 analyzer.

The uniaxial linear accelerometers calibrated were PCB Model J353B04 SN's 11849, 11850, and 11851. The frequency response of the accelerometers (± 5 %) is 1 Hz to 7 kHz. The J indicates that the accelerometer is electrically isolated. The required external 4 mA constant current source was provided by the SD390 analyzer.

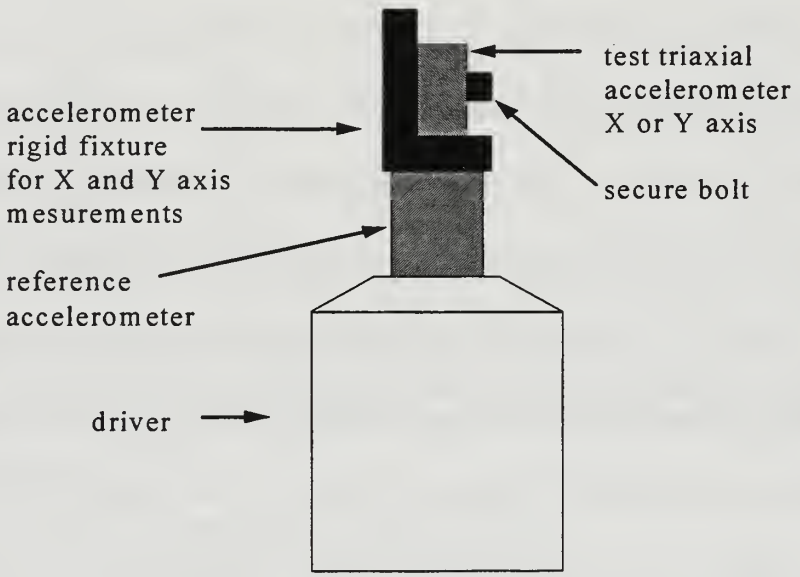

Figure 4.1. Mounting of the calibration reference and triaxial accelerometers on a fixture for measurements in the triaxials's X- and Y- axis direction.

2. Procedures

Two linear accelerometers calibrations experiments were performed. For both the SD390's Signal Source Generator (SSG) provided a 100 Hz, 300 mV sine wave input for the mini-shaker.

For the first calibration experiment, each accelerometer was connected to the SD390 in their assigned channel as described in Chapter III. The output voltage measured by each channel was recorded in volts peak (Vp). This was corrected for each channel's gain (Table 4.1) and converted into gp for comparison to the calibration reference accelerometer. The output voltage of the calibration reference accelerometer was read from the lock-in amplifier in Vrms and converted into Vp. From the Kistler 5010B settings, the Vp equals gp. This procedure was performed for each of the eight live-fire test accelerometer and SD390 channel configurations.

For the second calibration experiment, the output of each accelerometers was measured using channel one of the SD390. Each accelerometer was stud-mounted on the reference accelerometer, one at a time, and the voltage outputs of the test accelerometer and of the reference accelerometer were read from the SD390 and from the lock-in amplifier, respectively.

3. Results

The results of the first calibration are tabulated in Tables 4.3 through 4.10, each table corresponds to one live-fire test configuration. The results of the second calibration experiment are listed in Table 4.11.

CH #	Name	SER #	Calibration reference accelerometer (gp)	Accelerometer (gp)	Difference (%)
1	A	11849	0.6385	0.6500	+2
2	B	454	0.4116	.40590	-1
3	C	5968	0.6540	0.6649	+2
4	D	453	0.4078	0.4076	-0.1
5	E	5969	0.6543	0.6472	-1
6	F	455	0.4060	0.4045	-0.3

Table 4.3. Voltage and g's for the reference accelerometer and test firing one's assigned accelerometers input into their assigned channel and percentage difference between the measurements

CH #	Name	SER #	Calibration reference accelerometer (gp)	Accelerometer (gp)	Difference (%)
1	A	11849	0.6427	0.6436	+0.2
2	B	454	0.4173	0.4159	-0.3
3	C	5968	0.6453	0.6514	-0.9
4	D	453	0.4184	.41740	-0.2
5	E	5969	0.6492	0.6466	-0.2
6	F	455	0 .4182	0 .4179	-0.05

Table 4.4. Voltage and g's for the reference accelerometer and test firing two's assigned accelerometers input into their assigned channel and percentage difference between the measurements.

CH #	Name	SER #	Calibration reference accelerometer (gp)	Accelerometer (gp)	Difference (%)
1	A	11849	0.6507	0.6622	+1
2	B	454	0.4186	0.4124	-0.6
3	C	454	0.5812	0.5918	+2
4	D	453	0.4141	0.4139	-0.05
5	E	453	0.5773	0.5813	+0.7
6	F	453	0 .4169	0 .4131	-0.9

Table 4.5. Voltage and g's for the reference accelerometer and test firing three's assigned accelerometers input into their assigned channel and percentage difference between the measurements

CH #	Name	SER #	Calibration reference accelerometer (gp)	Accelerometer (gp)	Difference (%)
1	B	454	0.4065	0.3980	-2
2	B	454	0.5781	0.5829	+0.8
3	B	454	0.4182	0.4189	+0.07
4	D	453	0.5827	0.5894	+1
5	D	453	0.4165	0.4155	-0.2
6	D	453	0 .4082	0 .4039	- 1

Table 4.6. Voltage and g's for the reference accelerometer and test firing four's assigned accelerometers input into their assigned channel and percentage difference between the measurements.

CH #	Name	SER #	Calibration reference accelerometer (gp)	Accelerometer (gp)	Difference (%)
1	A	11849	0.6479	0.6605	+2
4	B	454	0.4141	0.4139	-0.04
5	B	454	0.4138	0.4076	-2
6	B	454	0 .5734	0 .5776	+0.7

Table 4.7. Voltage and g's for the reference accelerometer and test firing five's assigned accelerometers input into their assigned channel and percentage difference between the measurements.

CH #	Name	SER #	Calibration reference accelerometer (gp)	Accelerometer (gp)	Difference (%)
1	A	11849	0.6455	0.6586	+2
2	C	11850	0.6509	0.6639	+2
3	E	11851	0.6457	0.6586	+2
4	D	453	0.5778	0.5870	+2
5	B	454	0.5727	0.5778	+0.9
6	F	455	0.5721	0.5771	+0.8
7	B	454	0.4187	0.4119	-2
8	F	455	0 .4188	0 .4168	-0.4

Table 4.8. Voltage and g's for the reference accelerometer and test firing six's assigned accelerometers input into their assigned channel and percentage difference between the measurements.

CH #	Name	SER #	Calibration reference accelerometer (gp)	Accelerometer (gp)	Difference (%)
1	A	11849	0.6731	0.6865	+2
3	D	11851	0.5653	0.5822	+3
4	D	453	0.4125	0.4117	-0.1
5	B	454	0.5785	0.5841	+0.9
6	B	454	0.4126	0.4119	-0.1
7	F	455	0.5786	0.5832	+0.7
8	F	455	0 .4188	0 .4189	-0.01

Table 4.9. Voltage and g's for the reference accelerometer and test firing seven's assigned accelerometers input into their assigned channel and percentage difference between the measurements.

CH #	Name	SER #	Calibration reference accelerometer (gp)	Accelerometer (gp)	Difference (%)
1	D	453	0.3483	0.3470	-0.3
2	D	453	0.3500	0.3465	-1
3	D	453	0.4904	0.4940	+0.7
4	F	455	0.3415	0.3395	-0.5
5	F	455	0.3411	0.3422	+0.3
6	F	455	0 .4806	0 .4845	+0.8

Table 4.10. Voltage and g's for the reference accelerometer and test firing eight's assigned accelerometers input into their assigned channel and percentage difference between the measurements

SD390 channel number	Accel model number	Accel SN	Test accel axis	Cal ref accel (gp)	Test accel (gp)	Difference %
1	354B33	453	X Y Z	0.3591 0.3545 0.4986	0.3559 0.3515 0.4989	-0.8 -0.8 +0.06
1	354B33	454	X Y Z	0.3510 0.3521 0.4890	0.3478 0.3485 0.4919	-0.6 -0.9 +1
1	354B33	455	X Y Z	0.3521 0.3518 0.4887	0.3495 0.3517 0.4924	-0.7 -0.01 +0.7
1	J353B04	11849	n/a	0.5402	0.5697	+5
1	J353B04	11850	n/a	0.5416	0.5727	+6
1	J353B04	11851	n/a	0.5398	0.5716	+6

Table 4.11. Calibration reference and test accelerometer gp and the percent difference.

D. THE FIRST COMPARISON OF ANGULAR AND LINEAR ACCELEROMETERS MEASURING ANGULAR ACCELERATION

1. Equipment

A jig was manufactured at NPS to create an angular acceleration source to compare the angular acceleration extracted from measurements of linear acceleration to that measured by an angular accelerometer. The jig consisted of a solid ⅝-inch square aluminum bar attached to a thin flexible strip of metal on one side and a single axis linear shaker on the other side, as shown in Figure 4.2. Earlier designs utilized ball bearings at the pivot and drive point, but proved to have too much play to be usable for accurate measurements. The bar was only free to rotate about the thin metal hinged (horizontal) axis during the test. At the center of the bar, a TAP system angular accelerometer was

mounted with Petro wax. At equal distances from the center of the bar, 10-32 holes were tapped for mounting triaxial accelerometers. Triaxial accelerometers were to be used to extract angular acceleration during the live fire test; therefore, they were used for this calibration.

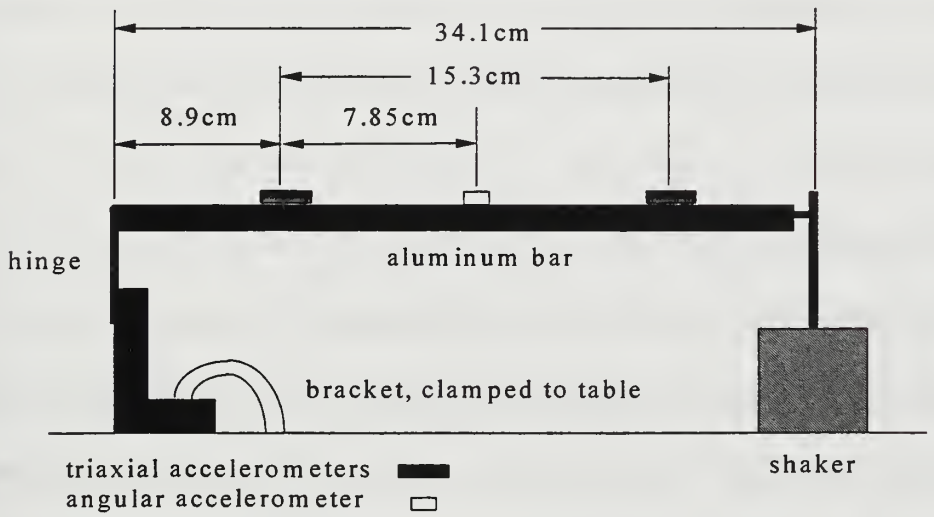

Figure 4.2. The jig manufactured at NPS and the relative locations of the accelerometers during the first angular comparison test.

The shaker was a Bruel & Kjaer type 4810 mini-shaker designed for dynamic testing and calibration of accelerometers and small objects. The shaker was connected to the bar by a 10-32 threaded steel rod screwed into the shaker and into a threaded pin at the end of the bar opposite to the hinged side.

The angular accelerometer used in this comparison is a Kistler Model 8832 Translational-Angular PiezoBEAM (TAP) accelerometer System. The TAP system is composed of a Model 8696 accelerometer and a Model 5130 signal coupler. The actual

system used was accelerometer model 8696 SN C103694 and coupler model 5130 SN C40185. The angular sensitivity was factory-calibrated to an NIST-traceable source at 250 Hz and 130 rad/s^2 to be 0.480 mV/rad/s^2; the linear sensitivity was calibrated at 100 Hz 3 g rms to be 1009 mV/g.

Two PCB Model 354B33 triaxial linear accelerometers were stud mounted to the two tapped holes. The actual accelerometers used were model 354B33 SN 454 and 455. The linear sensitivity was calibrated at 103.2 and 103.0 mV/g for SN 454 and 455, respectively, at 100 Hz.

2. Procedures

The Scientific Atlanta Model SD390 Signal Analyzer was used to drive the shaker through a HP467A power amplifier to collect the data. The accelerometers were mounted as shown in Figure 3-2 and connected to the SD390. The TAP system angular and linear outputs were connected to SD390 channels one and two, respectively. The angular signal gain amplifier on the Kistler 5130 coupler for the TAP system was set to 1x (no amplification). The linear accelerometers were connected to SD390 channels four and five for accelerometers 454 and 455, respectively. The SD390 signal generator provided a 100 Hz sine wave at 300 mV to the power amplifier, which voltage gain was set to one. The sampling frequency was 512 Hz.

3. Results

Angular acceleration (α) from two linear accelerometers is calculated from the difference between their linear acceleration in m/s^2 (Δa) divided by the distance between them in meters (Δx):

$$\alpha = \Delta a / \Delta x \qquad 4.1$$

The distance between the two linear accelerometers was 0.153 m.

The test was conducted for sixteen different magnitudes of linear and angular acceleration. The driver frequency was a constant 100 Hz sine wave for each test. However, the linear amplitude of the driver was successively increased for each successive test, which increased the angular and linear acceleration of the bar. The shaker was driven so that its acceleration amplitude ranged from a minimum of 0.01 g's of linear and 7 rad/s^2 of angular acceleration to a maximum of 1.1 g's of linear and 60 rad/s^2 of angular acceleration. After correcting for SD390 channel voltage, the difference between the two measures of angular acceleration ranged from 3.0 to 4.4 percent. The angular acceleration extracted from linear accelerations is consistently greater than that measured by the angular accelerometer by an average of 3.70%. The results of the comparison are shown in Table 4.12.

TEST #	Linear g measured by TAP System (gp)	Angular Acceleration from TAP System (rad/s^2)	Angular Acceleration from Linear Accelerometers (rad/s^2)	Difference between angular and linear conversion (%)
1	0.014	7.84	8.14	3.8
2	0.094	6.97	7.24	3.8
3	0.103	7.71	8.05	4.4
4	0.134	8.43	8.75	3.9
5	0.124	9.16	9.53	4.0
6	0.164	12.1	12.5	3.7
7	0.203	15.2	15.8	4.3
8	0.244	18.1	18.7	3.5
9	0.282	21.0	21.8	3.9
10	0.323	23.9	24.6	3.2
11	0.845	44.8	46.4	3.7
12	0 .901	47.5	49.0	3.1
13	0.959	50.6	52.2	3.1
14	1.01	53.5	55.1	3.0
15	1.06	56.4	58.1	3.1
16	1.11	59.4	61.5	3.5

Table 4.12. Angular and converted linear to angular accelerations in rad/s^2 and percentage difference for sixteen different linear acceleration on a bar.

E. THE SECOND COMPARISON OF ANGULAR AND LINEAR ACCELEROMETERS MEASURING ANGULAR ACCELERATION

1. Equipment

For a second comparison of angular acceleration from linear and angular acceleration measurements, the original jig was modified as shown in Figure 4.3. On the bottom side of the jig, two 10-32 flexible steel rods connected the bar to two APS shaker tables [APS, 1984, p. 1]. This enabled each end of the jig to be independently driven. As before, at the center of the bar, a TAP system angular accelerometer was mounted. However, this time the TAP accelerometer was mounted with super glue as it would be for the live-fire tests. Two linear triaxial accelerometers were mounted at equal distances from the center of the bar.

The shakers were two Acoustic Power Systems Inc (APS) model 120S, SN's 035 and 036. Each shaker was connected to an APS model 114 amplifier which received a signal from a separate signal generator. In the 0 to 2000 Hz frequency range, the APS model 120 can produce a maximum of 50 lbs (222 N) of force with a weight load of 25 lbs (11 kg) and a maximum stroke of 0.2 inches (0.51 cm).
The signal generators were two Hewlett-Packard Model HP33120A, SN's 34000183 and 34003130.

2. Procedures

The two HP signal generators were set to generate a 75, 150, 225, 300, 375, or 450 Hz sine wave. The signal generators were not synchronized. However, both signal

generators were set to the same frequency and magnitude for each test. The accelerometers were mounted as shown in Figure 3-3 and connected to the SD390. The TAP system for angular and linear outputs were connected to SD390 channels one, respectively. The linear accelerometers were connected to SD390 channels four and five

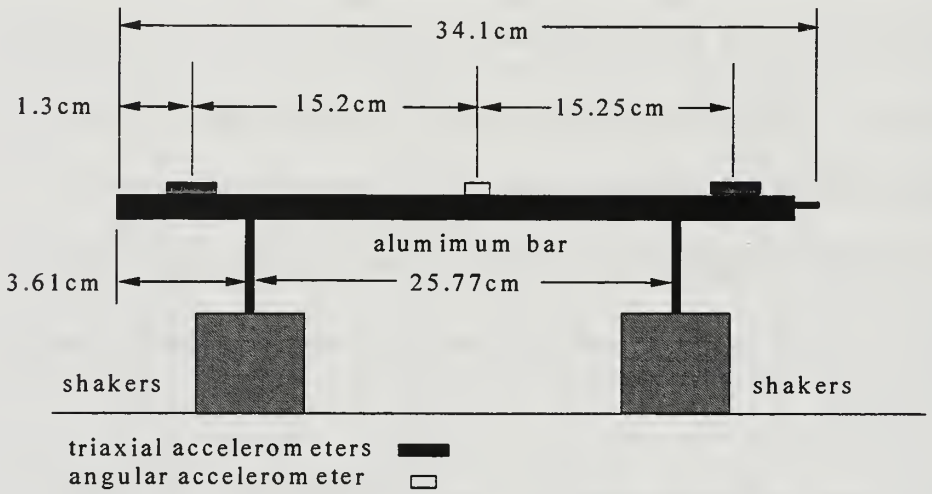

Figure 4.3. The modified jig and the relative locations of the accelerometers during the second angular comparison test

for accelerometers 454 and 455, respectively. Each test was conducted at the maximum amplitude the shaker systems would accept for the frequency of the test.

3. Results

As before, Equation 3.1 was used to convert linear acceleration to angular acceleration. For the second angular acceleration comparison test, the distance between the two linear accelerometers was 0.3036 m.

The test was conducted for eight different frequencies and magnitudes of linear and angular acceleration. The results are shown in Table 4.13. The amplitude of linear

and angular acceleration of the bar ranged from a minimum of 1.9 m/s^2 and 39 rad/s^2 to a maximum of 8.7 m/s^2 and 240 rad/s^2 respectively. The difference between the two measurements of angular acceleration range from -3.9 to +5.4 percent. Unlike the first test, here the angular acceleration extracted from linear accelerations is not consistently greater than that measured using the TAP System. In this test, angular acceleration calculated from linear acceleration is greater than that measured by the angular accelerometer by an average of 2%. From the results of both comparisons, one can expect the angular acceleration calculated from linear acceleration is within 4% of that measured by a TAP system accelerometer.

Frequency (Hz)	75	100	150	225	300	375	450
Percentage difference between angular accel measurements from linear accelerometers to the TAP system. (%)	+4.0	-3.9	+2.6	+4.3	+3.6	+5.4	-2.9
Maximum magnitude of linear acceleration at the TAP accelerometer. (m/s^2)	1.3	6.5	8.7	2.3	1.9	3.1	7.6
Maximum angular acceleration of TAP system during test. (rad/s^2)	227	451	222	93	124	31	68
Maximum angular acceleration calculated from liner acceleration during test. (rad/s^2)	237	437	240	97	127	33	39

Table 4.13. The results of the second angular acceleration comparison test showing the percentage difference between angular acceleration measurements from linear accelerometers to the TAP system, the maximum magnitude of linear acceleration at the TAP accelerometer, the maximum angular acceleration of TAP system, and the maximum angular acceleration calculated from liner acceleration for the seven tested frequencies.

F. MAGNITUDE AND PHASE CALIBRATIONS OF THE TRIAXIAL ACCELEROMETERS

After the live fire tests, a calibration of the triaxial accelerometers for voltage sensitivity magnitude and phase was conducted. Before the tests began, the manufacturer of the accelerometers was consulted regarding the phase calibrations of the accelerometers. The sensitivity calibration provided with the accelerometers provides magnitude, but no phase information. An applications engineer at PCB reported the phase of the sensitivity is less than one-half degree in the 20 to 2000 Hz band in each axis, and that the calibration should not have changed since the manufacturer's calibration of February 6, 1996.

1. Equipment

With one exception, the equipment and set-up used for this experiment was identical to the first accelerometer calibration test described in section B. For this experiment a HP4192 impedance analyzer was used to validate the phase in the same manner that the SR530 lock-in amplifier was used in section B. The HP4192A analyzer was used here because it is more accurate then the SR530 (See section II.B.4 and II.B.5).

2. Procedures

The procedures followed were the same as described above in section B with the exception of using the HP4192 instead of the SR530.

3. Results

The results of the calibration showed that the sensitivity phase of the triaxial accelerometers was less than one-half degree, as stated by the applications engineer, and

the magnitude was extremely close to the manufacturer's calibration. From this result, and due to the recent manufacturer's calibration, the presumably more accurate manufacture's sensitivity calibration was used for the analysis of the test data. A MATLAB program was written to linearly interpolate the magnitude of the sensitivity provided by the manufacturer for frequencies between 20 and 2000 Hz. The phase of the sensitivity was taken to be zero.

G. CALIBRATION OF THE REFERENCE ACCELEROMETER

1. Equipment

With one exception, the equipment and set-up was identical to the first accelerometer calibration test described in section B. For this experiment, a HP4192 impedance analyzer was used in the same manner that the SR530 lock-in amplifier was used in section B.

2. Procedures

The procedures followed were the same as described above in section B, with the exception of the HP4192 instead of the SR530.

3. Results

The results of the calibration showed that the sensitivity of the reference accelerometer differed slightly from the manufacturers calibration of 9.7 mV/g. The results of our calibration are shown in Table 4.14. These calibration data were used in the analysis of the test data. A MATLAB program was written to linearly interpolate the sensitivity magnitude for all frequencies between 20 and 2000 Hz. The phase of the sensitivity was taken to be zero.

Frequency (Hz)	Calibration magnitude (mV/g)	Calibration phase (degrees)	Frequency (Hz)	Calibration magnitude (mV/g)	Calibration phase (degrees)
10	10.68	1.21	300	10.34	0.620
15	10.15	1.15	500	10.30	0.877
30	10.35	0.748	1000	10.32	1.00
50	10.22	0.484	2000	10.42	1.09
100	10.27	0.333			

Table 4.14. The magnitude and phase calibration results for the uniaxial reference accelerometers SN 11849.

V. RESULTS OF THE LIVE-FIRE TESTS

The first four live-fire tests were conducted on July 30, 1996. Test firings five through eight were conducted on August 1, 1996. The test firings were conducted on two days due to mechanical problems with the PHALANX gun.

Two short-burst firings were conducted before the actual test firings on July 30. The two short-bursts comprised approximately 90 rounds and were used to determine the correct full-scale voltage settings for the SD390 input channels. Most of the data from the two short-burst firings exceeded the full-scale settings of the SD390, and none of these data were used in later analyses.

After completing the planned eight test firings, several additional firings were conducted by HMSC to support other evaluations of the PSUM. Acceleration data were collected during some of these additional firings, examined, and used in later analyses.

The data collected during each test firing by the SD390 were saved as Extended Record Memory (XRC) Files on the SD390 internal (DOS) hard disk and on an external disk immediately after collection. The external disk was hand-carried back to NPS and the XRC files were converted into MATLAB-readable (.MAT) files using a Scientific Atlanta conversion program. The .MAT file for each test contains a 184320 x 8 matrix of data. Each column of the matrix corresponds to the voltages recorded from the same numbered channel of the SD390 for a single test firing. A MATLAB code to analyze the data was written and executed as described below.

A. DATA ORGANIZATION BY FILE NAME

The data files have been renamed to simplify identification of their origin. The file name identifies the test firing and the configuration of the SD390 by the simple system described below. Each data file begins with the abbreviation "cf" for "configuration ", then the test fire plan number (1-8), underscore, then the data series number (1-3), underscore, then the approximate time duration the gun was fired, in seconds (1, 3, or 5). As an example, for the file named "cf1_1_5s.mat", the .mat represents a MATLAB readable data file containing a 184320x8 matrix, the cf1 represents that the eight matrix data columns represent the first test firing configuration, the _1 represents that this is the first time this data was collected in this configuration, and the _5s represents that the firing lasted for approximately 5 seconds.

The one-second test firings are the two approximately 100-round bursts conducted on July 30 conducted to adjust the full scale settings on the SD390, mentioned previously. The three-second firings are the approximately 250-round obscuration test-firings conducted during the afternoon of August 1. The five-second firings are the approximately 410-round jitter test-firings that occurred on July 30 and August 1, 1996.

Two “baseline” recordings were made of the accelerations on the stabilizer without the gun firing. The data file for the first one is labeled cf0_ 0_bl and consists of 7.2 seconds of accelerations recorded with all PHALANX systems were turned off. The location of accelerometers and channel assignments are detailed in Appendix H. The second baseline data file is labeled cf5_0_bl. These data were recorded before the fifth test firing, with the PHALANX electronics operating, waiting for the countdown to

begin the fifth test firing. The location of accelerometers and channel assignments are detailed in the test plan in Appendix H.

B. TEST FIRE CONFIGURATION MATRICES

The tables in Appendix H list the configuration of the accelerometers and the SD390 channel assignments for each baseline data acquisition and live-fire test conducted. The tables follow the approved test plan and specify the SD390 channels, accelerometers, manufacturer's calibrations, and the polarity of the accelerometer axis with respect to the corresponding test coordinate axis for each firing. These matrices were strictly followed during data collection.

The test configuration tables are broken into ten columns. The first column is the letter name assigned (by us) to each accelerometer. The next three columns identify the manufacturer, model, and serial number of the accelerometer. For triaxial and angular accelerometers, the fourth column gives the cable exit direction in the test coordinate axes. For triaxial accelerometers, the sixth column identifies which accelerometer axis corresponds to which test axis. For uniaxial accelerometers, this column also identifies when the polarity of the accelerometer measurement axis with respect to the test axis is negative. The seventh column identifies the SD390 channel assigned to the accelerometer. The eighth column identifies the full scale voltage assigned to the channel. The ninth column is the test location by numbered position on the stabilizer (as per the test plan) and also gives the data collection axis in the test coordinate axes. The tenth column lists the manufacturers calibration factor for the accelerometer at 100 Hz.

C. REVIEW OF THE TEST-FIRE TIME RECORD DATA

After each test-firing, the time record of each SD390 channel was given a cursory review to verify the integrity of the data. Figures 5.1 and 5.2 are representative of the time records acquired for each live-firing and show the relative amplitude of the signal and the noise. Figures 5.1 and 5.2 could only be plotted using one out of every 500 points (51.2 Hz sampling rate) due to the limitations of the word processor used. Nevertheless, it can be seen the signal-to-noise ratio of the data is very good.

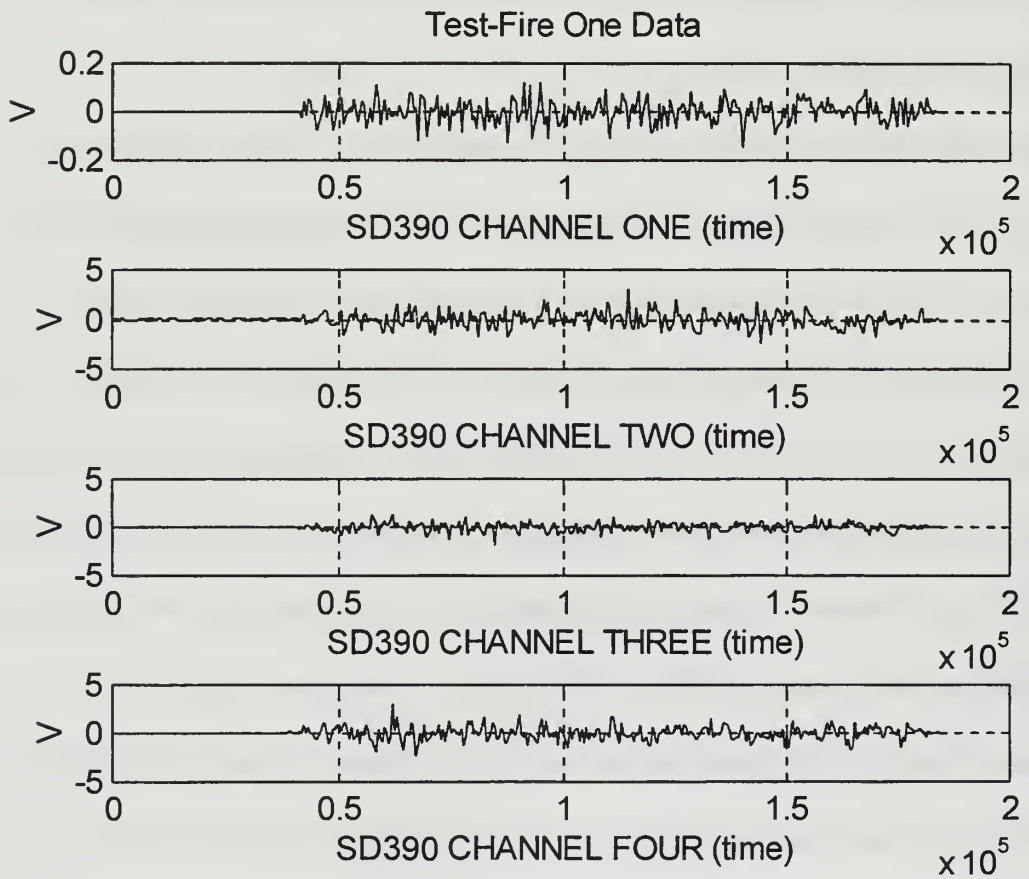

Figure 5.1. The 7.2 seconds (184320 points) of raw data as saved by the SD390 from test-fire one (cf_1_5s) in volts for channels one through four.

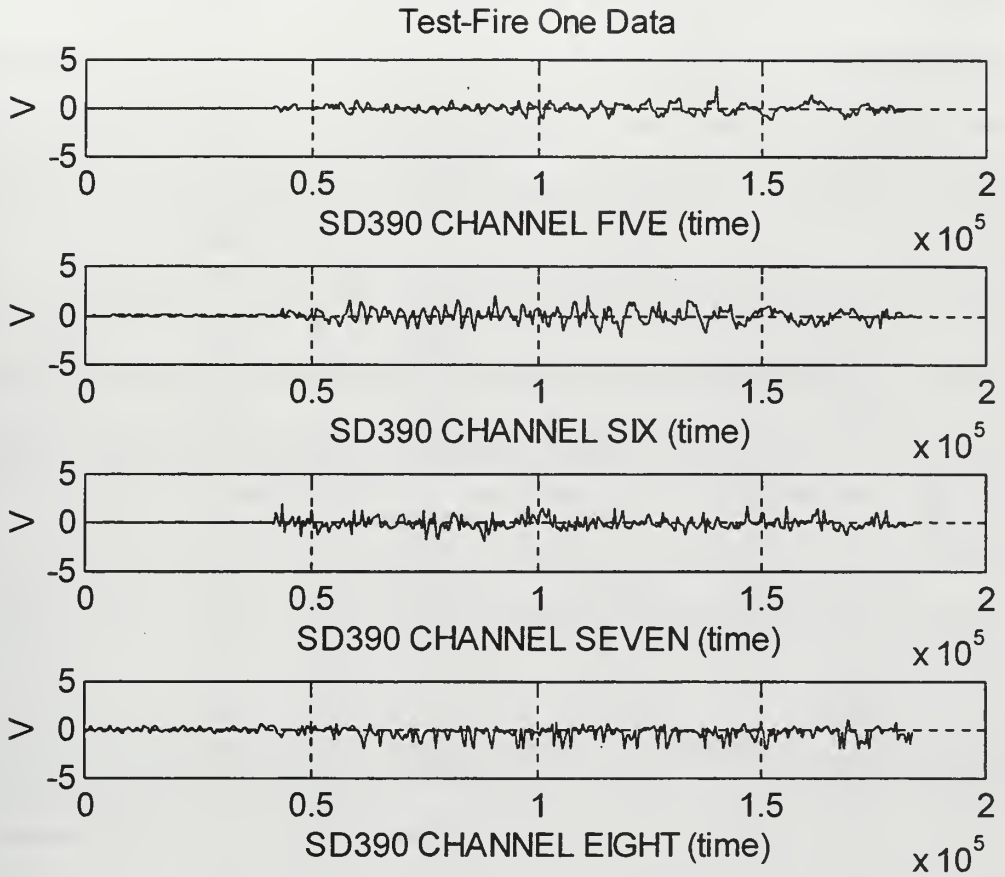

Figure 5.2. The 7.2 seconds (184320 points) of raw data as saved by the SD390 from test-fire one (cf_1_5s) in volts for channels five through eight.

D. LINEAR ACCELEROMETER BASELINE ACCELERATION

A " baseline" measurement of accelerations with the PHALANX CWIS ready to fire was made for each firing by examining the 1.2 seconds of data before the first round was fired. These data represent the sum of all electrical and mechanical noise present before the gun is fired. The observed baseline accelerations ranged from 0.0908 to 0.6063 g rms in a 20 to 2000 Hz band, with an average value of 0.2209 g rms. The baseline acceleration for each accelerometer by location number and test axis direction is

show in Table 5.1. The power spectral density plots below include a plot of the 1.2 second pre-firing data.

Accel location and axis direction	Baseline (g rms)		Accel location and axis direction	Baseline (g rms)		Accel location and axis direction	Baseline (g rms)
1 X	0.113		7 X	0.165		13 Y	0.146
2 Y	0.186		7 Y	0.116		13 Z	0.172
2 Z	0.239		7 Z	0.118		14 X	0.396
3 X	0.114		10 X	0.179		14 Y	0.342
3 Y	0.162		10 Y	0.165		15 X	0.412
3 Z	0.250		11 X	0.091		15 Y	0.403
4 X	0.096		11 Y	0.113		16 X	0.606
4 Y	0.255		11 Z	0.090		19 X	0.343
4 Z	0.190		12 X	0.134		19 Y	0.336
6 X	0.313		12 Y	0.181		19 Z	0.270
6 Y	0.273		12 Z	0.137			
6 Z	0.288		13 X	0.109			

Table 5.1. The baseline acceleration measured for each accelerometer location by location number and axis direction, from 20 to 2000 Hz . Data are from 1.2 seconds prior to firing the five-second long test firings.

E. POWER SPECTRAL DENSITY (PSD) AND G'S RMS FOR LINEAR ACCELEROMETERS

The estimated (one-sided) power spectral density (PSD), or autospectrum, $G_{xx}(f)$, is given by Bendat and Piersol (Bendat and Piersol, 1993, p.71) by

$$G_{xx}(f) = \frac{2}{T\, n_d} \sum_{i=1}^{n_d} | X_i(f, T) |^2 , \qquad 5.1$$

where n_d is the number of disjoint (independent) time records of length T and $X_i(f,T)$ is the finite Fourier transform of the i_{th} record (Bendat and Piersol, 1993, p.54),

$$X_i(f, T) = \int_0^T x_i(t)\, e^{-j2\pi f t}\, dt. \qquad 5.2$$

For a periodically-sampled signal, $X_i(f,T)$ is related to the N-point discrete Fourier transform (DFT), $X_i(f)$, computed, for example, using MATLAB, by

$$X_i(f_k, T) = T\, X_i(f_k)\ ;\ f_k = k f_1 = \frac{k}{T} = \frac{k f_s}{N}\ ;\quad k = 0, 1, \ldots, N-1, \qquad 5.3$$

where $f_1 = 1/T$ is the discrete frequency spacing, f_s is the sampling frequency, and N is the number of samples in one time record.

It is convenient to introduce the one-sided, normalized DFT, which we designate $Pn(f_k)$, and is given by (MATLAB Signal Processing Toolbox Math Works, 1994, p. 2-92)

$$Pn(f_k) = \frac{2\, X(f_k)}{N}\ ;\quad k = 0, 1, \ldots, \frac{N-1}{2}. \qquad 5.4$$

Normalized this way, a single sine wave of unit amplitude and frequency f_k will result in a value of $|\, Pn(f_k)\,|$ of unity. In terms of the one-sided DFT, the estimated PSD is given by

$$G_{xx}(f_k) = \frac{T}{2}\frac{1}{n_b}\sum_{i=1}^{n_b} |\, Pn_i(f_k)\,|^2 \qquad 5.5$$

Using equation 5.5, a MATLAB M-file was written to calculate the PSD for each linear accelerometer data record. A sample MATLAB code is provided in Appendix I. The MATLAB code calculated the acceleration PSD and g's rms by first applying a correction for the SD390 channel voltage gain and then converting the recorded channel voltages into g's using linearly interpolated sensitivities (calibration "constants") between 20 and 2000 Hz.

A 5.12-second block of data from the middle of the firing was extracted from each 7.2-second time record. A 5.12 second block of samples, at the sampling frequency rate of 25.6 kHz, consists of 131072 (2^{17}) data. Larger and smaller blocks of points were examined, but some of them included non-firing, ramp-up, or ramp-down portions of the time record, and gave the same results as the 5.12-second time block. For the 3-second test firings, a 2.56-second time window was used centered on the firing portion of the record.

1. Frequency Resolution of the DFT

The 5.12-second (2^{17} points) time record block was divided into eight 0.64-second (2^{14} points) time record sub-blocks, and the one-sided DFT for each sub-block was calculated, as described above. The frequency resolution of each one-sided DFT is 1.56 Hz ($1/T$). This is also the frequency resolution of the resulting PSD.

2. The Hanning Window Correction Factor

A Hanning window was applied to the time records before the DFT's were computed to reduce the "leakage"(Bendat and Piersol, 1993, p. 74). However, application of the Hanning window results in some energy loss. This requires the application of a Hanning window correction factor to the DFT for the lost energy. The proper method to correct for the Hanning window, as calculated by Bendat and Piersol, is to multiply the DFT values by the square root of 8/3 (Bendat and Piersol, 1993, p.76).

F. INPUT ACCELERATION AT THE PEDESTAL MOUNTS

The input acceleration at each pedestal mount in the three test axis directions was computed with the MATLAB code described above. The results in the 20 to 2000 Hz frequency band show that the input acceleration across the gun bore sight, in the X- and Y- axis directions, is about five g rms at each of the three pedestal mounts. This is about what was expected for the cross-bore-sight input. The input acceleration in the bore-sight axis (Z) direction was higher than expected, about 6.5 g rms. Although higher than expected, bore-sight jitter is not significant for the operation of the FLIR camera. Table 5.1 shows the input acceleration in g rms from 20 to 2000 Hz at each pedestal mount. The rms acceleration over all frequencies computed from either the time record or the PSD is about 1 g rms, or about 20%, higher than that in the 20 to 2000 Hz frequency band. Figures 5.3 through 5.14 show the firing and the baseline acceleration PSDs at each pedestal mount.

Location description and test plan location number	X accel (g rms)	Y accel (g rms)	Z accel (g rms)	accel magnitude in all axes (g rms)
Pedestal mount, #1 (forward, upper mount)	4.09	7.26	7.44	11.1
Pedestal mount, #2 (forward, lower mount)	3.78	6.62	6.12	9.77
Pedestal mount, #3 (rear mount)	4.23	6.55	6.90	10.4

Table 5.2. The input acceleration from 20 tp 2000 Hz at the pedestal mounts in the X-, Y-, Z-directions, and the magnitude in all directions from test-firing one (cf1_1_5s) and two (cf2_1_5s) data.

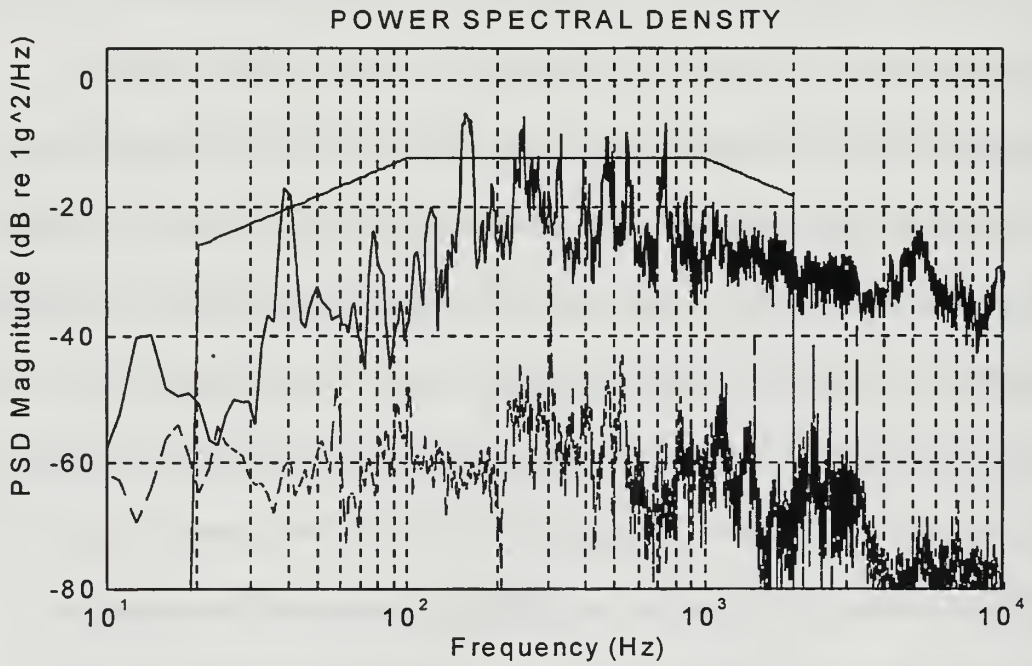

Figure 5.3. Plot of the PSD (solid line), pre-firing noise (dashed line), and specification for location one in the X-direction; from test firing one (cf1_1_5s) data. The acceleration in the 20 to 2000 Hz frequency band is 4.0871 g rms.

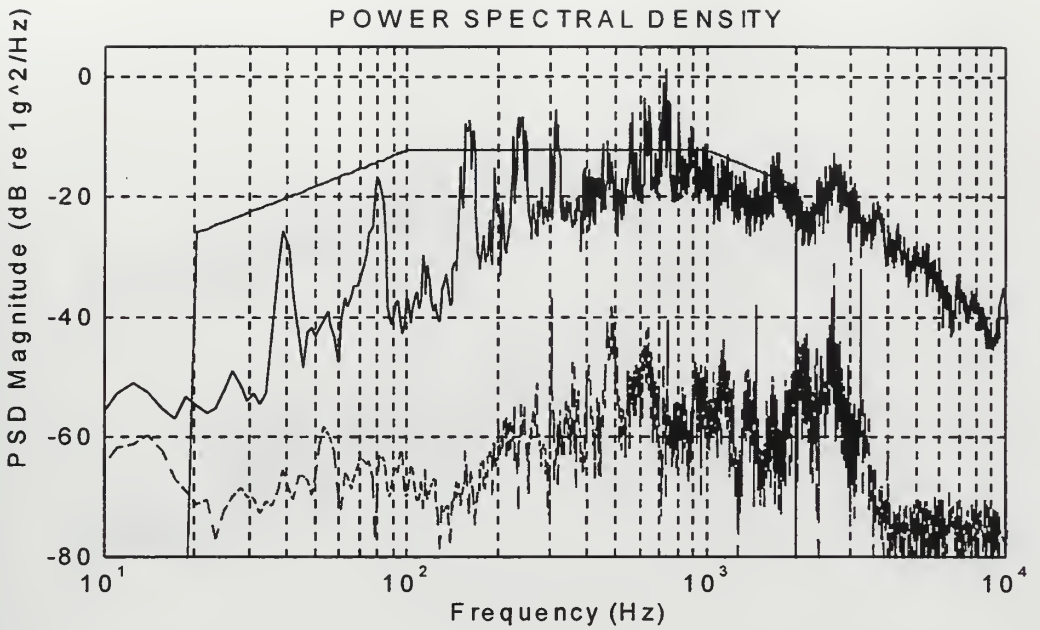

Figure 5.4. Plot of the PSD (solid line), pre-firing noise (dashed line), and specification for location two in the Y-direction; from test firing one (cf1_1_5s) data. The acceleration in the 20 to 2000 Hz frequency band is 7.257 g rms.

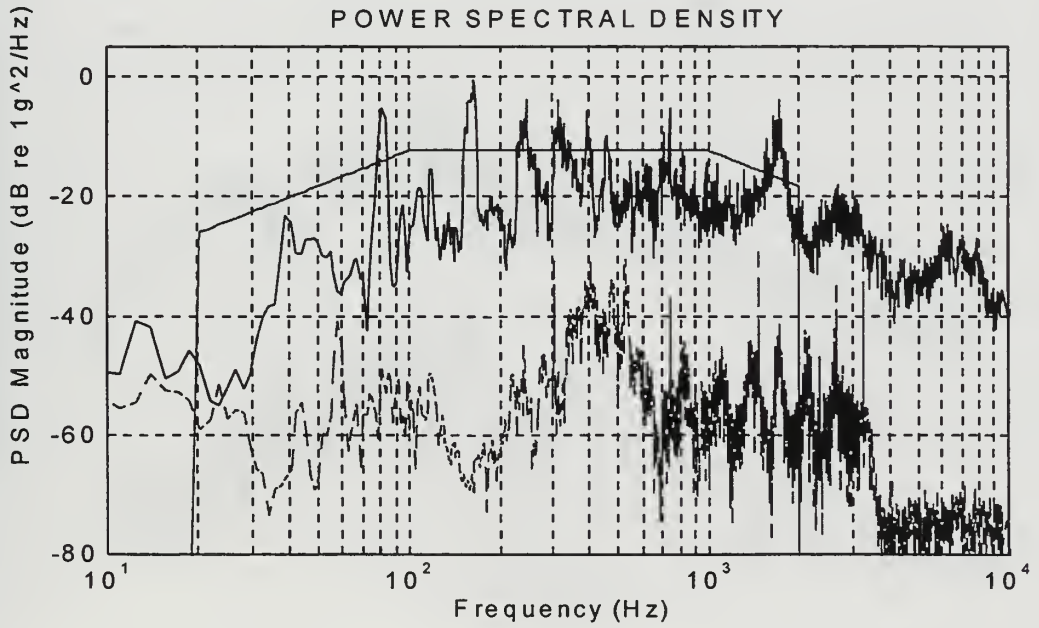

Figure 5.5. Plot of the PSD (solid line), pre-firing noise (dashed line), and specification for location two in the Z-direction; from test firing one (cf1_1_5s) data. The acceleration in the 20 to 2000 Hz frequency band is 7.435 g rms.

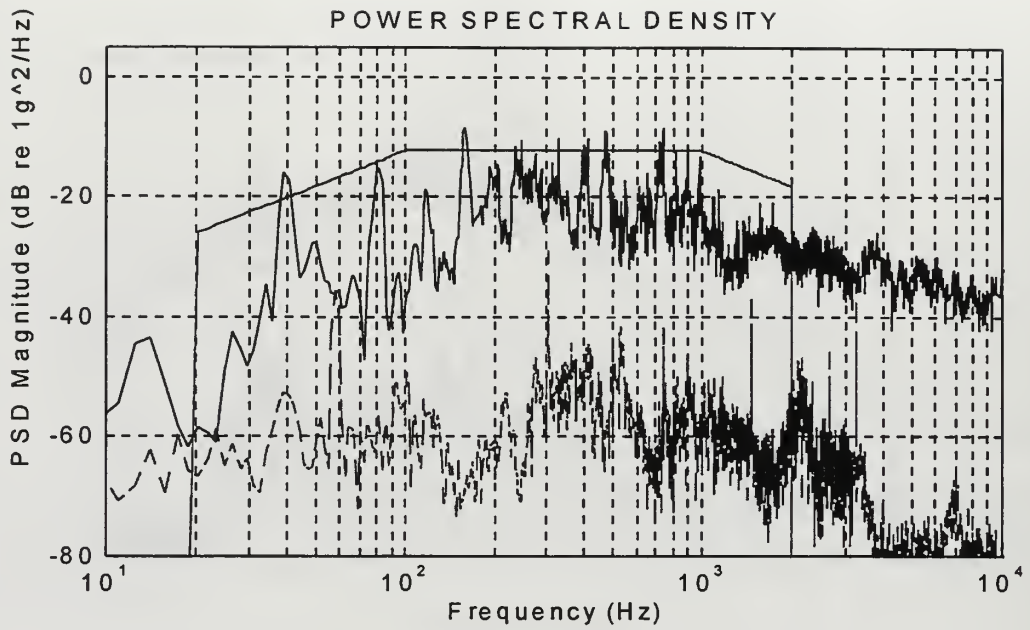

Figure 5.6. Plot of the PSD (solid line), pre-firing noise (dashed line), and specification for location three in the X-direction; from test firing one (cf1_1_5s) data. The acceleration in the 20 to 2000 Hz frequency band is 3.773 g rms.

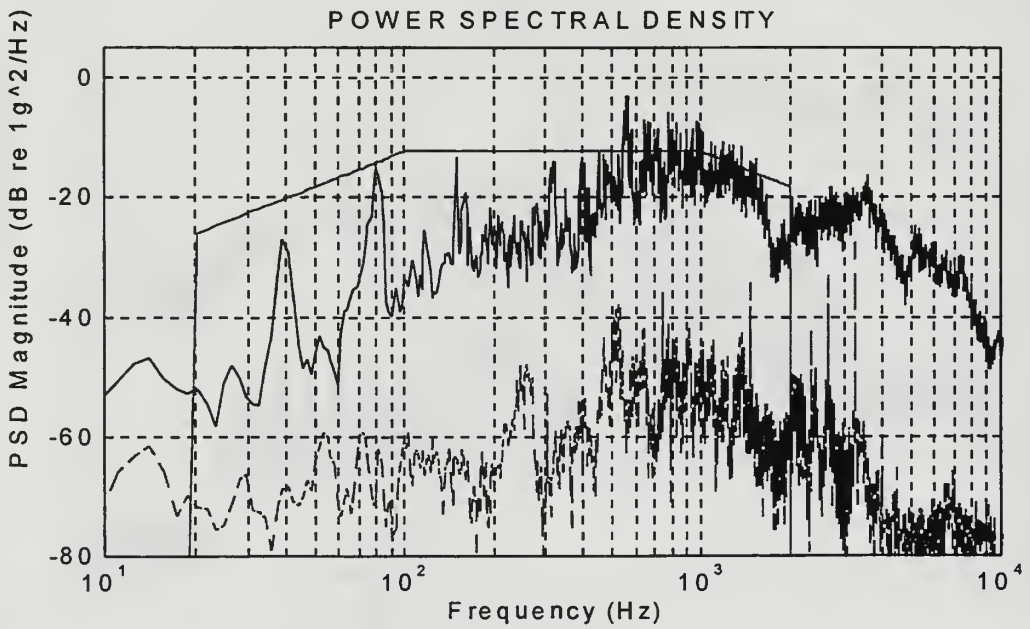

Figure 5.7. Plot of the PSD (solid line), pre-firing noise (dashed line), and specification for location three in the Y-direction; from test firing one (cf1_1_5s) data. The acceleration in the 20 to 2000 Hz frequency band is 6.619 g rms.

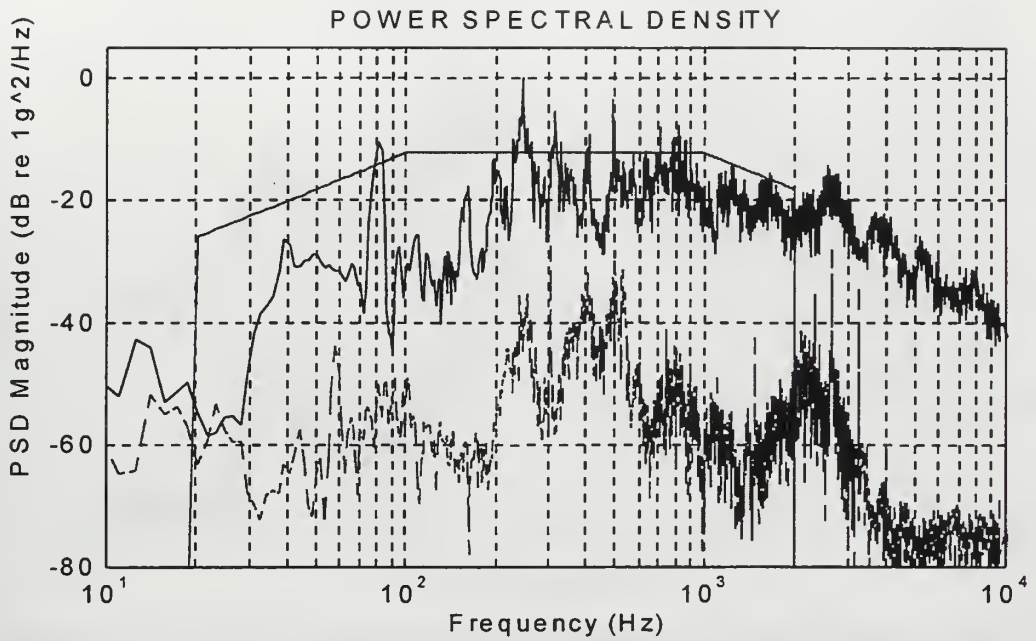

Figure 5.8. Plot of the PSD (solid line), pre-firing noise (dashed line), and specification for location three in the Z-direction; from test firing one (cf1_1_5s) data. The acceleration in the 20 to 2000 Hz frequency band is 6.116 g rms.

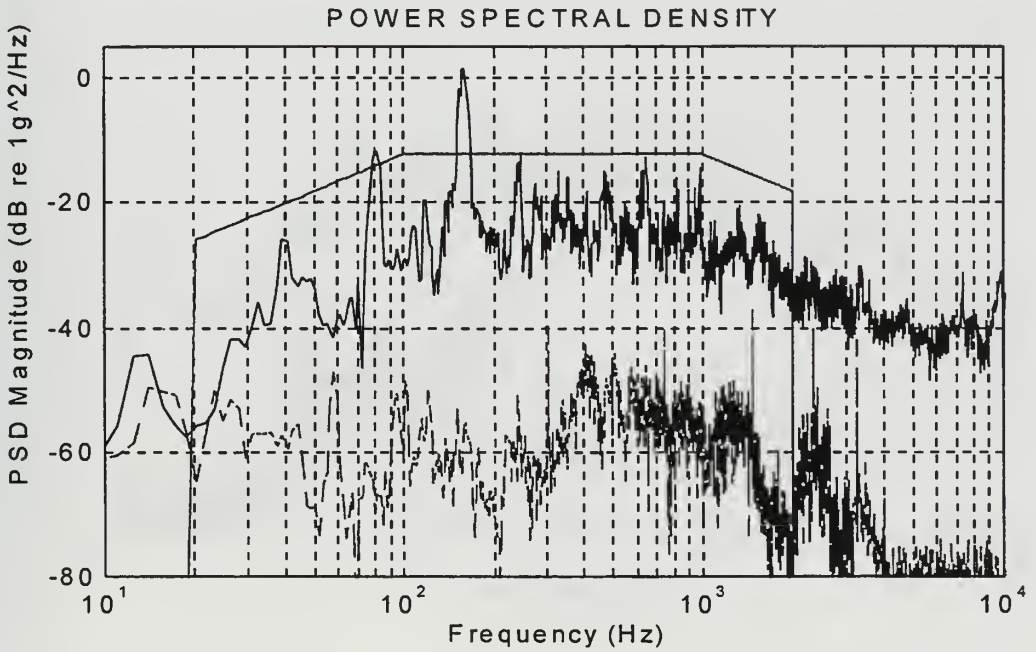

Figure 5.9. Plot of the PSD (solid line), pre-firing noise (dashed line), and specification for location four in the X-direction; from test firing one (cf1_1_5s) data. The acceleration in the 20 to 2000 Hz frequency band is 4.227 g rms.

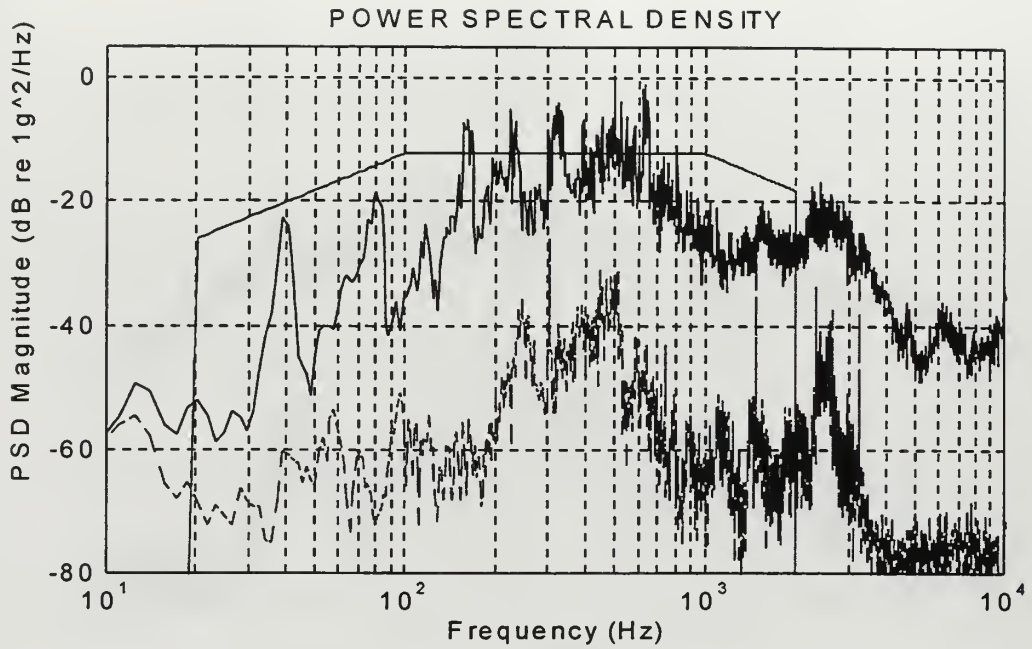

Figure 5.10. Plot of the PSD (solid line), pre-firing noise (dashed line), and specification for location four in the Y-direction; from test firing one (cf1_1_5s) data. The acceleration in the 20 to 2000 Hz frequency band is 6.549 g rms.

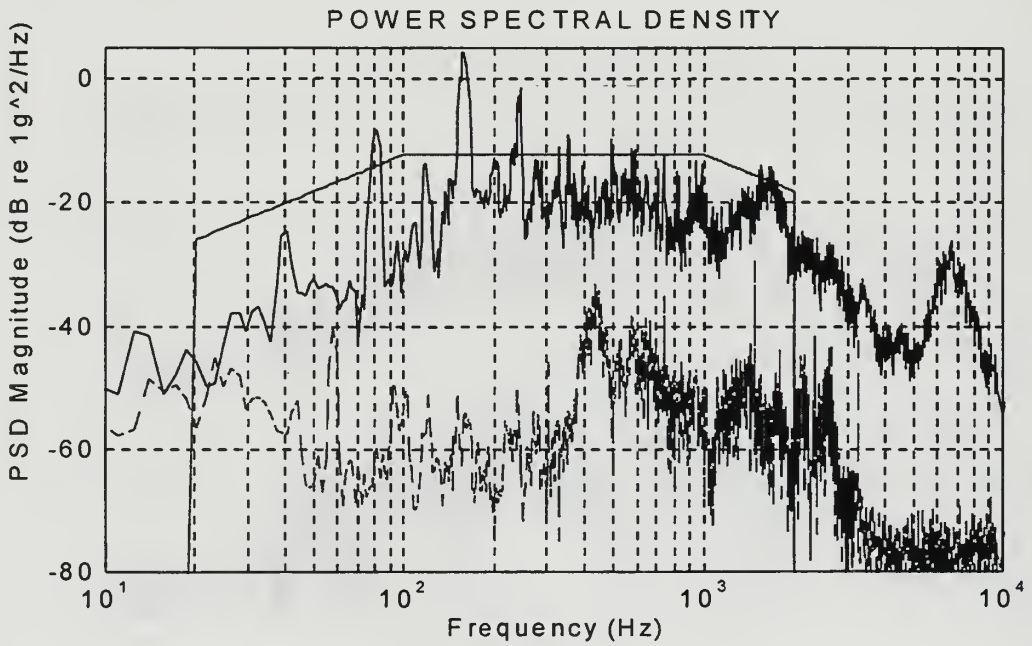

Figure 5.11. Plot of the PSD (solid line), pre-firing noise (dashed line), and specification for location four in the Z-direction; from test firing one (cf1_1_5s) data. The acceleration in the 20 to 2000 Hz frequency band is 6.8971 g rms.

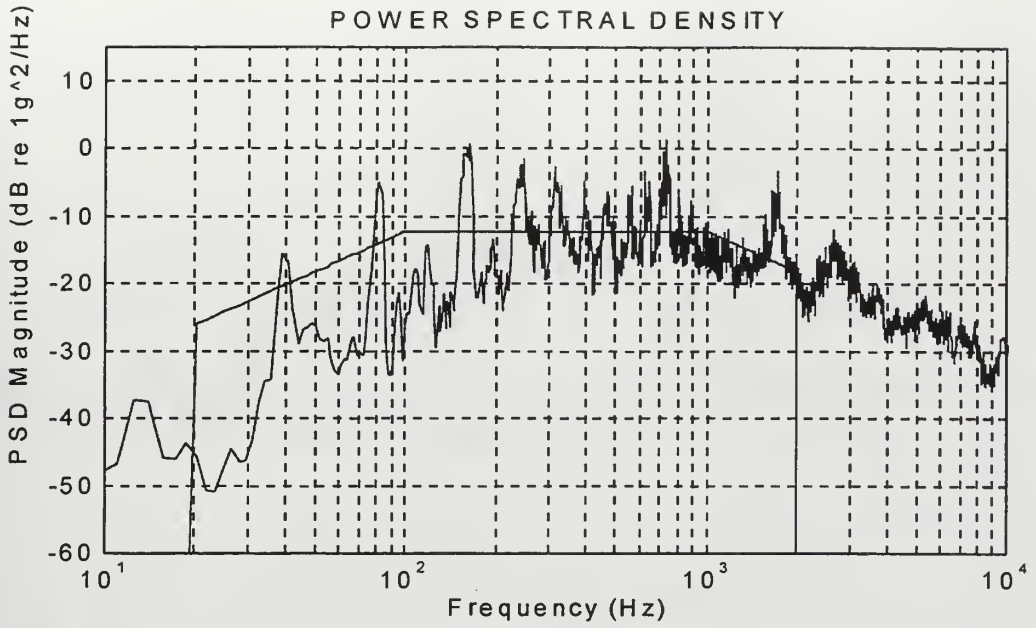

Figure 5.12. Plot of the overall acceleration magnitude PSD and the specification for pedestal mount one from test firing one (cf1_1_5s) and test firing two (cf2_1_5s) data. The g rms in the 20 to 2000 Hz frequency band is 11.16 g rms.

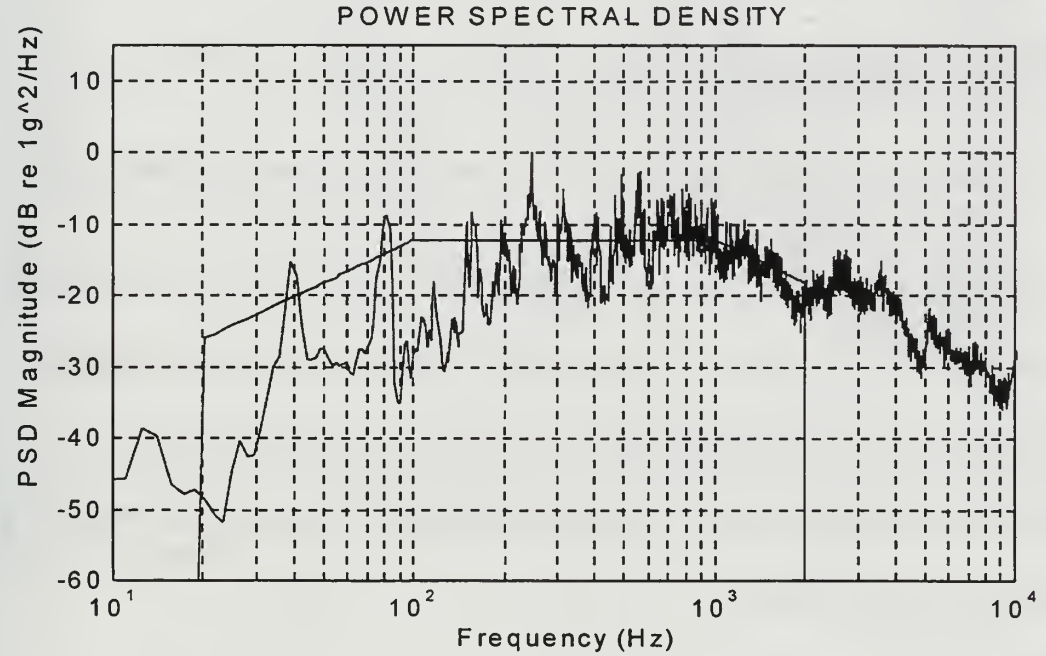

Figure 5.13. Plot of the overall acceleration magnitude PSD and the specification for pedestal mount two from test firing one (cf1_1_5s) and test firing two (cf2_1_5s) data. The g rms in the 20 to 2000 Hz frequency band is 9.769 g rms.

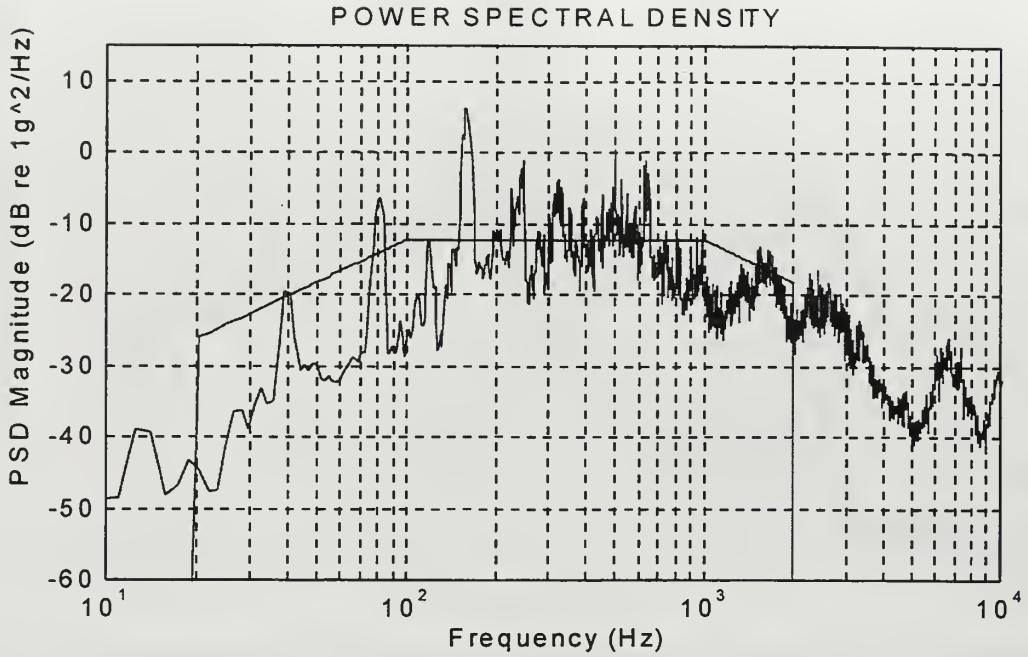

Figure 5.14. Plot of the overall acceleration magnitude PSD and the specification for pedestal mount three from test firing one (cf1_1_5s) and test firing two (cf2_1_5s) data. The g rms in the 20 to 2000 Hz frequency band is 10.40 g rms.

G. LINEAR ACCELERATION FROM LINEAR ACCELEROMETERS LOCATED ON THE STABILIZER

1. Linear Acceleration from Linear Accelerometers Located on the FLIR Camera Mount ("rocky")

The linear accelerations from 20 to 2000 Hz in all axial directions were calculated using the same MATLAB code previously described. The results for the rms values are shown in Table 5.3 and the power spectral densities are plotted in Figures from 5.15 through 5.20. It is generally observed that the FLIR camera mount experiences about 1 g rms acceleration in each direction.

Location description and test plan location number	g rms in X axis direction	g rms in Y axis direction	g rms in Z axis direction	g rms in all axis directions
Front surface of FLIR mount, #6	0.978	0.880	0.718	1.50
Rear surface of FLIR mount, #7	0.862	1.02	0.726	1.52

Table 5.3. The magnitude of the linear acceleration in all axis directions from 20 to 2000 Hz at the FLIR camera mount; from test firing eight (cf8_1_ 5s).

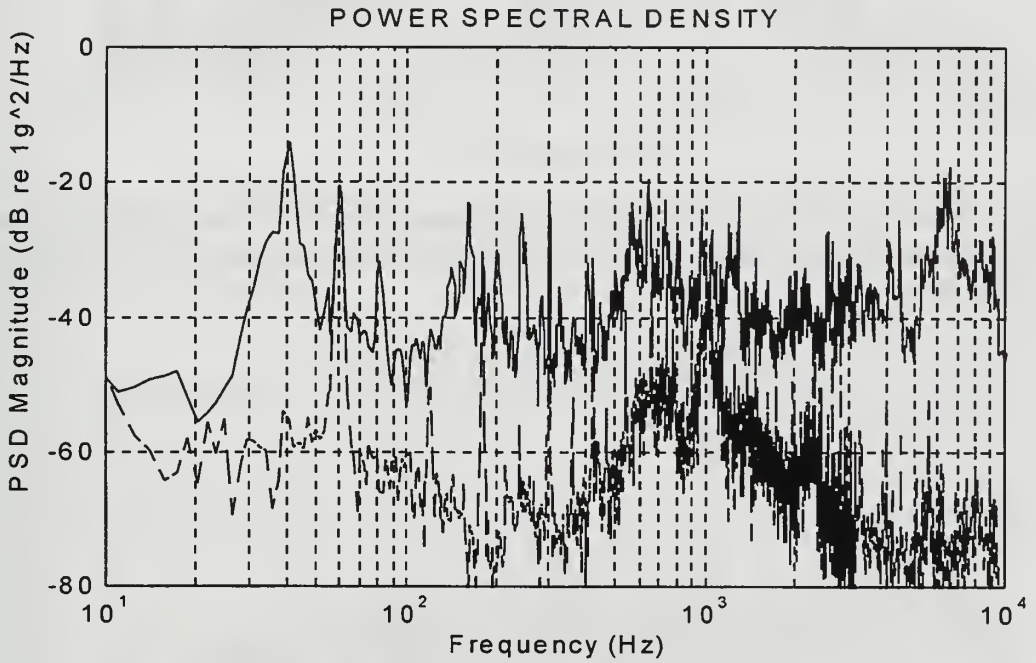

Figure 5.15. Plot of the PSD (solid line) and pre-firing noise (dashed line) for location six in the X-direction; from test firing one (cf8_1_5s) data. The g rms in the 20 to 2000 Hz band is 0.978 g rms.

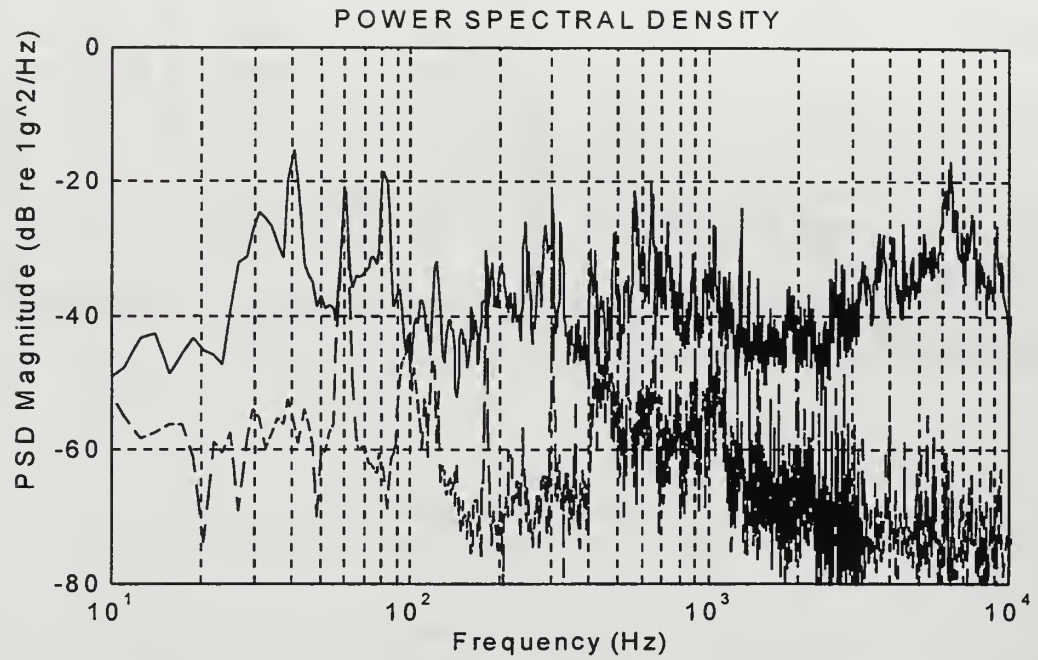

Figure 5.16. Plot of the PSD (solid line) and pre-firing noise (dashed line) for location six in the Y- direction; from test firing one (cf8_1_5s) data. The g rms in the 20 to 2000 Hz band is 0.880 g rms.

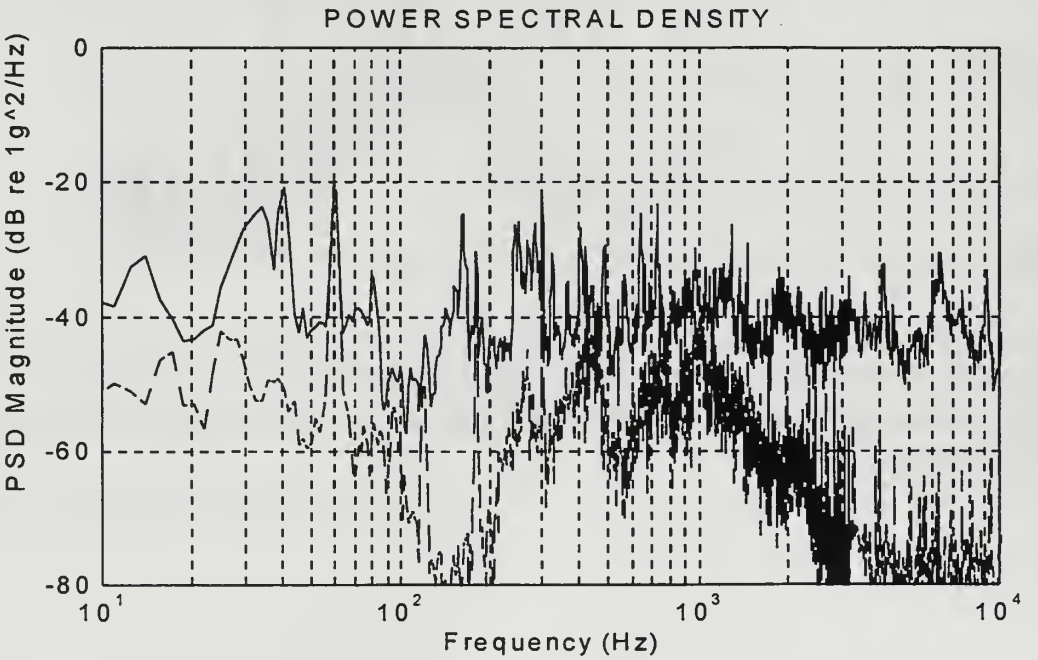

Figure 5.17. Plot of the PSD (solid line) and pre-firing noise (dashed line)for location six in the Z- direction; from test firing one (cf8_1_5s) data. The g rms in the 20 to 2000 Hz band is 0.718 g rms.

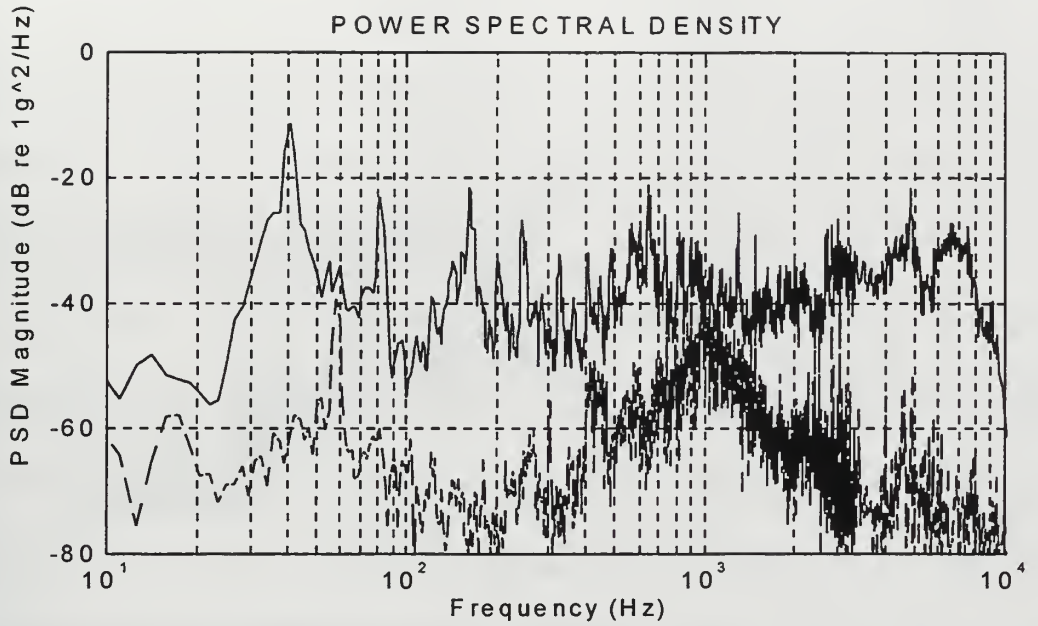

Figure 5.18. Plot of the PSD (solid line) and pre-firing noise (dashed line) for location seven in the X- direction; from test firing one (cf8_1_5s) data. The g rms in the 20 to 2000 Hz band is 0.862 g rms.

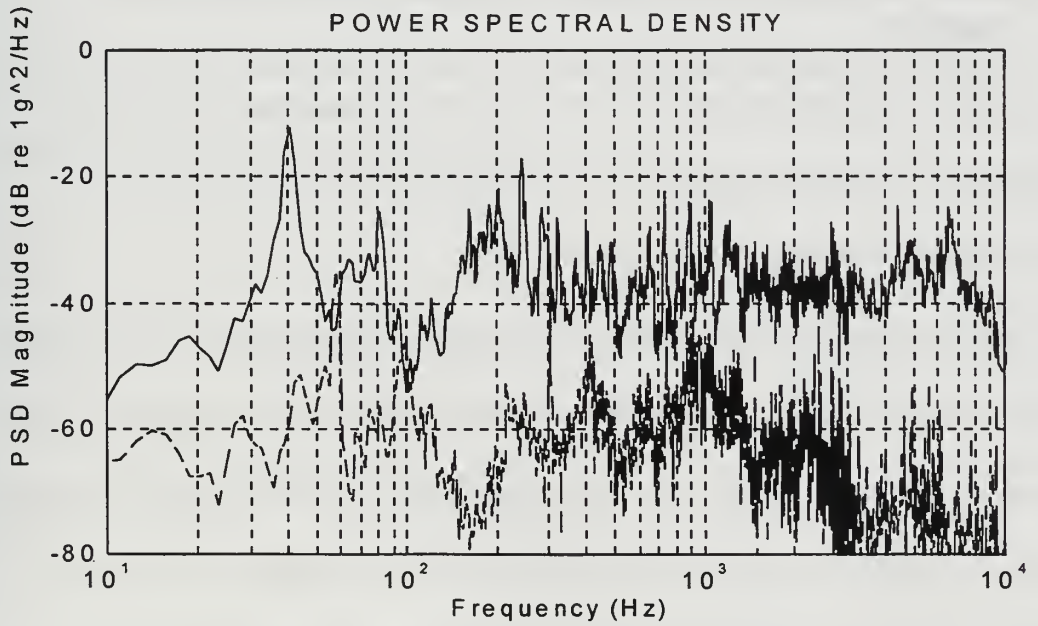

Figure 5.19. Plot of the PSD (solid line) and pre-firing noise (dashed line) for location seven in the Y- direction; from test firing one (cf8_1_5s) data. The g rms in the 20 to 2000 Hz band is 1.02 g rms.

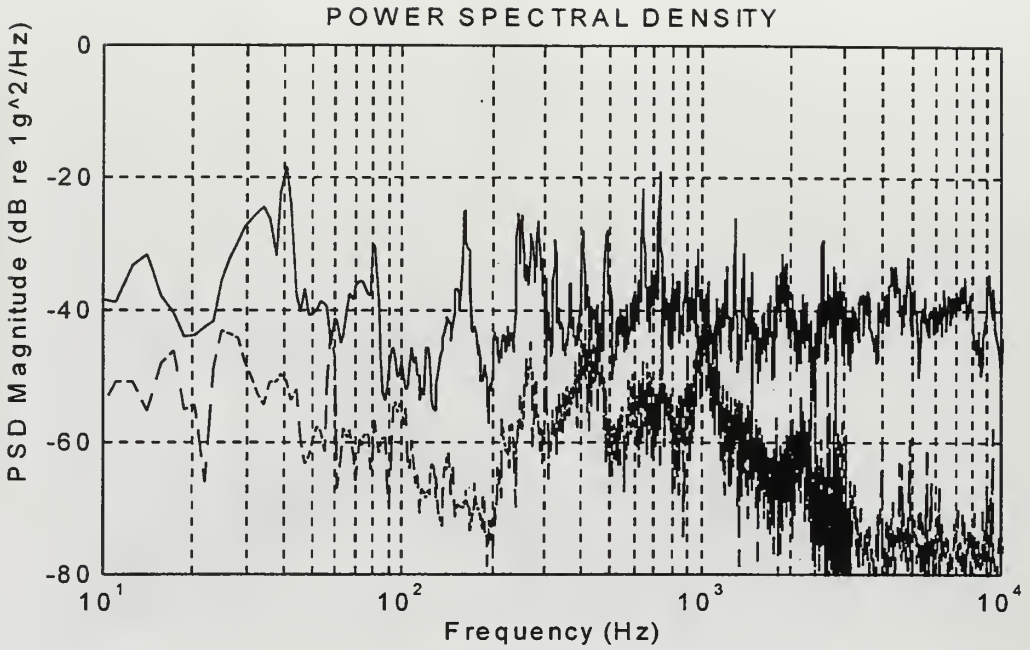

Figure 5.20. Plot of the PSD (solid line) and pre-firing noise (dashed line) for location seven in the Z- direction; from test firing one (cf8_1_5s) data. The g rms in the 20 to 2000 Hz band is 0.726 g rms.

2. Linear Acceleration from Linear Accelerometers Located on the Stabilizer

The linear accelerations over the 20 to 2000 Hz frequency band measured by accelerometers located on the stabilizer were calculated with the MATLAB code described above. The results are shown in Table 5.4.

Comparing these results with those of the pedestal mounts (Table 5.2), the input acceleration appears to be unabated from the pedestal mounts across the dampers to the base assembly (locations 14, 15, 16). The acceleration may even intensify, as in the case of location 16 in the X-axis direction. The acceleration at this location and direction is in excess of 13 g rms. This is the largest acceleration recorded during this study.

The linear accelerations measured on the FLIR camera housing (locations 10 and 11) and lens housing (locations 12 and 13) range from 0.923 to 1.93 g rms. This is slightly greater than the accelerations measured on the FLIR camera mount. The accelerations on the FLIR camera and lens housing in the X- and Y-direction are slightly less than in the Z-direction.

The linear acceleration at the elevation assembly (location 19) in the Y-direction is less than in the X-direction. The magnitude in the Y-direction is of the same magnitude as that observed on the FLIR camera mount and the camera housing. The acceleration in the X- and Z-directions is decreased from that at the base assembly but is still greater than that on the FLIR camera mount or camera housing.

The results for the overall acceleration magnitudes are greater than expected at each location listed in Table 5.4, especially on the lens housing (locations 12 and 13), where the acceleration magnitude is nearly 3 g rms and on the elevation assembly (location 19) where it is more than 4 g rms.

Location description and test plan location number	Axis of acceleration relative to stabilizer	Acceleration (g rms)
Top rear of FLIR camera, #10	X	1.68
	Y	1.77
Top middle of FLIR camera, #11	X	1.29
	Y	1.28
	Z	.923
Magnitude of g rms for all directions for #11	all	2.04
Side of lens housing, #12	X	1.70
	Y	1.93
	Z	1.36
Magnitude of g rms for all directions for #12	all	2.91
Side of lens housing, #13	X	1.50
	Y	1.09
	Z	1.64
Magnitude of g rms for all directions for #13	all	2.47
Base assembly, #14	X	8.66
	Y	6.16
Base assembly, #15	X	8.53
	Y	4.77
Base assembly, #16	Z	13.4
Elevation assembly, #19	X	1.59
	Y	1.64
	Z	3.53
Magnitude of g rms for all directions for #19	all	4.21

Table 5.4. The acceleration from 20 to 2000 Hz by location and axial direction for linear accelerometers located on the stabilizer; from test firings three through eight.

H. ANGULAR ACCELERATION FROM ANGULAR ACCELEROMETERS LOCATED ON THE FLIR CAMERA MOUNT

A MATLAB code similar to that described previously for computing linear acceleration PSDs and rms values was written to compute angular jitter (displacement) PSDs and rms values using TAP system angular acceleration data. A sample is provided in Appendix J. Figure 5.21 shows the results of the MATLAB code for test fire one (cf1_1_5s), location eight (azimuth) data. This figure is representative of typical results for this angular accelerometer. The discrete peaks seen in all the linear accelerometer PSDs are not apparent in the angular displacement PSD. The rms angular jitter in the 20 to 2000 Hz frequency band is 4.34×10^4 microradians. This value is much greater than expected and leads us to suspect that something is wrong with the data. Several hypotheses as to the cause of these results were investigated.

The first hypothesis investigated was that the MATLAB code was not functioning properly. However, the code functioned properly for the linear calculations and it also functioned properly when tested with a synthetic (sine wave) signal.

The second hypothesis investigated was that the TAP system signal coupler was improperly connected during the test firing. The signal coupler has two connectors on its back panel. One is for angular output and the other is for linear output. The following tests were performed to determine whether or not the cables were connected to the angular outputs of the signal coupler. First, each presumed angular acceleration data file was processed using the calibration constant for its system's linear output. This result was compared to that of the closest linear accelerometer measuring linear acceleration in

the same direction as the direction sensed by the TAP system. If the linear output of the TAP system had been taken by mistake, we should expect these two results to be comparable. They were not. Next, pre-firing noise data collected from the presumed TAP angular output were compared for measurements made on three different days that accelerometers were hooked-up at the test site. The accelerometers were connected the first time by Professor Baker for the baseline tests and by LCDR Schmidt during the firing tests. The observed PSDs were essentially identical, making it very unlikely that they were improperly connected during any of the testing.

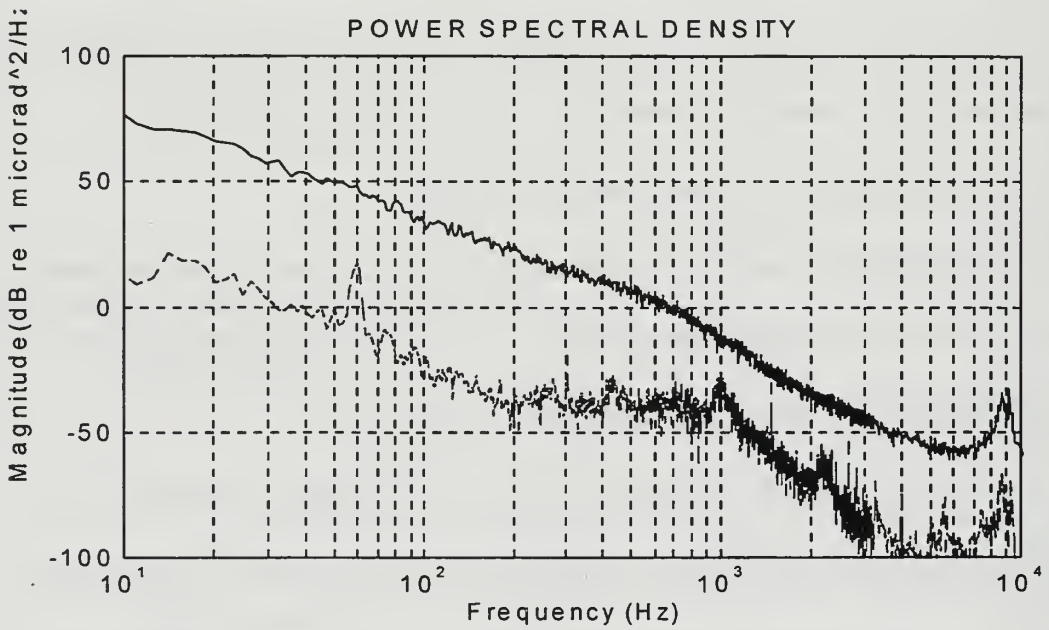

Figure 5.21. Plot of the angular displacement PSD (solid line) and the pre-firing noise (dashed line) for location eight, rotation about the Y-axis (azimuth); from test firing one (cf1_1_5s).

The reason for the suspicious data from the angular accelerometers remains not understood. The angular accelerometers are constructed from two closely-spaced cantilever PZT linear accelerometers. By summing and differencing the outputs from

these in the signal coupler, the TAP System provides one output signal proportional to the linear acceleration normal to the accelerometer base and another output proportional to the angular acceleration about an axis parallel to the accelerometer cable connector. Good agreement (within 4%) was obtained in the lab at NPS between the angular acceleration measured using two linear accelerometers and that obtained using the TAP system , as described in Chapter IV. Also, from the rotational acceleration time record (cf1_1_5s, Figure 5.1), the signal-to-noise ratio appeared to be more than adequate for a good measurement. Nevertheless, we lacked confidence in the angular accelerometer data, and decided to obtain the angular jitter results from linear acceleration measurements. Further investigation of the angular accelerometer data is suggested for follow-on work.

I. ANGULAR ACCELERATION CALCULATED FROM LINEAR ACCELEROMETERS LOCATED ON THE FLIR CAMERA MOUNT

Due to the misfortunes experienced with the angular accelerometers, the calculation of angular acceleration and displacement on the FLIR mount using two linear accelerometers was performed. A sample MATLAB code to accomplish this is provided in Appendix K.

Figures 5.22 and 5.23 show the one-sided linear DFT magnitude and phase in the X- and Y-direction measured at the front left and back right side corners of the FLIR camera mount, locations 6 and 7, respectively. From these figures, it appears that there is sufficient signal-to-noise ratio to measure the difference in the two linear accelerations at about 75 Hz to better than 25% accuracy.

Azimuthal and elevation angular displacement (jitter) PSDs and 20 to 2000 Hz band rms values were computed for the FLIR camera mount. The band rms values and their estimated standard errors are listed in Table 5.5 as "not corrected for coherence." Also listed for comparison are Johns Hopkins University's (JHU) values obtained from optical measurements made at the same time as the acceleration measurements (Johns Hopkins University: Analysis Summary of FLIR LOS Jitter Data, 1996, p. 6). The NPS values for azimuthal and angular jitter are 2.0 and 4.6 times the JHU values. It should be noted that the optical data were obtained from video images scanned at 33 Hz, and that no anti-aliasing filter could be applied to the pre-sampled signal; the rms values for these data were estimated directly from the time series.

Because of the nature of the calculation of angular displacement from linear accelerations, amounting to the difference of two quantities which may be nearly equal, we are especially concerned that our estimates may be contaminated by random noise, resulting in excessively large values, as appears to be the case. The uncorrected estimated PSDs and band rms values contain "power" due to both the desired "signal" and contaminating "noise." Bendat and Piersol (Bendat and Piersol, 1993, pp. 83-85) describe the use of the "coherence function" to estimate the PSD of a signal, uncontaminated by noise. If $x(t)$ is the source (input) of the uncontaminated "signal" (ideal output) $v(t)$, and $y(t)$ is the measured, contaminated (actual output) signal, then, if the noise is introduced at the measurement point (output), and not at the source (input), the estimated PSD of the uncontaminated signal, $G_{vv}(f)$, is given by

$$G_{vv}(f) = \gamma_{xy}^2(f)\, G_{yy}(f), \qquad 5.6$$

where $\gamma_{xy}^2(f)$ is the so-called coherence function between x and y, and $G_{yy}(f)$ is the (uncorrected) PSD of the contaminated signal. The coherence function is given by

$$\gamma_{xy}^2(f) = \frac{|G_{xy}(f)|^2}{G_{xx}(f)\, G_{yy}(f)} \qquad 5.7$$

where $G_{xy}(f)$ is the cross-spectral density (CSD), and $G_{xx}(f)$ and $G_{yy}(f)$ are the PSDs of x and y, respectively (Bendat and Piersol, 1993, p. 71). The coherence function in the frequency domain is similar to the square correlation coefficient in statistical analysis in the time domain (Bendat and Piersol, 1993, pp. 49, 59). It can be interpreted as the fraction of the power of x and y at frequency f due to a linear relationship between them. The remainder is attributed to noise.

We computed the coherence functions between the two linear acceleration signals which were used to extract azimuthal and elevation angular jitter using the built-in MATLAB function "cohere" (MATLAB Signal Processing Toolbox, Math Works, 1994, pp. 2-52). On the assumption that these are good estimates of the coherence functions between the source of azimuthal and elevation angular jitter and the angular jitter that results from this source, we corrected the "raw" angular displacement PSDs using Eqn. 5.6 to obtain better estimates. These are shown in Figures 5.24 and 5.25. The corrected 20 to 2000 Hz band rms jitter values and their estimated standard errors are listed in Table 5.6 as "corrected for coherence." The corrected NPS values for azimuthal and

angular jitter are still 1.7 and 4.2 times the JHU values.

We are disappointed that the reduction in band rms values after correcting for coherence was not greater, and so we have conducted the following further analyses. Figures 5.26 and 5.28 show a plot of the angular jitter PSD over the frequency range 20 to 240 Hz. This range includes the predominant portion of the spectra. In Figures 5.27 and 5.28 are plotted the coherence function and the "normalized difference in acceleration" between the two acceleration signals used to extract the angular jitter. We define the normalized difference in acceleration between the phasor accelerations a_1 and a_2 to be

$$\frac{| a_2 - a_1 |}{(|a_2| + |a_1|)}. \qquad 5.8$$

Absent noise, this normalized difference is a measure of the fraction of the acceleration measured at two locations due to rotation versus translation. In the presence of noise, interpretation of the normalized difference in acceleration is more difficult. Where the coherence is large, the interpretation of it as a measure of rotation present is more reliable; where the coherence is small, it is less so. In any case, if the normalized difference is very small, this indicates that the accelerometer sensitivities need to be very well known to extract the rotation. The number of digits required of the sensitivity calibration is approximately -log10 (norm diff) + the number of digits of precision desired in the extracted rotation. For example, if the normalized difference is approximately 10^{-3}, then the calibration constants need to be known to 4 digits for 10% precision in the extracted rotation.

We do not observe particularly small values of normalized differences in Figures 5.27 and 5.29. This implies that our PSD and band rms estimates would not likely be improved with more precise sensitivity calibration constants (i.e. more digits of precision). Our PSD and rms estimates might be improved if the calibration constants were more accurately known; our best estimates for those are the manufacturer's values (see Chapter IV). Note the tendency that where the normalized difference is large, the coherence is small. Also note that at the frequencies of the predominant peaks in the PSDs, the coherence is not particularly large. Our conclusion is that either the accuracy of the linear accelerometer sensitivities is not good enough, or the coherence between the two accelerometer signals is not great enough to extract accurate angular displacement PSD and band rms values.

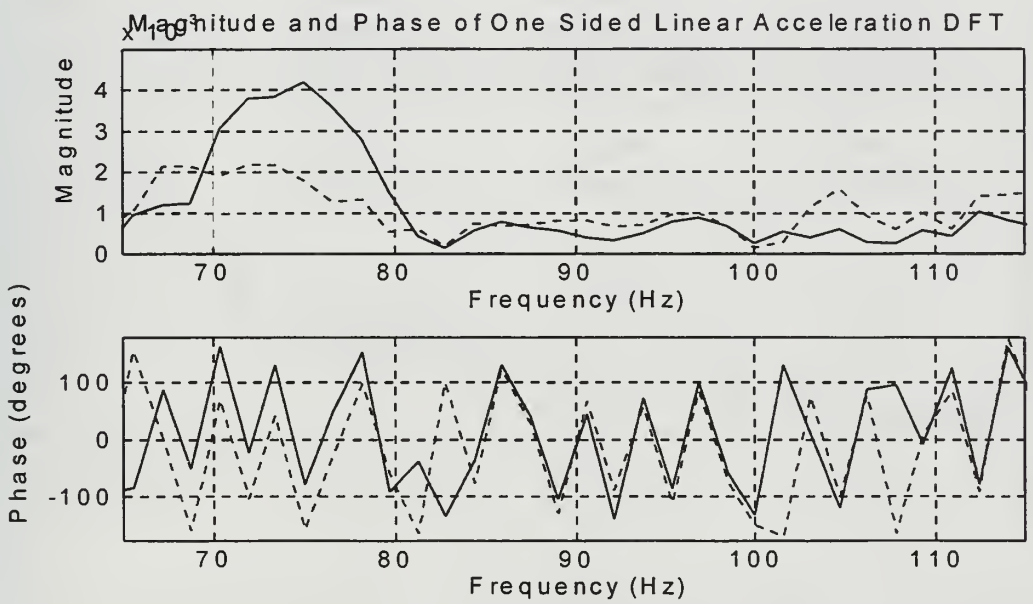

Figure 5.22. Plot of the magnitude and phase (degrees) of the one-sided linear acceleration DFT of accelerometers located at 6 and 7 on "rocky" in the X-direction from 65 to 115 Hz; for extracting azimuth jitter; data from firing eight (cf8_1_5s).

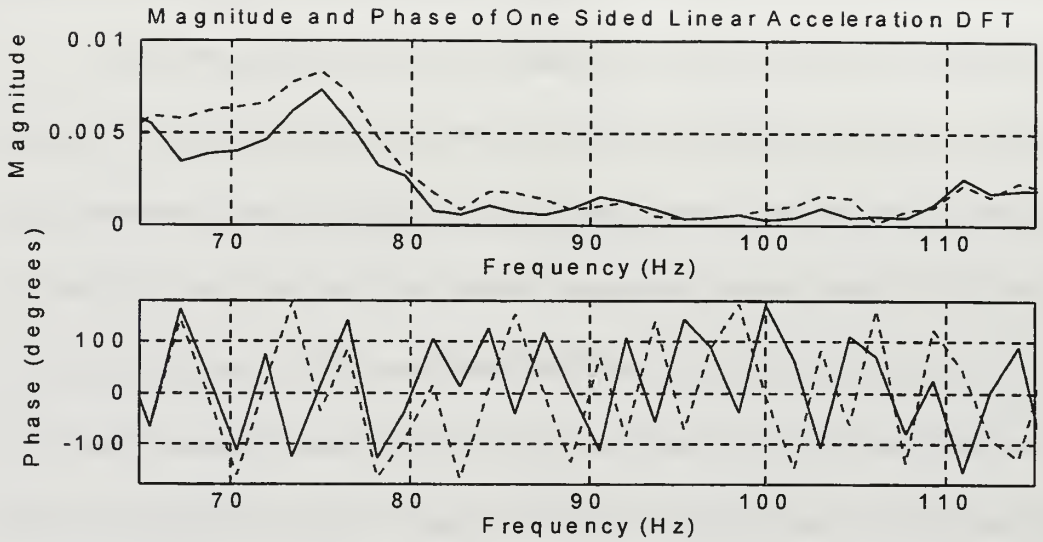

Figure 5.23. Plot of the magnitude and phase (degrees) of the one-sided linear acceleration DFT of accelerometers located at 6 and 7 on "rocky" in the Y-direction from 65 to 115 Hz; for extracting azimuth jitter; data from firing eight (cf8_1_5s).

Type of rotation, location, and distance between accel-erometers	uncorrected for coherence rms angular acceleration in 20 to 2 kHz band (microrad/s^2)	uncorrected for coherence rms angular displacement in 20 to 2 kHz band (microrad)	corrected for coherence rms angular acceleration in 20 to 2 kHz band (microrad/s^2)	corrected for coherence rms angular displacement in 20 to 2 kHz band (microrad)
Azimuth 6 X - 7 X 0.241m (9.5in)	1.9×10^7 ($\pm 1.7 \times 10^4$; 0.08%)	59.1 (± 2.2; 3%)	1.35×10^7 ($\pm 1.6 \times 10^6$; 10%)	51.9 (± 2.5; 3%)
Elevation 6 Y - 7 Y 0.241m (9.5in)	3.1×10^7 ($\pm 5.5 \times 10^4$; 0.8%)	157 (± 4.4; 3%)	2.50×10^7 ($\pm 2.3 \times 10^6$; 10%)	142.8 (±3.3; 2.3%)

Table 5.5. The coherence corrected and uncorrected rms azimuth and elevation angular acceleration, displacement, and standard error of the mean PSD in the 20 to 2000 Hz band as calculated from linear accelerometers mounted on the FLIR camera mount.

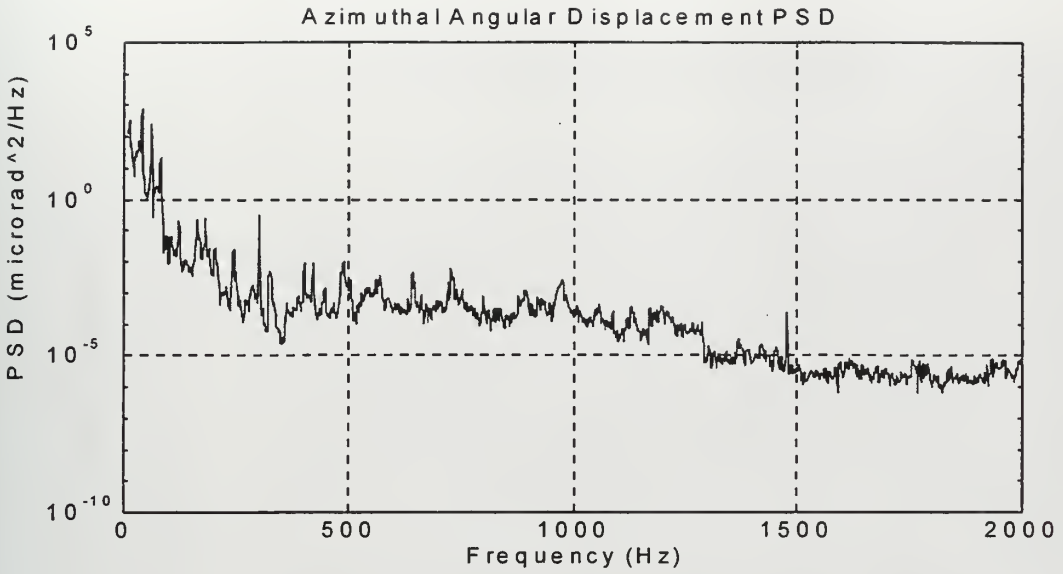

Figure 5.24. Plot of the Azimuthal Angular Displacement PSD for FLIR camera mount; from test firing eight (cf8_1_5s) data. The rms displacement in the 20 to 2000 Hz frequency band is 59.1 microrad.

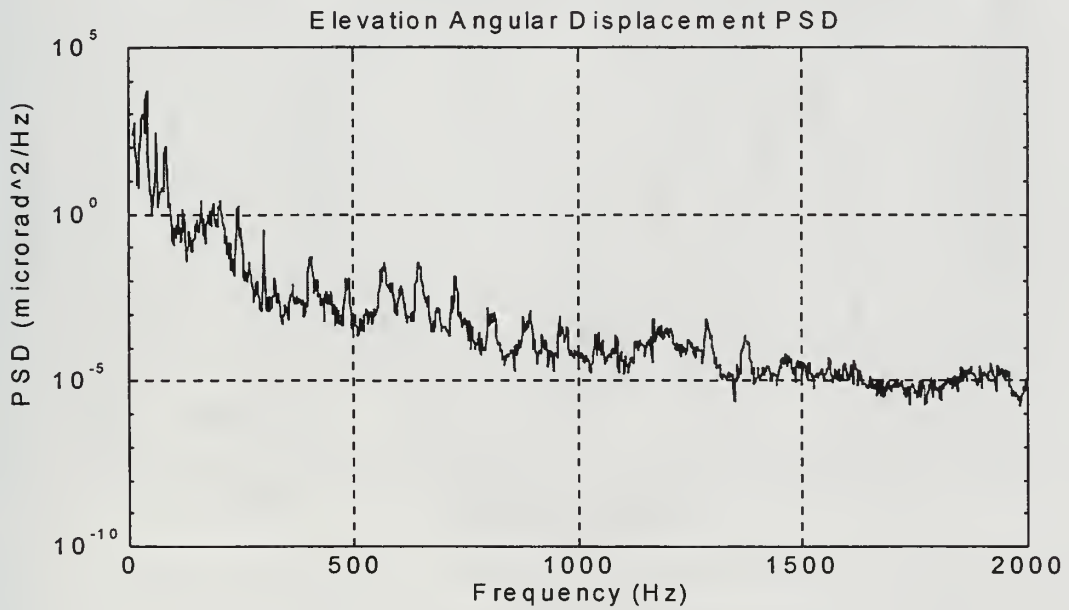

Figure 5. 25. Plot of the Elevation Angular Displacement PSD for FLIR camera mount; from test firing eight (cf8_1_5s) data. The rms displacement in the 20 to 2000 Hz frequency band is 157 microrad

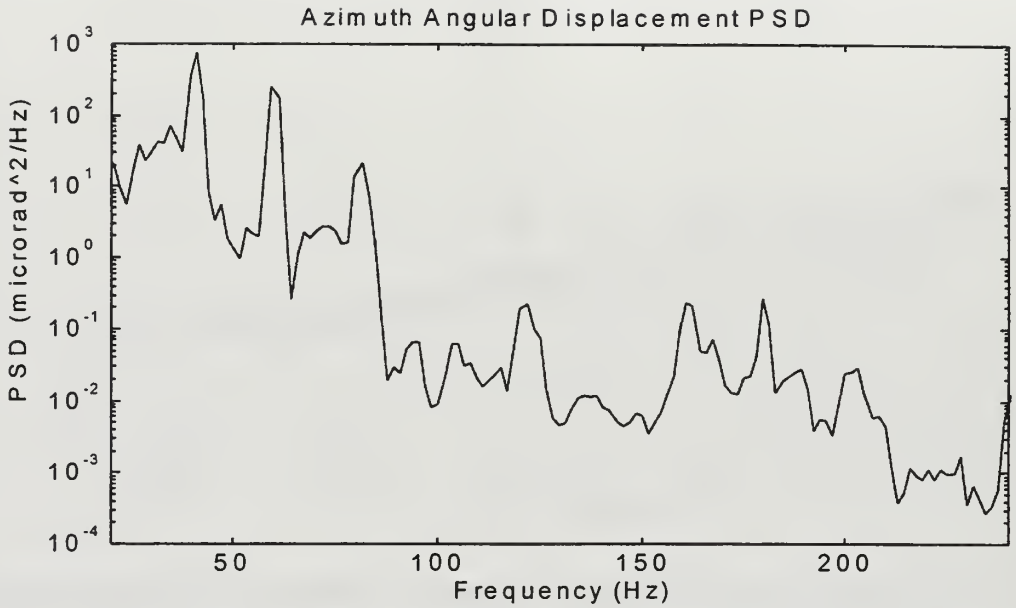

Figure 5.26. Plot of the azimuth displacment PSD 20 to 240 Hz after correcting for coherence.

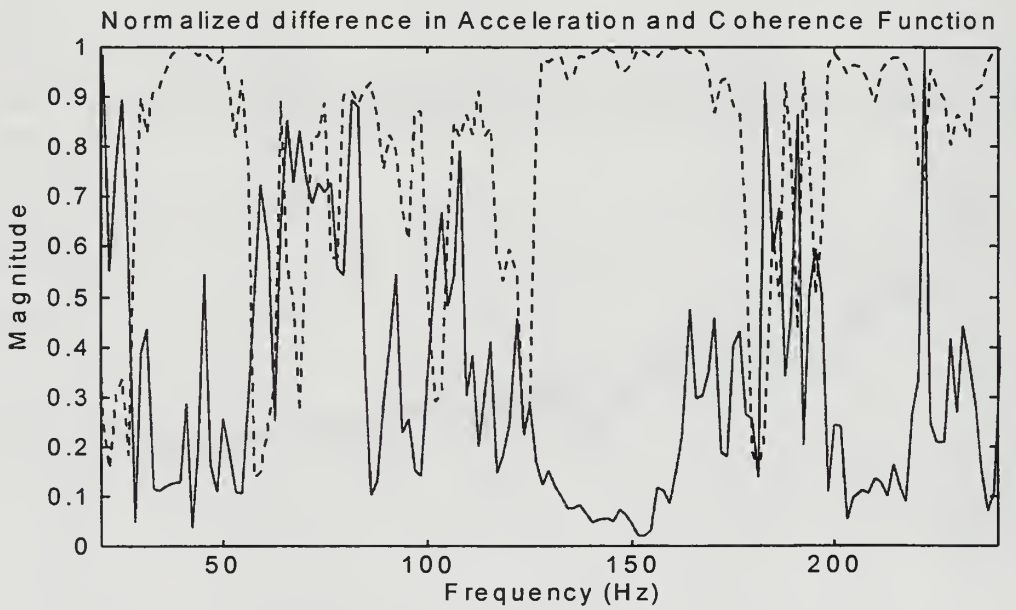

Figure 5.27. Plot of the normalized difference in acceleration (solid line) and coherence (dashed line) from 20 to 240 Hz from accelerometers mounted on 6X and 7X used in extracting the azimuthal jitter of the FLIR camera mount.

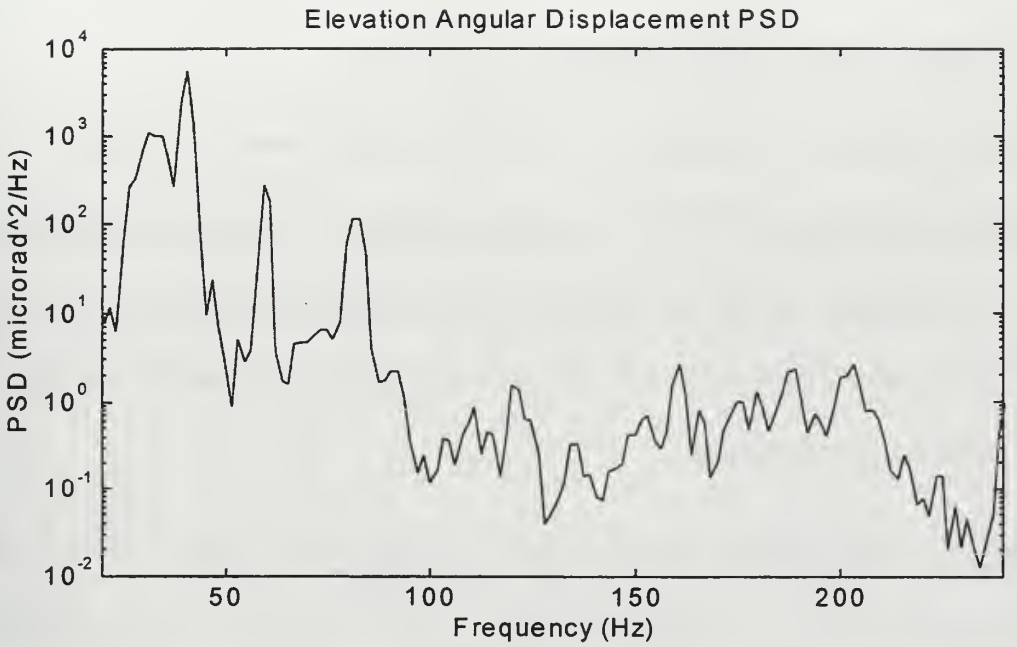

Figure 5.28. Plot of the elevation displacment PSD 20 to 240 Hz after correcting for coherence.

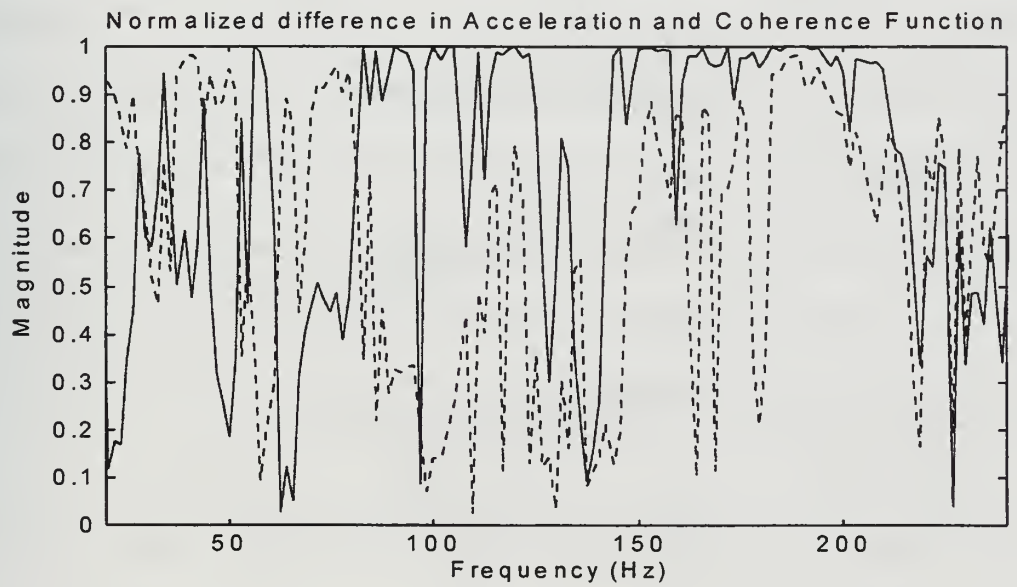

Figure 5.29. Plot of the normalized difference in acceleration (solid line) and coherence (dashed line) from 20 to 240 Hz from accelerometers mounted on 6X and 7X used in extracting the elevation jitter of the FLIR camera mount

J. ANGULAR MOTION OF THE PEDESTAL MOUNTS

Figure 5.30 depicts the three pedestal feet, which define a plane. We take this plane to have coordinate value X=0. The Y- and Z-coordinate values of the pedestal feet were obtained by HMSC. The vector, ***R***, from pedestal number three to the point bisecting the line from pedestal one to two, lies in the X=0 plane and is parallel to the Z-axis (barrel axis). It has coordinates

$$\boldsymbol{R} = \left(\frac{x_1 + x_2}{2} - x_3 \;,\; \frac{y_1 + y_2}{2} - y_3 \;,\; \frac{z_1 + z_2}{2} - z_3 \right), \qquad 5.9$$

where x_i, y_i, and z_i, with i= 1, 2, and 3, are the X-, Y-, and Z- coordinates of pedestals 1, 2, and 3, respectively.

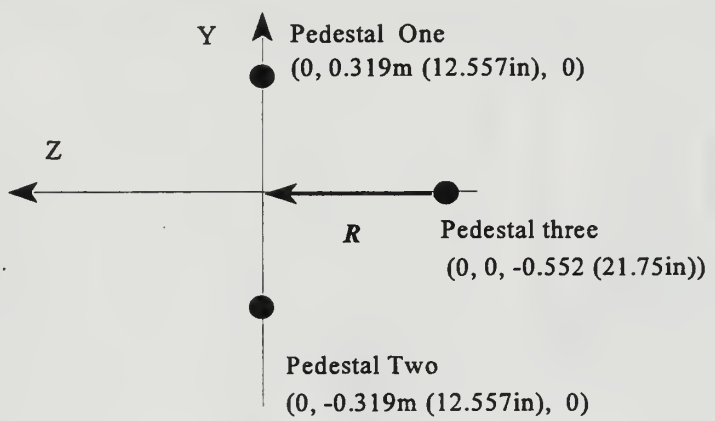

Figure 5.30. The locations of the pedestal feet in the X-, Y-, Z-coordinate system.

For small vibration amplitude, using the small angle approximation, the relationship between elevation angle of input rotation of the pedestal feet, $\delta\theta_{el}$, and

changes in their y-coordinates is

$$R\ \delta\Theta_{el} = \frac{\delta y_1 + \delta y_2}{2} - \delta y_3 \ . \qquad 5.10$$

Where R is the length of $\boldsymbol{R}$. The corresponding relationship between the azimuth angle of input rotations of the pedestal feet , $\delta\theta_{az}$, and changes in their x-coordinates is

$$R\ \delta\Theta_{az} = \frac{\delta x_1 + \delta x_2}{2} - \delta x_3 \ . \qquad 5.11$$

A MATLAB program to extract $\delta\theta_{az}$ and $\delta\theta_{el}$ was written and is included as Appendix L. Using data from the test fires one (cf1_1_5s) and two (cf2_1_5s), rotation of the pedestal-foot plane was calculated in radians and degrees for azimuth and elevation.

Elevation and azimuth displacement coherence function were estimated by computing the coherence between $\delta y_1 + \delta y_2$ and δy_3, and $\delta x_1 + \delta x_2$ and δx_3,, respectively. These were used to correct the "raw" angular displacement PSDs, as was done for the FLIR camera mount. The uncorrected and corrected values of pedestal plane elevation and azimuth rms angular jitter in the 20 to 2000 Hz band are listed in Table 5.6. Figures 5.31 through 5.34 show the coherence functions and the corrected PSDs.

	Uncorrected rms jitter in 20 to 2000 Hz band (microrad)	Corrected rms jitter in 20 to 2000 Hz band (microrad)
Azimuth	62.4	58.1
Elevation	37.6	35.8

Table 5.6 The rms azimuth and elevation angular jitter in the 20 to 2000 Hz band, of the plane of the pedestal feet uncorrected and corrected for coherence; data from firing one (cf1_1_5s) and two (cf2_1_5s) .

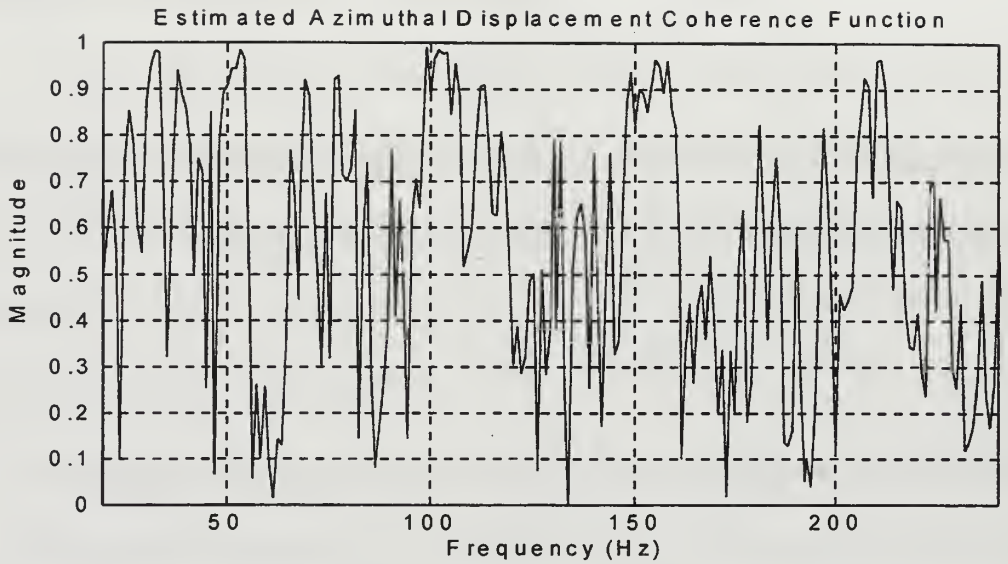

Figure 5.31. Plot of the coherence function from 20 to 240 Hz between the mean Y-acceleration of pedestal mounts one and two and Y-acceleration of pedestal three for azimuth; data from test fire one (cf1_1_5s).

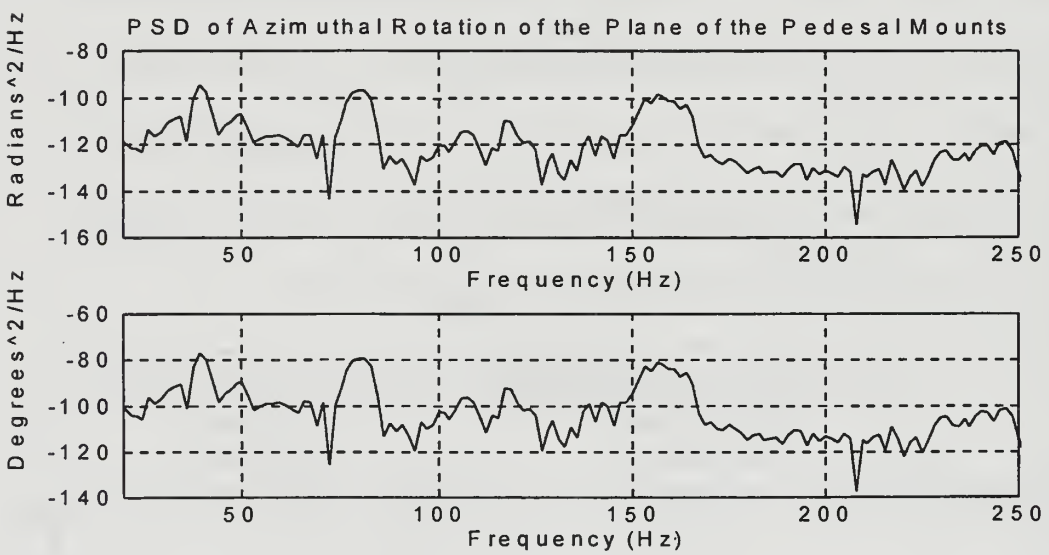

Figure 5.32. Plot of the PSD of azimuth rotation of the plane of the pedestal mounts for frequencies from 20 to 240 Hz; from test fire one (cf1_1_5s).

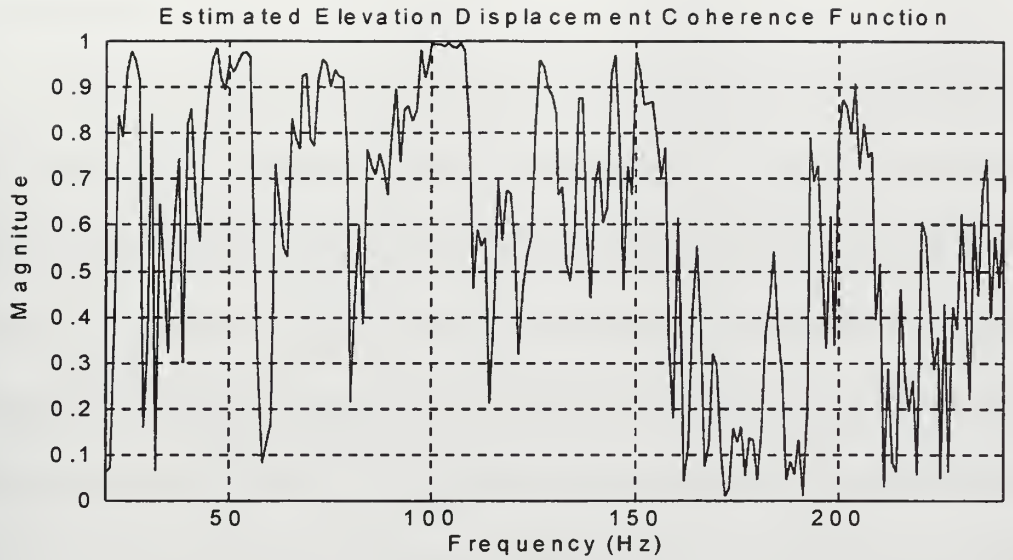

Figure 5.33. Plot of the coherence function from 20 to 240 Hz between the mean Y-acceleration of pedestal mounts one and two and Y-acceleration of pedestal three for azimuth; data from test fire two (cf2_1_5s).

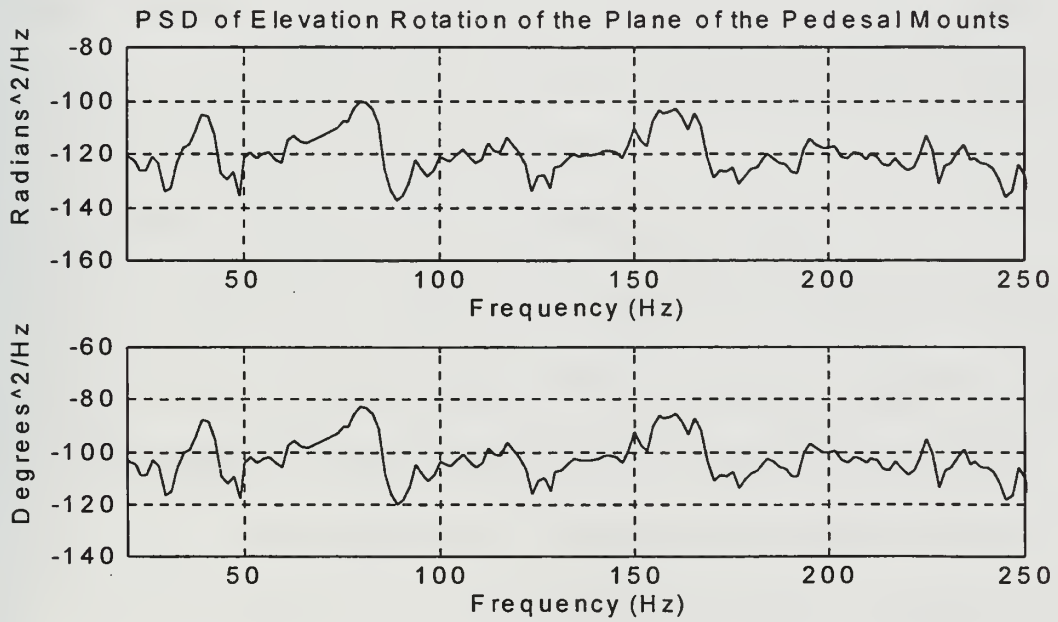

Figure 5.34. Plot fo the PSD of elevation rotation of the plane of the pedestal moounts for frequencies from 20 to 240 Hz; from test fire two (cf2_1_5s).

VI. CONCLUSIONS

A. SUMMARY

The purpose of this study was to measure the linear and angular acceleration at various locations on the PHALANX Surface Mode (PSUM) Upgrade FLIR camera and stabilizer system during live-fire tests conducted a NSWC, Dahlgren, Virginia. And from these tests determine the acceleration input at the pedestal feet and resulting angular jitter displacement of the FLIR camera mount to assist NSWC to determine if the prototype stabilizer meets its specifications. We find the input acceleration at each pedestal foot is about 5 g rms in the 20 to 2000 Hz frequency band in each of the three axial directions. The rms (20 to 2000 Hz) angular displacement of the FLIR camera mount extracted from linear acceleration measurements is 59.1 microrad in azimuth and 157 microrad in elevation. For unknown reasons, data from the angular accelerometers was suspect, and was not used. The rms (20 to 2000 Hz) rotation of the plane of the pedestal mount is 62 microrad in azimuth and 59 microrad in elevation.

B. SUGGESTION FOR FOLLOW-ON INVESTIGATIONS

1. Laboratory calibration tests conducted on the TAP system angular accelerometers prior to the live-fire tests gave no indication of difficulty measuring angular acceleration. Also, signal-to-noise ratio of the measured live-fire data appeared to be more than adequate to make a quality measurement. It is suggested that the behavior of the TAP system angular accelerometers be further investigated by laboratory experiments in which the live-fire vibration is simulated.

2. Unfortunately, because of the timetable of events, it was not possible to study the

transfer functions for vibration input to the pedestal feet through the stabilizer system to the FLIR camera. It would be useful to compute these.

APPENDIX A. TEST PLAN MEMORANDUM FAXED TO NSWC DAHLGREN VA

10 June 1996

MEMORANDUM

From: Prof. Steve Baker & LCDR Jim Schmidt, Naval Postgraduate School
To: LCDR Iain Buckle RN & Dr. Chris Yeaw , NSWC, Dahlgren Division

Subj: PHALANX EO Stabilization System Vibration Test Plan, 10 JUN REV

This document describes the methods and procedures which will be employed to measure the vibration of the PHALANX Electro-Optical (EO) Stabilization System during live firing tests at NSWC, Dahlgren. The measurements are planned for the week of 15 July 1996.

1. Data collection

Vibration data will be collected using a Scientific Atlanta Model SD390 8-Channel Dynamic Signal Analyzer. The SD390 has been previously employed by NPS to acquire vibration data on a firing PHALANX gun at China Lake. Each channel has an independent 16-bit A/D converter, with a maximum sampling rate exceeding 40 kHz with all channels active. Channels are simultaneously sampled. A sampling rate of 25.6 kHz for a duration of approximately 6.5 seconds (166400 samples/channel) will be employed to capture the data of a single firing event, which lasts approximately 5 seconds. This sampling rate exceeds the maximum bullet firing rate by more than a factor of 250, allowing data processing for frequencies well in excess of 1 kHz. The SD390 will be manually triggered and begin sampling approximately 0.5 seconds before firing begins. It takes about 2.7 MB of disk space to store the data for all 8 channels from one test firing. Internal and external disk storage capacity greatly exceeds the required amount anticipated for testing.

As the SD390 can only acquire 8 channels of data, and it is desired to measure the vibration for more than 8 locations and/or directions, a series of measurements employing different accelerometer location and direction combinations is planned. These are described in following sections.

2. Accelerometers

Three types of accelerometers will be employed: (1) uniaxial linear accelerometers, (2) triaxial linear accelerometers, and (3) combination uniaxial linear and uniaxial angular accelerometers

The uniaxial linear accelerometers will be PCB Model J353B03 (side-mounted connector) or J353B04 (top-mounted connector). These are small (½-in hex, 0.8-in H), lightweight (10 g), electrically-isolated units which employ quartz sensing elements and

have a built-in charge amplifier. The frequency response of the accelerometers (± 5 %) is 1 Hz to 7 kHz. They require an external 4 mA constant current source, which will be provided by the SD390 Analyzer.

The triaxial linear accelerometers will be PCB Model 354B33. These are small (0.8-in hex, 0.4-in H), lightweight (15.5 g), electrically-isolated units which employ quartz sensing elements and have a built-in charge amplifier. The frequency response of the accelerometers (± 5 %) is 1 Hz to 2 kHz. They require an external 4 mA constant current source, which will be provided by the SD390 Analyzer.

The combination uniaxial linear and uniaxial angular accelerometers will be Kistler Model 8832 (their so-called "TAP" System, for Transnational-Angular PiezoBEAM accelerometer System). The TAP system is composed of a Model 8696 accelerometer and a Model 5130 signal processor (includes a power supply). The accelerometers are small (5/8-in square, ½-in H), lightweight (10 g), units which employ two piezoelectric ceramic bimorph sensing elements and have a built-in charge amplifier. They are not electrically isolated. By summing and differencing the individual sensor outputs in the signal processor, the TAP System provides one output signal proportional to the linear acceleration normal to the accelerometer base and another output proportional to the angular acceleration about an axis parallel to the accelerometer cable connector. The frequency response of the system (± 5 %) is 0.5 Hz to 2 kHz.

3. Sensor Calibration

Accurate measurement of the relative phase between accelerometers is very important to extract a platform rotation component from linear acceleration data. Amplitude and phase calibration of each accelerometer and each measurement channel will be performed at selected frequencies from 100 Hz to 1 kHz in the lab at NPS. A new, NIST-traceable, Bruel&Kjaer calibration standard accelerometer was procured for this purpose.

Additionally, a hinged beam calibration jig was constructed and used to compare the angular acceleration obtained from measurements of linear acceleration at two locations to that obtained using a TAP angular accelerometer. Results of first experiments made at 100 Hz show a random difference between the two measurements of from 3.0 to 4.4 percent, with a separation between linear accelerometers of 15.3 cm and an average linear acceleration of from 0.014 g pk to 1.11 g pk.

4. Mounting of accelerometers

The uniaxial accelerometers have a 10-32 tapped hole for stud mounting. The triaxial accelerometers have a through hole for an insulated 10-32 cap screw. For most locations, these will be mounted to adhesive mounting bases bonded to the structure with a cyanoacrylate ester "super glue" gelatin or epoxy. Bonding of the bases may require a slight amount of roughing of the surface with steel wool or fine sand paper. It is preferable to bond the mounts the day prior to the test to allow for overnight drying of the adhesive. For several locations it is planned to stud- or screw-mount the accelerometers to tapped holes. The method of mounting at each location is identified in next section.

The angular accelerometers have no provision for stud or screw mounting. The owner's manual recommends that no glue be used on the bottom cover plate of the accelerometer, which occupies most of that surface; petro wax is the recommended adhesive. The units are supplied with petro wax for use at nominally 70 F. We are concerned that the ambient temperature at the test site may considerably exceed this. We have consulted with an application engineer at the manufacturer, and he advised us that it is acceptable to adhesively bond the outer edges of the bottom of the accelerometer, outside of the cover plate, to the structure. We plan to adhesively bond the angular accelerometers to the structure.

5. Accelerometer mounting locations

A description and reference number for each location is provided in Table 1. A diagram of the accelerometer locations by reference number is provided by Figures 1 and 2. The diagrams also indicate the directions of the X, Y, and Z axes.

Accelerometer locations are broken into two categories, primary and secondary, which denotes the priority of that location. Once mounted, accelerometer locations relative to the structure will be carefully measured with 14-inch calipers. We will require the sponsor's or his contractors' assistance in determining the precise coordinates of the sensor locations on the structure. This is crucial for those linear accelerometers which will be used to extract angular acceleration.

Locations and orientations of linear accelerometers, particularly on the camera mount, have been chosen to optimize the extraction of angular acceleration. Azimuthal angular acceleration is obtained from the difference in the X component of acceleration with Y position or the difference in the Y component of acceleration with X position. Elevation angular acceleration is obtained from the difference in the X component of acceleration with Z position or the difference in the Z component of acceleration with X position.

TABLE 1. ACCELEROMETER LOCATIONS

PRIMARY LOCATIONS

Linear accelerometer locations on pedestal mounts:

1. Single-axis, Y-dir, top front pedestal mount, stud-mounted to adhesive-bonded base.
2. Tri-axial, top front pedestal mount, screw-mounted.
3. Tri-axial, bottom front pedestal mount, screw-mounted.
4. Tri-axial, back pedestal mount, screw-mounted.

Note: the triaxial accelerometers are mounted using a through-screw, not a stud. It was discussed at our meeting in Tucson that we would like to mount them to bolts securing the pedestal feet. To do this we must replace one of the production bolts used to secure each foot to the mounting flange on the radome with a bolt which has a 10-32 hole

tapped in its head. Since that meeting, we have obtained production bolts of two different lengths from Hughes. We have purchased bolts that are one-half inch longer than these, drilled and tapped each bolt head with a 10-32 hole, and manufactured one-half inch extension spacers (bushings) for each bolt. These bolts will replace one production bolt on each foot, and will be used to mount the triaxial accelerometers. Using the drawings we have from Hughes, we have estimated that the triaxial accelerometers will not interfere with the feet using these bolts and spacers.

Linear accelerometer locations on FLIR mount ("Rocky"):

5. Single-axis, Y-dir, left surface of FLIR mount (when facing front), to the rear, stud-mounted to adhesive-bonded base.

6. Tri-axial, front surface of FLIR mount (when facing front), to the left. The hole at this location is tapped with 8-32 threads 3/8 inch deep per e-mail from Mr. Bruce Bartholomew of HMSC dated 17 April 1996. We will stud mount this accelerometer with a 8-32 bolt.

7. Tri-axial, rear surface of FLIR mount (when facing front), to the right, stud-mounted to adhesive-bonded base. This location is diagonally opposite location 6.

Angular accelerometer locations on FLIR mount:

8. Angular, Z-axis (azimuth) (w/cable exiting up), mounted on left surface of FLIR mount (when facing front), to the front, adhesively-mounted. Also provides-dir linear acceleration (at a separate output connector).

9. Angular, Y-axis (elevation) (w/cable exiting out, away from radome), mounted on top of the lower surface of the cutout on the left side of FLIR mount (when facing front), close to the center, adhesively-mounted. Also provides Z-dir linear acceleration (at a separate output connector).

Linear accelerometer locations on FLIR:

10. Tri-axial, top surface of FLIR, at rear (Pilkington location 10), stud-mounted to adhesive-bonded base.

11. Tri-axial, top surface of FLIR, near center (Pilkington location 4), stud-mounted to adhesive-bonded base.

12. Tri-axial, top of lens housing (Pilkington location 1).

13. Tri-axial, left side of lens housing (when facing front; Pilkington location 2).

Note: For locations 12 and 13, a machined mounting block which can be bonded to the lens housing is required. This will have to be provided by either Hughes or Contraves or Pilkington.

SECONDARY LOCATIONS

Linear accelerometer locations on base assembly:

14. Tri-axial, on base assembly adjacent to top front pedestal mount, stud-mounted to adhesive-bonded base.

15. Tri-axial, on base assembly adjacent to bottom front pedestal mount, stud-mounted to adhesive-bonded base.

16. Tri-axial, on base assembly adjacent to rear pedestal mount, stud-mounted to adhesive-bonded base.

Angular accelerometer locations on elevation assembly:

17. Angular, Z-axis (azimuth) (w/cable exiting down), on left surface of motor box (?) at front of elevation assembly. Also provides Y-dir linear acceleration (at a separate output connector), adhesively-mounted.

18. Angular, Y-axis (elevation) (w/cable exiting out, away from radome), on bottom surface of motor box (?) at front of elevation assembly. Also provides Z-dir linear acceleration (at a separate output connector), adhesively-mounted.

19. Tri-axial, at front of elevation assembly on top of gear housing (?), stud-mounted to adhesive-bonded base.

6. Reference accelerometers

It is planned to designate two uniaxial linear accelerometers as references, and to keep them mounted in the same place for the duration of the testing, and to dedicate one to two measurement channels to record their signal outputs for every test firing. The purpose is to be able to merge data from different firing runs by normalizing to these references. These will be at locations 1 (Y-dir on one pedestal foot) and 5 (Y-dir on side of FLIR camera mount).

7. Description of each firing

A listing by priority and a description of each firing is provided in Table 2. Each test firing will collect data to calculate the broad-band and narrow-band spectrum levels, displacement levels, coherence (amplitude and phase) components of linear and angular acceleration. The
elevation and azimuth accelerations of the pedestal mounts and base assembly will be measured as will the the angular accelerations of the FLIR camera, camera mount, and base assembly. Between each firing, accelerometers will be moved to the next location while the data is transferred to the external drive and evaluated for completeness.

Prior to each test firing, 10-20 seconds of data will be recorded with the stabilization and FLIR system energized to establish a static baseline for the test.

TABLE 2. ORDER OF TEST FIRINGS AND ACCELEROMETER LOCATIONS

PRIMARY FIRINGS

Firing One: The purpose of this firing is to obtain the Y- and X-components of the input linear accelerations at the pedestal feet and the resulting azimuth and elevation angular accelerations of the FLIR camera mount. One reference single-axis (Y) linear

accelerometer will be mounted at location 1 (top front foot). Triaxial accelerometers at the three pedestal feet will measure the remaining Y- and X-components of input linear acceleration. Two angular accelerometers will be mounted at locations 8 and 9, on the FLIR camera mount ("Rocky"), measuring its elevation and azimuth angular acceleration.

Ch	Type	Loc&Dir/Axis
1	Uni	1Y
2	Tri	2X
3	Tri	3Y
4	Tri	3X
5	Tri	4Y
6	Tri	4X
7	TAP	8Z (Angular Output)
8	TAP	9Y (Angular Output)

Firing Two: The purpose of this firing is to obtain the Y- and Z-components of the input linear accelerations at the pedestal feet and the resulting azimuth and elevation angular accelerations of the FLIR camera mount. One reference single-axis (Y) linear accelerometer will be mounted at location 1 (top front foot). Triaxial accelerometers at the three pedestal feet will measure the remaining Y- and Z-components of input linear acceleration. Two angular accelerometers will be mounted at locations 8 and 9, on the FLIR camera mount ("Rocky"), measuring its elevation and azimuth angular acceleration.

Ch	Type	Loc&Dir/Axis
1	Uni	1Y
2	Tri	2Z
3	Tri	3Y
4	Tri	3Z
5	Tri	4Y
6	Tri	4Z
7	TAP	8Z (Angular Output)
8	TAP	9Y (Angular Output)

Firing Three: The purpose of this firing is to accommodate Pilkington's request for data on the FLIR camera. One references will be used, on the top front pedestal foot (1Y). Two triaxial accelerometers will measure the Y- and Z- components of linear acceleration at the rear and center of the top of the camera. From these measurements, elevation and azimuthal angular acceleration can be computed. The X- component of linear acceleration will also be measured at the center of the top of the camera, as well as the azimuthal and elevation angular acceleration of the FLIR camera mount.

Ch	Type	Loc&Dir/Axis
1	Uni	1Y
2	Tri	10Y
3	Tri	10X
4	Tri	11Y
5	Tri	11Z
6	Tri	11X
7	TAP	8Z (Angular Output)
8	TAP	9Y (Angular Output)

Firing Four: The purpose of this firing is to compare elevation and azimuthal angular acceleration measurements made with linear and angular accelerometers. Two tri-axial accelerometers will be mounted at locations 6 and 7 and collect linear acceleration data in the Y-, Z-, and X-directions. Angular accelerometers at positions 8 and 9 will simultaneously measure azimuth and elevation angular acceleration.

Ch	Type	Loc&Dir/Axis
1	Tri	6Y
2	Tri	6Z
3	Tri	6X
4	Tri	7Y
5	Tri	7Z
6	Tri	7X
7	TAP	8Z(Angular Output)
8	TAP	9Y (Angular Output)

Firing Five: The purpose of this firing is to measure the vibration of the FLIR camera lens housing. Two tri-axial accelerometers will be mounted at locations 12 and 13 and collect data in the X, Y, and Z axis if a suitable mounting block can be manufactured. From these measurements angular and linear acceleration can be computed for the FLIR lens housing relative to the angular acceleration of the camera mount. This firing requires suitable accelerometer mounting blocks manufactured as noted above.

Ch	Type	Loc&Dir/Axis
1	Tri	12Y
2	Tri	12Z
3	Tri	12X
4	Tri	13Y
5	Tri	13Z
6	Tri	13X
7	TAP	8Z (Angular Output)
8	TAP	9Y (Angular Output)

SECONDARY FIRINGS

Firing Six: The purpose of this firing is to obtain the linear Y- and X-components of the input accelerations at the pedestal feet and the base assembly. One reference single-axis (Y) linear accelerometer will be mounted at location 1 (top front foot). Triaxial accelerometers at the base assembly (14, 15, 16) will measure the Y- and X-components of linear acceleration of the base assembly.

Ch	Type	Loc&Dir/Axis
1	Uni	1Y
2	Tri	14Y
3	Tri	3Y
4	Tri	15Y
5	Tri	4Y
6	Tri	16Y
7	Tri	4X
8	Tri	16X

Firing Seven: The purpose of this firing is to obtain the linear Y- and Z-components of the input accelerations at two pedestals and base assembly locations. One reference single-axis (Y) linear accelerometer will be mounted at location 1 (top front foot). Triaxial accelerometers at the base assembly (14 and 15) will measure the Y- and Z-components of linear acceleration of the base assembly.

Ch	Type	Loc&Dir/Axis
1	Uni	1Y
2	Tri	2Z
3	Tri	3Y
4	Tri	3Z
5	Tri	14Y
6	Tri	14Z
7	Tri	15Y
8	Tri	15Z

Firing Eight: The purpose of the firing is to measure the linear and angular acceleration of the elevation axis assembly. One reference will be used, on the top front pedestal foot (1Y). Two angular accelerometers will measure the elevation and azimuthal angular acceleration of the elevation axis assembly at positions 17 and 18. Angular accelerometers at positions 8 and 9 will simultaneously measure azimuth and elevation angular acceleration of the FLIR camera mount. A triaxial accelerometer at location 19 will simultaneously measure the linear component for all axes.

Ch	Type	Loc&Dir/Axis
1	Uni	1Y
2	TAP	8Z (Angular Output)
3	TAP	9Y (Angular Output)
4	TAP	17Z (Angular Output)
5	TAP	18Y (Angular Output)
6	Tri	19Y
7	Tri	19Z
8	Tri	19X

8. Post test

After each firing, the data can quickly be examined for any problems that may have occurred in data collection. After all firings, the test equipment will be removed and packaged for return to NPS. It would be preferable to retain the adhesive mounting bases on the stabilizer until it is confirmed that no further testing is required. This would enable any future test to be conducted at the exact same locations. If further testing is unnecessary, the mounting bases can easily be removed and mailed to NPS.

9. Data Analysis

A utility program, provided by Scientific Atlanta, will be used to convert the SD390 data files into ASCII text files. These will be imported into MATLAB for analysis. Broad-band (rms) and narrow-band spectrum levels of acceleration and displacement will be computed for each measured acceleration component. Segments of the time records that represent the ramp-up and steady-state time periods will be selected for analysis. All measured and calculated angular quantities will be converted into milliradians of angle in the elevation or azimuth axis. The amplitude and phase of each acceleration component will be computed. In particular, the components of linear acceleration at each of the pedestal feet and the azimuth and elevation angular acceleration of the FLIR camera mount will be computed, the latter from both angular and linear accelerometer measurements taken on the FLIR camera mount. Also, the components of angular acceleration of the plane containing the pedestal feet will be computed from the linear acceleration measurements taken at each foot.

Power spectra for acceleration-derived quantities will be reported in mks units and their equivalent english units, e.g. mm/s^2/root Hz, g/root Hz, g^2/Hz for linear acceleration, mm/root Hz for linear displacement, mradians/s^2/root Hz for angular acceleration, mradians/root Hz for angular displacement. Other acceleration-derived quantities of interest, e.g. transfer functions, will be computed as the need arises. Raw and processed acceleration data will be made available to interested parties with permission of the sponsor. It is planned to establish an ftp site for this purpose.

APPENDIX B. SCIENTIFIC ATLANTA MODEL SD390 SPECIFICATIONS

SA390 Specifications

General

Number of Channels	Standard: two (SA610 and SA610DC four channels)
	Optional: four, six or eight (SA390DC and SA610DC limited to four channels maximum)
Frequency Ranges	dc to 100 kHz full scale in 1, 2, 4, 5 sequence less 50 kHz range, two channels active
	dc to 40 kHz full scale 1, 2, 4, 5 sequence, four to eight channels active
Anti-Aliasing Filter	Standard on each Channel with 120 dB/Octave rolloff
A/D Conversion	Ranges up to 40 kHz: 16 Bit Resolution - All channels parallel sampled
	100 kHz range: 12 Bit Resolution - Two channels parallel sampled
Sampling Rate	2.56 x upper frequency range
Maximum Composite Sampling Rate	819, 200 samples per second
DSP Operation	32 Bit 40 MHz Floating Point Primary Processor (20 Million Floating Point Operations per Second)
	16 Bit Secondary Processor for each channel pair (20 Million Operations per Second)
Dynamic Range (analog board type 1)	0.05 Vrms F.S. to 20.0 Vrms F.S. 0–40 kHz, >90 dB below F.S. with 8 avg.
	40 kHz–100 kHz, >80 dB below F.S. with 8 avg.
Noise Floor	0.05 Vrms F.S. to 20.0 Vrms F.S.
(analog board type 1)	0–40 kHz >90 dB below F.S. with 8 avg.
	40 kHz–100 kHz, >80 dB below F.S. with 8 avg.
Real Time Performance	>20 kHz real time rate on dual spectrum calculation
Full Scale Voltage Range	0.001 Vrms to 20 Vrms in 1, 2, 5 sequence with autoranging, independently selectable on each channel

Channel to Channel Match (analog board Type 1)	
Amplitude:	± 0.25 dB, 0–40 kHz, I mVrms F.S. to 1.0 Vrms F.S.
	± 0.5 dB, 0–40 kHz, 2 Vrms F.S. to 20 Vrms F.S.
	±0.5 dB, 40 kHz–100 kHz, 1 mVrms F.S. to 20 Vrms F.S.
Phase:	± 1.0°, 0–40 kHz, 1 mVrms F.S. to 1.0 Vrms F.S.
	± 3.0°, 0–40 kHz, 2 Vrms F.S. to 20 Vrms F.S.
	±3.0°, 40–100 kHz, 1 mVrms F.S. to 20 Vrms F.S.
Cross Talk:	0.05 Vrms F.S. to 20.0 Vrms F.S.
	0–40 kHz, >85 dB below F.S. with 8 avg.
	40 kHz–100 kHz, >75 dB below F.S. with 8 avg.
Input Impedance	1 MΩ shunted by less than 100 picofarads
Input Coupling	dc or ac (-3 dB at 0.5 Hz), selectable each channel
Constant Current Power (ICP®)	4 mA constant current, 24 Vdc maximum, selectable each channel
Overload Protection	100 Vpk input on each channel
Triggering	Internally selectable for any channel, single or repeat;
	External single or repeat
	Slope: Rising or Falling Edge
	Delay: Selectable pre- and post- trigger delay in one sample increments
Frequency Resolution	200, 400, 800, or 1600 lines selectable
Input Recorder Memory	Standard configuration 7.5 MB distributed between active channels
Replay Mode	Auto scan of input recorder memory within user defined boundaries at selected overlap factor
	View time record or processed function results

APPENDIX C. UNIAXIAL ACCELEROMETERS CALIBRATION DATA CARDS

Baker **Calibration Data Card**
Sp004 **SHEAR ACCELEROMETER**
MODEL # J353B04
SERIAL # 11849

VOLTAGE SENSITIVITY: 9.70 mV/g
FREQUENCY RANGE: 1-5000 Hz
OUTPUT BIAS LEVEL: 8.6 V
Date: 5/20/94 By: LC

For further information please refer to Calibration Certificate.

PCB PIEZOTRONICS

3425 Walden Ave • Depew, NY•14043
(716) 684-0001

Baker **Calibration Data Card**
Sp004 **SHEAR ACCELEROMETER**
MODEL # J353B04
SERIAL # 11850

VOLTAGE SENSITIVITY: 9.63 mV/g
FREQUENCY RANGE: 1-5000 Hz
OUTPUT BIAS LEVEL: 8.6 V
Date: 5/20/94 By: LC

For further information please refer to Calibration Certificate.

PCB PIEZOTRONICS

3425 Walden Ave • Depew, NY•14043
(716) 684-0001

Baker **Calibration Data Card**
Sp004 **SHEAR ACCELEROMETER**
MODEL # J353B04
SERIAL # 11851

VOLTAGE SENSITIVITY: 9.73 mV/g
FREQUENCY RANGE: 1-5000 Hz
OUTPUT BIAS LEVEL: 8.7 V
Date: 5/20/94 By: LC

For further information please refer to Calibration Certificate.

PCB PIEZOTRONICS

3425 Walden Ave • Depew, NY•14043
(716) 684-0001

APPENDIX D. TRIAXIAL ACCELEROMETER CALIBRATION CERTIFICATES

— *Calibration Certificate* —
Per ISA-RP37.2

833
F3 (X-AXIS)
Customer
e to NIST thru Project No. 822/255630

ICP® ACCELEROMETER
with built-in electronics
Calibration procedure is in compl
MIL-STD-45662A and traceable

ATION DATA

Sensitivity	102.3	mV/g
rse Sensitivity	2.8	%
it Frequency	12.0	kHz
Bias Level	9.8	V
onstent	1.8	s

KEY SPECIFICATIONS

Range	50	± g
Resolution	0.003	g
Temp. Range	-65/+250	°F

METRIC C
me^4 = .
°C = 5

Reference Freq.

Hz		10	15	30	50	100	300	500	1000	2000				
on %		-1.0	-1.3	-0.9	-0.5	0.0	0.4	0.5	1.1	2.5				

EQUENCY RESPONSE

onics, Inc. 3425 Walden Avenue Depew, NY 14043-2495 USA
0001

Calibrated by Thomas Witne
Date 02-06-1996

453 X

— *Calibration Certificate* —
Per ISA-RP37.2

833
F2 (Y-AXIS)
Customer
le to NIST thru Project No. 822/255630

ICP® ACCELEROMETER
with built-in electronics
Calibration procedure is in comp
MIL-STD-45662A and traceable

ATION DATA

Sensitivity	103.0	mV/g
rse Sensitivity	3.6	%
nt Frequency	15.5	kHz
Bias Level	9.7	V
onstent	1.3	s

KEY SPECIFICATIONS

Range	50	± g
Resolution	0.003	g
Temp. Range	-65/+250	°F

METRIC
me^4 =
°C =

Reference Freq.

Hz		10	15	30	50	100	300	500	1000	2000				
ion %		-1.3	-1.7	-1.1	-0.3	0.0	0.6	0.8	1.3	2.8				

EQUENCY RESPONSE

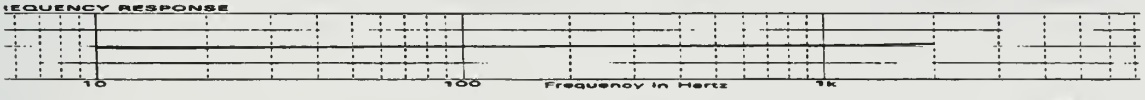

onics, Inc. 3425 Walden Avenue Depew, NY 14043-2495 USA
0001

Calibrated by Thomas Witn
Date 02-06-1996

453 Y

— Calibration Certificate —

Per ISA-RP37.2

B33
453 (Z-AXIS)

Customer

ls to NIST thru Project No. 822/255630

ICP® ACCELEROMETER
with built-in electronics

Calibration procedure is in comp
MIL-STD-45662A and traceable

IATION DATA

Sensitivity	104.8	mV/g
erse Sensitivity	0.9	%
nt Frequency	22.5	kHz
Bias Level	9.7	V
onstant	0.5	s

KEY SPECIFICATIONS

Range	50	± g
Resolution	0.003	g
Temp. Range	-65/+250	°F

METRIC
ms⁻² =
°C = (

Reference Freq.

Hz		10	15	30	50	100	300	500	1000	2000				
ion %		-0.4	-1.4	-0.6	-0.5	0.0	0.6	0.9	1.2	1.7				

REQUENCY RESPONSE

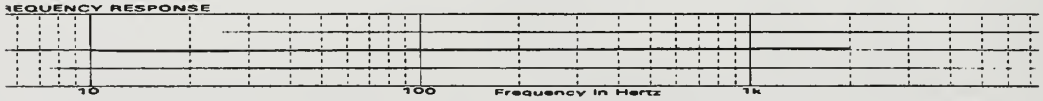

onics, Inc. 3425 Walden Avenue Depew, NY 14043-2495 USA
0001

Calibrated by Thomas Witn
Date 02-06-1996

453 Z

— Calibration Certificate —

Per ISA-RP37.2

4B33
454 (X-AXIS)

Customer

able to NIST thru Project No. 822/255630

ICP® ACCELEROMETER
with built-in electronic

Calibration procedure is in co
MIL-STD-45662A and traceab

IRATION DATA

ge Sensitivity	106.0	mV/g
verse Sensitivity	2.1	%
ent Frequency	14.5	kHz
it Bias Level	9.9	V
Constant	1.4	s

KEY SPECIFICATIONS

Range	50	± g
Resolution	0.003	g
Temp. Range	-65/+250	°F

METR
ms
°C

Reference Freq.

y Hz		10	15	30	50	100	300	500	1000	2000				
ation %		-0.2	-0.7	-0.6	-0.3	0.0	0.3	0.6	1.1	2.0				

FREQUENCY RESPONSE

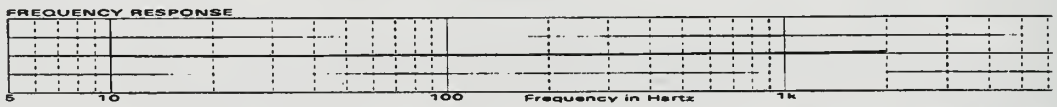

tronics, Inc. 3425 Walden Avenue Depew, NY 14043-2495 USA
4-0001

Calibrated by Thomas Wi
Date 02-06-199

454 X

— Calibration Certificate —

Per ISA-RP37.2

3B33
454 (Y-AXIS)
Customer
ble to NIST thru Project No. 822/255630

ICP® ACCELEROMETER
with built-in electronic
Calibration procedure is in co
MIL-STD-45662A and traceat

RATION DATA

ie Sensitivity	100.0	mV/g
/erse Sensitivity	3.8	%
ant Frequency	17.0	kHz
t Bias Level	9.7	V
Constant	1.8	s

KEY SPECIFICATIONS

Range	50	±g
Resolution	0.003	g
Temp. Range	-65/+250	°F

METRI
ms²
°C -

Reference Freq.

Hz		10	15	30	50	100	300	500	1000	2000			
tion %		-0.5	-1.1	-0.5	-0.3	0.0	0.2	0.4	0.7	1.7			

FREQUENCY RESPONSE

tronics, Inc. 3425 Walden Avenue Depew, NY 14043-2495 USA
:0001

Calibrated by Thomas Wi
Date 02-06-199

454 Y

— Calibration Certificate —

Per ISA-RP37.2

B33
454 (Z-AXIS)
Customer
le to NIST thru Project No. 822/255630

ICP® ACCELEROMETER
with built-in electronics
Calibration procedure is in com
MIL-STD-45662A and traceable

ATION DATA

Sensitivity	103.2	mV/g
rse Sensitivity	0.6	%
nt Frequency	23.0	kHz
Bias Level	9.6	V
onstant	1.2	s

KEY SPECIFICATIONS

Range	50	±g
Resolution	0.003	g
Temp. Range	-65/+250	°F

METRIC
ms² —
°C —

Reference Freq.

Hz		10	15	30	50	100	300	500	1000	2000			
ion %		-0.1	-0.8	-0.3	-0.3	0.0	0.4	0.6	0.9	1.4			

EQUENCY RESPONSE

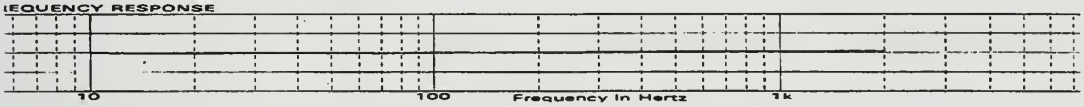

onics, Inc. 3425 Walden Avenue Depew, NY 14043-2495 USA
0001

Calibrated by Thomas Witn
Date 02-06-1996

454 Z

APPENDIX E. ANGULAR ACCELEROMETERS CALIBRATION CERTIFICATES

Piezo-Instrumentation KISTLER

piezoelectric transducers & instrumentation for pressure, force, multi-component force, & acceleration

Type 8832 Translational-Angular PiezoBEAM® (TAP)™ System

Data Bulletin K8.8832 08/90 Page 1 of 2

Features

- Simultaneous measurement of angular and translational vibrations.
- High sensitivity, very low cross talk.
- Ultra low base strain sensitivity.
- Low mass and low profile.
- Selectable gain for the angular signal.

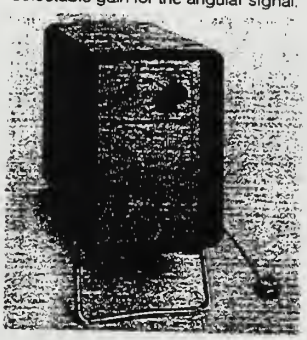

8832 System

Technical Data

		8832
Range*		
Linear	*g*	±10
Angular	rad/s²	±18,000
Overload*		
Linear	*g*	±16
Angular	rad/s²	±28,800
Sensitivity, ±2%		
Linear	mV/*g*	1,000
Angular (selectable)	mV/rad/s²	0.5, 5, 50
Threshold		
Linear	μg_{rms}	300
Angular	rad/s²	0.6
Amplitude Linearity, nom.	%	±1
Resonant frequency (mounted)	kHz	8
Frequency response, ±5%	Hz	0.5 ... 2k
Phase shift, 4 to 2000Hz	°	<5
Time constant, nom.	s	1
Transverse sensitivity, max	%	2
Operating temperature range	°C	0 ... 65
Storage temperature range	°C	–20 ... 90
Temperature coefficient of sensitivity	%/°C	–0.04
Shock Limit (0.2ms pulse)		
Linear	*g*	5,000
Angular	rad/s²	500,000
Weight of transducer (type 8696)	g	10
Housing material (type 8696)		Stainless Steel
Power supply	V AC	110/220
	Hz	50/60
	VA	7.5
Dimensions (type 5130)	inch	3.7Wx5.9Hx7.7D
Mass (type 5130)	kg	1.5

*Acceleration range and overload are determined under pure linear and pure angular acceleration conditions. The decrease in range or limit is directly proportional to the ratio of linear to angular acceleration (for example, if linear acceleration is present at half range, angular range is limited to half range)

1 *g* = 9.80665 m/s², 1 m/s² = 0.1019 *g*; 1inch=25.4mm; 1 g = 0.03527...oz

Description

The 8832 Translational-Angular PiezoBEAM (TAP) system consists of a low impedance accelerometer (8696) and a signal processor (5130). The single piezoelectric sensing element of the 8696 accelerometer simultaneously measures translational and angular accelerations.

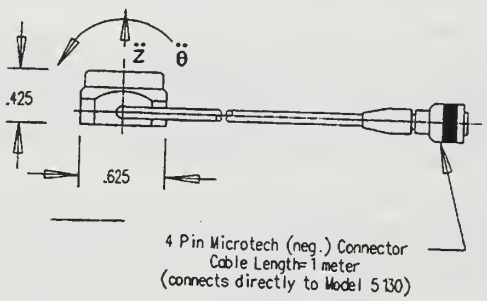

8696 Accelerometer

The main sensing element is a pair of cantilever beams made of a piezoelectric ceramic bimorph. The two beams are arranged as shown in figure 1. The output of the beams is an electrical charge signal whose charge polarity is shown in figure 1. The beam will experience a slight deflection upon acceleration. The example shown in figure 1 is exaggerated for clarity. If the acceleration is purely

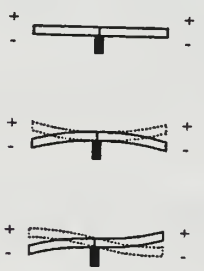

Figure 1

linear (for example in vertical direction), the beams will flex in the same direction. Under angular acceleration, the two beams will flex in opposite directions.

To summarize, linear acceleration of the transducer produces signals from each beam which are in phase, whereas angular acceleration produces signals which have opposite phase. Stimuli which contain linear and angular accelerations will produce two complex signals which are

KISTLER INSTRUMENT CORPORATION

75 John Glenn Drive, Amherst, NY 14228-2171 ■ Phone: 716-691-5100 ■ Fax: 716-691-5226

processed by the 5130 to yield the angular and linear components.

Each beam is connected to an internal hybridized charge amplifier which converts the two charge signals into two high level, low impedance voltage signals.

An integral multiconductor cable connects the 8696 accelerometer to the 5130 signal processor. The two voltage signals are then processed in the 5130 by amplifiers which take their sum and difference. The in-phase linear signals will produce maximum output in the summing amplifier and will also cancel in the difference amplifier. At the same time, out-of-phase angular signals will cancel in the summing amplifier and produce maximum output in the difference amplifier.

The front panel includes a line power switch, a line test LED and a 1,10,100x gain switch for the angular signal. Two rear panel mounted BNC connectors provide output for both the translational and angular signals.

Application

The TAP system is ideally suited for angular and translational mobility measurements. The high sensitivities of 1000mV/g and up to 50mV/rad/sec^2 with very low transverse sensitivity, allow accurate measurement of structural vibrations. The TAP system completes the link between Finite Element Analysis (FEA) and Experimental Modal Analysis (EMA).

Mounting

Special wax for adhesive mounting is supplied. Apply a thin layer of the wax to the test structure's surface. Attach the accelerometer to the structure with firm finger pressure in an alternating twisting motion.

Accessories

Standard accessories

Type 8432 mounting-wax for 8696
Type 1508 Power cord for 5130
Type 1511 Output cable (2 each)

Optional accessories

Type 1578A extension cable between 8696 and 5130
4 pin Microtech pos to 4 pin Microtech neg (l = 2m)

Type 1578Asp same as 1578A, specify length.

Ordering Information

1. Specify Type 8832 TAP system.
2. Specify wired for 220V AC operation as required.
3. Specify 1578A extension cable as required.

Note: 8832 TAP system includes special system calibration of 8896 accelerometer and 5130 signal processor. Accordingly, 8696 and 5130 should be ordered together.

0 ■ Fax: 716-691-5226

KISTLER

Calibration Certificate

TAP™

TRANSLATIONAL ANGULAR PIEZOBEAM SYSTEM MODEL 8832

Accelerometer Model 8696.....SN C103693
Coupler Model 5130.....SN C40184

Angular Sensitivity at 250 Hz, 130 rad/s²	0.472 mV/rad/s²
Linear Sensitivity at 100 Hz, $3g_{rms}$	1004 mV/g

Linear Range	±10 g
Angular Range	±18,000 rad/s²
Mounted Resonant Frequency (nom.)	8 kHz
Transverse Sensitivity max.	2%
Bias Voltage	11 ±3 VDC
Time Constant (nom.)	1.0 s

All measurements at 23°C
g = 9.807 m/s²

NIST TRACEABILITY

This accelerometer was calibrated using a back to back comparison technique against a Kistler Working Standard. The Working Standard is periodically calibrated against a Kistler Reference Standard System which in turn is periodically recertified by the National Institute of Standards and Technology. The calibration of all Kistler acceptance test instrumentation is in conformance with MIL-STD-45662A.

	Working Standard	Reference Standard
Linear Acceleration:		
Accelerometer	Model 809K112 SN C51785	Model 8002K SN C17447
Charge Amplifier	Model 5020 SN C31904	Model 5020 SN C4870
NIST Test Report Number:		822/250337
Angular Acceleration:		
Accelerometers	Model 8602A500M1 SN C36072/SN C36073	Model 8002K SN C17447
Charge Amplifiers	Model 504E10 SN C4797/SN C4623	Model 5020 SN C4870
Summing Amplifier	Model 5217 SN 186396	

By: Michael A. Ferrio
Michael A. Ferrio

FEB 27 1996
Date: 02-23-96

Kistler Instrument Corporation 75 John Glenn Drive Amherst, NY 14120-5091

KISTLER

Calibration Certificate

TAP™

TRANSLATIONAL ANGULAR PIEZOBEAM SYSTEM MODEL 8832

Accelerometer Model 8696.....SN C103694
Coupler Model 5130.....SN C40185

Angular Sensitivity at 250 Hz, 130 rad/s²	0.480 mV/rad/s²
Linear Sensitivity at 100 Hz, $3g_{rms}$	1009 mV/g

Linear Range	±10 g
Angular Range	±18,000 rad/s²
Mounted Resonant Frequency (nom.)	8 kHz
Transverse Sensitivity max.	2%
Bias Voltage	11 ±3 VDC
Time Constant (nom.)	1.0 s

All measurements at 23°C
g = 9.807 m/s²

NIST TRACEABILITY

This accelerometer was calibrated using a back to back comparison technique against a Kistler Working Standard. The Working Standard is periodically calibrated against a Kistler Reference Standard System which in turn is periodically recertified by the National Institute of Standards and Technology. The calibration of all Kistler acceptance test instrumentation is in conformance with MIL-STD-45662A.

	Working Standard	Reference Standard
Linear Acceleration:		
Accelerometer	Model 809K112 SN C51785	Model 8002K SN C17447
Charge Amplifier	Model 5020 SN C31904	Model 5020 SN C4870
NIST Test Report Number:		822/250337
Angular Acceleration:		
Accelerometers	Model 8602A500M1 SN C36072/SN C36073	Model 8002K SN C17447
Charge Amplifiers	Model 504E10 SN C4797/SN C4623	Model 5020 SN C4870
Summing Amplifier	Model 5217 SN 186396	

By: Michael A. Ferrio
Michael A. Ferrio

FEB 27 1996
Date: 02-23-96

Kistler Instrument Corporation 75 John Glenn Drive Amherst, NY 14120-5091

APPENDIX F. CALIBRATION REFERENCE ACCELEROMETER

Brüel & Kjær

BakerLab NPS 3/96 Physics

CERTIFICATE of CALIBRATION

Absolute Calibration by Laser-Interferometer*

(Estimated Uncertainty less than 0,5% at 95% Confidence Level)**

All absolute sensitivity values are transferred from DPLA document No. A1.00-1168

Reference Standard Accelerometer Type 8305 S Serial No. 1864983

Reference Sensitivity*** at 159,2 Hz (ω = 1000 s^{-1}), 50 ms^{-2} and 24.1 °C:

0.1286 pC/ms^{-2} or 1.261 pC/g†

Frequency Response

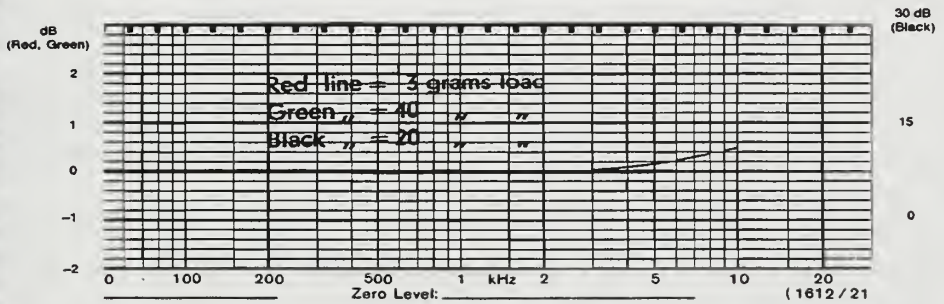

The frequency response curves are obtained with the base of the Reference Accelerometer mounted on an Exciter and with a special accelerometer, with high resonance frequency and high base stiffness, loading the top. Mounting is by 10–32 UNF screw, silicon grease and 2 Nm (17,7 lbf. in.) torque. The load acceleration is kept constant.

Maximum Transverse Sensitivity at 30 Hz 0.4 %

Accelerometer Capacitance 791 pF

Weight: 402 grams

Polarity is negative on the center of the connector for an acceleration directed from the base into the body of the accelerometer.

Resistance minimum $10^{12}\Omega$ at room temperature.

Environmental:

Humidity: Hermetically sealed.
(All welded and glass to metal diffusion seal)

Temperature Range: −74 to +200°C (−100 to +392°F)

Max. Shock Acceleration: 10 kms^{-2} peak

Typical Magnetic Sensitivity (50 Hz – 0,03 T): 1 ms^{-2}/T

Typical Acoustic Sensitivity: 0,008 ms^{-2} at 154 dB SPL (2–100 Hz)

Typical Base Strain Sensitivity (at 250 $\mu\varepsilon$). Base: 0,003 $ms^{-2}/\mu\varepsilon$. Top: 0,01 $ms^{-2}/\mu\varepsilon$

Typical Temperature Transient Sensitivity (3 Hz LLF): 0,5 ms^{-2}/°C

Specifications obtained in accordance with ANSI S2.11-1969

Physical:

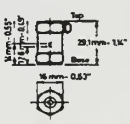

Material: Stainless Steel AISI 316
Mounting Thread: 10-32 UNF-2 B
Electrical Connector: Coaxial 10-32 UNF-2 A thread
Seismic Mass: 7,1 gram
Centre of gravity: "0" seismic mass
"X" whole assembly

Typical Temperature Sensitivity deviation rel. to the Reference Value

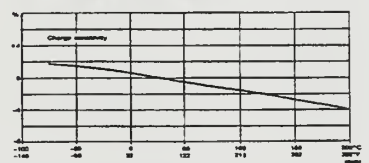

* In accordance with ISO 5347

** Following ISO 5347, NAMAS Information Sheet No.3003 or BIPM Recommendation (CI-1981)

*** This calibration is in compliance with MIL-STD-45662A, and is traceable to:

NIST – National Institute of Standards and Technology, U.S.A., and

PTB – Physikalisch-Technische Bundesanstalt, Germany

† 1 g = 9.80665 ms^{-2}

Nærum on 28 FEB. 19 96

Approved: [signature]

Signed: [signature]

BC 0073–18

APPENDIX G. KISTLER MODEL 5010B DUAL MODE CHARGE AMPLIFIER CALIBRATION CERTIFICATE

KISTLER
Kistler Instrument Corporation
75 John Glenn Drive
Amherst, NY 14228-2171
Phone 716-691-5100
Fax 716-691-5226

Baker Lab
NPS Physics
3/96

Certificate of Calibration

Model: 5010B
Serial Number: C72093
MIL-STD-45662A
Environmental Conditions: Temperature 72 deg.F +/- 7 deg.F
Rel. Humidity 30% +/- 25%
Date: 02-26-1996
Certificate No.: 022696-C72093

Test Equipment Used:
Keithley 199 DMM, SN 0548534
Philips PM5138 Funct. Generator, SN LO5220B0
Kistler Precision Calibrator, SN 441977

Tested by: Kenneth R. Ozzimo
Signature: Kenneth R. Ozzimo

ACCURACY

Range (pC/MU)	Average Deviation	Maximum Measured Deviation
1.00 to 9.99	-0.08%	+0.11%
10.0 to 99.9	-0.01%	+0.06%
100.0 to 999.0	-0.05%	+0.08%
1000 to 9990	-0.03%	+0.07%
10000 to 99900	-0.04%	+0.05%

INTERNAL CALIBRATION CAPACITOR
Measured Value: 962 pF

NOISE
Noise in Reset (at 1pC/V Range): 0.3 mV
Noise in Operate (at 1pC/V Range): 0.8 mV

DRIFT
Drift at each range within 0.03 pC/Second specification

PIEZOTRON CURRENT
Measured Value: 3.9 mA

Kistler Instrument Corp. hereby certifies that the above product was calibrated in compliance with Military Standard Calibration Systems Requirements MIL-STD-45662A using applicable Kistler procedures. Standards used are traceable to the National Institute of Standards and Technology (NIST), or another recognized National Standard, or have been derived from accepted values of natural physical constants, or have been derived by the ratio type of calibration, or by comparison to consensus standards.

ISO 9001 CERTIFIED QUALITY SYSTEM

APPENDIX H. ACCELEROMETER ASSIGNMENT WORKSHEET

TEST FIRING CONFIGURATION ONE

NAME	MAKE	MODEL	SER #	CABLE EXIT DIR	ACC AXIS	CH #	F.S. Volt	TEST LOC/ AXIS	CAL
A	PCB	J353B04	11849	N/A	N/A	1	1	1-X	9.70 mV/g
B	PCB	354B33	454	DOWN (-Y)	TRI-Y	2	10	2-Z	103.2 mV/g
C	PCB	354B33	453	DOWN (-Y)	TRI-Z	3	10	3-X	104.8 mV/g
C	PCB	354B33	453	DOWN (-Y)	TRI-Y	4	10	3-Z	103.0 mV/g
D	PCB	354B33	455	DOWN (-Y)	TRI-Z	5	10	4-X	103.0 mV/g
D	PCB	354B33	455	DOWN (-Y)	TRI-Y	6	10	4-Z	102.3 mV/g
G	TAP	ACC-8696 SC- 5130	C-103694 C-40185	UP (+Y)	ANGLE	7	1	8-Y	0.480 mV/r/s 1009 mV/g
H	TAP	ACC-8696 SC- 5130	C-103693 C-40184	OUT (+X)	ANGLE	8	1	9-X	0.472 mV/r/s 1004 mV/g

Note: Applies to files cf1_1_5s, cf1_2_5s, and cf1_3_3s.

TEST FIRING CONFIGURATION TWO

NAME	MAKE	MOD	SER #	CABLE EXIT DIR	ACC AXIS	CH #	F.S. Volt	TEST LOC/ AXIS	CAL
A	PCB	J353B04	11849	N/A	N/A	1	1	1-X	9.70 mV/g
B	PCB	354B33	454	DOWN (-Y)	TRI-X	2	10	2-Y	106.0 mV/g
C	PCB	354B33	453	DOWN (-Y)	TRI-Z	3	10	3-X	104.8 mV/G
C	PCB	354B33	453	DOWN (-Y)	TRI-X	4	10	3-Y	102.3 mV/g
D	PCB	354B33	455	DOWN (-Y)	TRI-Z	5	10	4-X	103.0 mV/g
D	PCB	354B33	455	DOWN (-Y)	TRI-X	6	10	4-Y	102.8 mV/g
G	TAP	ACC-8696 SC-5130	C-103694 C-40185	UP (+Y)	ANGLE	7	1	8-Y	0.480 mV/r/s 1009 mV/g
H	TAP	ACC-8696 SC-5130	C-103693 C-40184	OUT (+X)	ANGLE	8	1	9-X	0.472 mV/r/s 1004 mV/g

Note: Applies to files cf2_1_5s, cf2_2_3s, and cf2_3_3s.

TEST FIRING CONFIGURATION THREE

NAME	MAKE	MOD	SER #	CABLE EXIT DIR	ACC AXIS	CH #	F.S. Volt	TEST LOC/ AXIS	CAL
A	PCB	J353B04	11849	N/A	N/A	1	1	1-X	9.70 mV/g
B	PCB	354B33	454	AFT (-Z)	TRI-Y	2	10	10-X	100.0 mV/g
B	PCB	354B33	454	AFT (-Z)	TRI-Z	3	10	10-Y	103.2 mV/g
C	PCB	354B33	453	AFT (-Z)	TRI-Y	4	10	11-X	103.0 mV/g
C	PCB	354B33	453	AFT (-Z)	TRI-Z	5	10	11-Y	104.8 mV/g
C	PCB	354B33	453	AFT (-Z)	TRI-X	6	10	11-Z	102.3 mV/g
G	TAP	ACC-8696 SC- 5130	C-103694 C-40185	UP (+Y)	ANGLE	7	2	8-Y	0.480 mV/r/s 1009 mV/g
H	TAP	ACC-8696 SC- 5130	C-103693 C-40184	OUT (+X)	ANGLE	8	2	9-X	0.472 mV/r/s 1004 mV/g

Note: Applies to file cf3_1_5s.

TEST FIRING CONFIGURATION FOUR

NAME	MAKE	MOD	SER #	CABLE EXIT DIR	ACC AXIS	CH #	F.S. Volt	TEST LOC/ AXIS	CAL
B	PCB	354B33	454	AFT (-Z)	TRI-Y	1	10	12-X	100.0 mV/g
B	PCB	354B33	454	AFT (-Z)	TRI-Z	2	10	12-Y	103.2 mV/g
B	PCB	354B33	454	AFT (-Z)	TRI-X	3	10	12-Z	106.0 mV/g
C	PCB	354B33	453	DOWN (-Y)	TRI-Z	4	10	13-X	104.8 mV/g
C	PCB	354B33	453	DOWN (-Y)	TRI-X	5	10	13-Y	102.3 mV/g
C	PCB	354B33	453	DOWN (-Y)	TRI-Y	6	10	13-Z	103.0 mV/g
G	TAP	ACC-8696 SC-5130	C-103694 C-40185	UP (+Y)	ANGLE	7	2	8-Y	0.480 mV/r/s 1009 mV/g
H	TAP	ACC-8696 SC-5130	C-103693 C-40184	OUT (+X)	ANGLE	8	2	9-X	0.472 mV/r/s 1004 mV/g

Note: Applies to file cf4_1_5s.

TEST FIRING CONFIGURATION FIVE

NAME	MAKE	MOD	SER #	CABLE EXIT DIR	ACC AXIS	CH #	F.S. Volt	TEST LOC/ AXIS	CAL
A	PCB	J353B04	11849	N/A	N/A	1	1	1-X	9.70 mV/g
I	TAP	ACC-8696 SC-5130	C-58089 C-34612	DOWN (-Y)	ANGLE	2	10	17-Y	0.478 mV/r/s 1019 mV/g
J	TAP	ACC-8696 SC-5130	C-58082 C-33393	OUT (+X)	ANGLE	3	10	18-X	0.485 mV/r/s 1014 mV/g
B	PCB	354B33	454	IN (-X)	TRI-X	4	10	19-X	106.0 mV/g
B	PCB	354B33	454	IN (-X)	TRI-Z	5	10	19-Y	103.2 mV/g
B	PCB	354B33	454	IN (-X)	TRI-(-Y)	6	10	19-Z (-)	100.0 mV/g
G	TAP	ACC-8696 SC- 5130	C-103694 C-40185	UP (+Y)	ANGLE	7	10	8-Y	0.480 mV/r/s 1009 mV/g
H	TAP	ACC-8696 SC- 5130	C-103693 C-40184	OUT (+X)	ANGLE	8	10	9-X	0.472 mV/r/s 1004 mV/g

Note: Applies to files cf5_1_5s and cf5_0_bl.

TEST FIRING CONFIGURATION SIX

NAME	MAKE	MOD	SER #	CABLE EXIT DIR	ACC AXIS	CH #	F.S. Volt	TEST LOC/ AXIS	CAL
A	PCB	J353B04	11849	N/A	N/A	1	1	1-X	9.70 mV/g
I	PCB	J353B04	11850	N/A	N/A	2	1	14-X (-)	9.63 mV/g
E	PCB	J353B04	11851	N/A	N/A	3	1	3-X	9.73 mV/g
C	PCB	354B33	453	DOWN (-Y)	TRI- (-Z)	4	10	15-X (-)	104.8 mV/g
B	PCB	354B33	454	DOWN (-Y)	TRI- Z	5	10	4-X	103.2 mV/g
D	PCB	354B33	455	DOWN (-Y)	TRI- (-Z)	6	10	16-X (-)	103.0 mV/g
B	PCB	354B33	454	DOWN (-Y)	TRI- Y	7	10	4-Z	100.0 mV/g
D	PCB	354B33	455	DOWN (-Y)	TRI- (-Y)	8	10	16-Z (-)	102.3 mV/g

Note: Applies to file cf6_1_5s.

TEST FIRING CONFIGURATION SEVEN

NAME	MAKE	MOD	SER #	CABLE EXIT DIR	ACC AXIS	CH #	F.S. Volt	TEST LOC/ AXIS	CAL
A	PCB	J353B04	11849	N/A	N/A	1	1	1-X	9.70 mV/g
X	PCB	J353B04	11851	N/A	N/A	2	1	2-Y	9.73 mV/g
C	PCB	354B33	453	DOWN (-Y)	TRI-Z	3	10	3-X	104.8 mV/g
C	PCB	354B33	453	DOWN (-Y)	TRI-X	4	10	3-Y	102.3 mV/g
B	PCB	354B33	454	UP (+Y)	TRI-Z	5	10	14-X (-)	103.2 mV/g
B	PCB	354B33	454	UP (+Y)	TRI-X	6	10	14-Y (-)	106.0 mV/g
D	PCB	354B33	455	DOWN (-Y)	TRI-Z	7	10	15-X (-)	103.0 mV/G
D	PCB	354B33	455	DOWN (-Y)	TRI-X	8	10	15-Y	102.8 mV/g

Note: Applies to file cf7_1_5s.

TEST FIRING CONFIGURATION EIGHT

NAME	MAKE	MOD	SER #	CABLE EXIT DIR	ACC AXIS	CH #	F.S. Volt	TEST LOC/ AXIS	CAL
C	PCB	354B33	453	DOWN (-Y)	TRI- (-Y)	1	10	6-X (-)	103.0 mV/g
C	PCB	354B33	453	DOWN (-Y)	TRI- X	2	10	6-Y	102.3 mV/g
C	PCB	354B33	453	DOWN (-Y)	TRI- Z	3	10	6-Z	104.8 mV/g
D	PCB	354B33	455	DOWN (-Y)	TRI- Y	4	10	7-X	102.3 mV/g
D	PCB	354B33	455	DOWN (-Y)	TRI- X	5	10	7-Y	102.8 mV/g
D	PCB	354B33	455	DOWN (-Y)	TRI- (-Z)	6	10	7-Z (-)	103.0 mV/g
G	TAP	ACC-8696 SC- 5130	C-103694 C-40185	UP (+Y)	ANGLE	7	10	8-Y	0.480 mV/r/s 1009 mV/g
H	TAP	ACC-8696 SC- 5130	C-103693 C-40184	OUT (+X)	ANGLE	8	10	9-X	0.472 mV/r/s 1004 mV/g

Note: Applies to file cf8_1_5s.

BASELINE CONFIGURATION ZERO

NAME	MAKE	MOD	SER #	CABLE EXIT DIR	ACC AXIS	CH #	F.S. Volt	TEST LOC/ AXIS	CAL
A	PCB	J353B04	11849	N/A	N/A	1	1	1-X	9.70 mV/g
I	TAP	ACC-8696 SC-5130	C-58089 C-34612	DOWN (-Y)	ANGLE	2	10	17-Y	0.478 mV/r/s 1019 mV/g
J	TAP	ACC-8696 SC-5130	C-58082 C-33393	OUT (+X)	ANGLE	3	10	18-X	0.485 mV/r/s 1014 mV/g
B	PCB	354B33	454	AFT (-Z)	TRI-Y	1	10	12-X	100.0 mV/g
B	PCB	354B33	454	AFT (-Z)	TRI-Z	2	10	12-Y	103.2 mV/g
B	PCB	354B33	454	AFT (-Z)	TRI-X	3	10	12-Z	106.0 mV/g
G	TAP	ACC-8696 SC- 5130	C-103694 C-40185	UP (+Y)	ANGLE	7	10	8-Y	0.480 mV/r/s 1009 mV/g
H	TAP	ACC-8696 SC- 5130	C-103693 C-40184	OUT (+X)	ANGLE	8	10	9-X	0.472 mV/r/s 1004 mV/g

Note: Applies to file cf0_0_bl.

FULL SCALE TEST CONFIGURATION ONE

NAME	MAKE	MOD	SER #	CABLE EXIT DIR	ACC AXIS	CH #	F.S. Volt	TEST LOC/ AXIS	CAL
A	PCB	J353B04	11849	N/A	N/A	1	1	1-X	9.70 mV/g
B	PCB	J353B04	454	DOWN (-Y)	TRI-Y	2	10	2-Z	100.0 mV/g
B	PCB	354B33	454	DOWN (-Y)	TRI-X	3	10	2-Y	106.0 mV/g
B	PCB	354B33	454	AFT (-Z)	TRI-Y	1	10	12-X	100.0 mV/g
B	PCB	354B33	454	AFT (-Z)	TRI-Z	2	10	12-Y	103.2 mV/g
B	PCB	354B33	454	AFT (-Z)	TRI-X	3	10	12-Z	106.0 mV/g
G	TAP	ACC-8696 SC- 5130	C-103694 C-40185	UP (+Y)	ANGLE	7	10	8-Y	0.480 mV/r/s 1009 mV/g
H	TAP	ACC-8696 SC- 5130	C-103693 C-40184	OUT (+X)	ANGLE	8	10	9-X	0.472 mV/r/s 1004 mV/g

Note: Applies to file cf0_1_1s.

FULL SCALE TEST CONFIGURATION TWO

NAME	MAKE	MOD	SER #	CABLE EXIT DIR	ACC AXIS	CH #	F.S. Volt	TEST LOC/ AXIS	CAL
B	PCB	354B33	454	AFT (-Z)	TRI-Y	1	10	12-X	100.0 mV/g
B	PCB	354B33	454	AFT (-Z)	TRI-Z	2	10	12-Y	103.2 mV/g
B	PCB	354B33	454	AFT (-Z)	TRI-X	3	10	12-Z	106.0 mV/g
B	PCB	354B33	454	IN (-X)	TRI-X	4	10	19-X	106.0 mV/g
B	PCB	354B33	454	IN (-X)	TRI-Z	5	10	19-Y	103.2 mV/g
B	PCB	354B33	454	IN (-X)	TRI-(-Y)	6	10	19-Z (-)	100.0 mV/g
G	TAP	ACC-8696 SC-5130	C-103694 C-40185	UP (+Y)	ANGLE	7	10	8-Y	0.480 mV/r/s 1009 mV/g
H	TAP	ACC-8696 SC-5130	C-103693 C-40184	OUT (+X)	ANGLE	8	10	9-X	0.472 mV/r/s 1004 mV/g

Note: Applies to file cf0_2_1s.

APPENDIX I. SAMPLE MATLAB CODE FOR CALCULATION OF POWER SPECTRAL DENSITIES FOR LINEAR ACCELEROMETERS

For a copy of this Appendix, contact:

Professor Steven R. Baker
Naval Postgraduate School
Physics Department Code PH/Ba
Monterey, California 93943
(408) 656-2732.

APPENDIX J. SAMPLE MATLAB CODE FOR CALCULATION OF POWER SPECTRAL DENSITIES FOR ANGULAR ACCELEROMETERS

For a copy of this Appendix, contact:

Professor Steven R. Baker
Naval Postgraduate School
Physics Department Code PH/Ba
Monterey, California 93943
(408) 656-2732.

APPENDIX K. SAMPLE MATLAB CODE FOR CALCULATION OF ANGULAR ACCELERATION FROM LINEAR ACCELEROMETERS

For a copy of this Appendix, contact:

Professor Steven R. Baker
Naval Postgraduate School
Physics Department Code PH/Ba
Monterey, California 93943
(408) 656-2732.

APPENDIX L. SAMPLE MATLAB CODE FOR CALCULATION OF ANGULAR ROTATION OF THE PLANE OF THE PEDESTAL FEET

For a copy of this Appendix, contact:

Professor Steven R. Baker
Naval Postgraduate School
Physics Department Code PH/Ba
Monterey, California 93943
(408) 656-2732.

LIST OF REFERENCES

APS, Acoustic Power Systems, Inc., Instruction Manual Model 120S Shaker, 1984, 5731 Palmer Way Suite A, Carlsbad, CA 92008. (619) 438-4848.

Bendat, J.S. and Piersol A.G., *Engineering Applications of Correlation and Spectral Analysis*, John Wiley & Sons, Inc., 1993.

Bruel & Kjaer, Sound and Vibration Catalogue, 1993. DK-Naerum, Denmark. (800) 442-1030.

Hewlett-Packard Company Catalog, 1996, Mail Stop 51LSJ, P.O. Box 58199, Santa Clara, CA 95952-9952. (800) 452-4844.

Hughes Missile Systems Company Contractor Technical Evaluation (CTE) Plan for PHALANX Block 1B, Hughes Missile Systems Company, Tucson, AZ January 1996.

Kistler, Kistler Instrument Corporation, 1995, 75 John Glen Drive, Amherst, NY 1422. (716) 691-5100.

Krauss, T.P., Shure, L., Little J.N., Signal Processing Toolbox for use with Matlab, The Math Works, Inc., 1994, 24 Prime Park Way, Natick, MA 01760. (508) 653-1415.

MATLAB, The Math Works, Inc. 1992, 24 Prime Park Way, Natick, MA 01760. (508) 653-1415.

PCB, Vibration and Shock Catalogue, 1993, 3425 Walden Avenue, Depew, NY 14043. (716) 684-0001.

Scientific Atlanta, Inc. Signal Processing Systems Instrumentation Group, 1996, 13112 Evening Creek Drive South, San Diego, CA 92128. (619) 679-6000.

Stanford Research Systems, 1986, 460 California Ave. Palo Alto, CA 94306

INITIAL DISTRIBUTION LIST

1. Defense Technical Information Center 2
   8725 John J. Kingsman Road., Ste 0944
   Ft. Belvoir, Virginia 22060-6218

2. Dudley Knox Library 2
   Naval Postgraduate School
   411 Dyer Rd.
   Monterey, California 93943-5101

3. Professor Steven R. Baker 2
   Department of Physics, Code PH/Ba
   Naval Postgraduate School
   Monterey, California 93943-5103
   (408) 656-2732

4. Professor Robert Keolian 1
   Department of Physic,s Code PH/Kn
   Naval Postgraduate School
   Monterey, California 93943-5103
   (408) 656-2732

4. Stan Wilson 1
   Port Hueneme Division
   Naval Surface Warfare Center, Code 4121
   Port Hueneme, California 94040

5. LCDR James E. Schmidt USN 2
   11593 Meadowbrook Dr
   Parma Hts., Ohio 44130

6. LCDR Iain Buckle RN 1
   Phalanx Program Office, Code G30
   Naval Surface Warfare Center
   Dahlgren Division
   Dahlgren, Virginia 22448-5000
   (540) 653-7587

7. Dr Christopher Yeaw 1
   Phalanx Program Office, Code G30
   Naval Surface Warfare Center
   Dahlgren Division
   Dahlgren, Virginia 22448-5000
   (540) 653-7587

8. Dr Sid Taylor 1
   John Hopkins University Advanced Physics Lab
   Building 1 West 257
   11100 John Hopkins Road
   Laural, MD 20723-6099
   (301) 953-6000

9. Dr Bruce Bartholomew 1
   Hughes Missile Systems Company
   1511 E. Herman Road
   Tucson, Arizona 85706
   (520) 794-2633